Article

Allosaurus europaeus (Theropoda: Allosauroidea) Revisited and Taxonomy of the Genus

André Burigo [1,*] and Octávio Mateus [1,2,3,*]

1   Faculdade de Ciências e Tecnoloogia, Universidade Nova de Lisboa, 2829-516 Caparica, Portugal
2   GeoBioTec, 2829-516 Caparica, Portugal
3   Museu da Lourinhã, 2530-158 Lourinhã, Portugal
*   Correspondence: andrepburigo@hotmail.com (A.B.); omateus@fct.unl.pt (O.M.)

Abstract: *Allosaurus* is one of the most famous theropod dinosaurs, but the validity and relationships between the different species have been confusing and often questioned. Portugal is relevant to the understanding of the genus in light of the discovery of *A. europaeus* ML415 from the Early Tithonian of Lourinhã and *Allosaurus* MNHNUL/AND.001 from Andrés. However, the exact classification and validity of these two specimens has always been controversial. The presence of *Allosaurus* in Portugal is strong evidence for a North America–Europe Late Jurassic dispersal, later supported by other taxa. A detailed cranial description and specimen-based phylogeny were performed and resolved many of the open questions: (1) The diversity of *Allosaurus* is limited to three named species: *A. fragilis*, *A. europaeus*, and *A. jimmadseni*. (2) Nine autapomorphies were found in *A. europaeus*, confirming the validity of the species. (3) Phylogenetic analyses place both Portuguese specimens in the genus *Allosaurus*, based on the following synapomorphies: jugal bone lateral view, relative heights of quadratojugal prongs, the dorsal prong is equal in height, the jugal bone in lateral view shows shallow accessory pneumatization of the antorbital fossa, the palatine pneumatic recess shape is small, and lacrimal horn morphology has a triangular horn. (4) The Andrés specimen is placed with the *A. europaeus* and they are considered here to be the same species, which is paleo-geographically and biochronologically congruent. (5) *A. europaeus* and *A. jimmadseni* are sister taxa and closer to each other than to *A. fragilis*. The genus is distributed in occurrences from the United States, Germany, and Portugal, and from the Late Kimmeridgian to the Late Tithonian, while the Cenomanian report from Japan is reidentified as *Segnosaurus*.

Keywords: *Allosaurus europaeus*; Allosauridae; theropods; Portugal; Tithonian; Lourinhã; specimen-based analysis

1. Introduction

Allosaurus Marsh, 1877 is the most iconic Jurassic theropod genus. Rauhut and Pol, 2019 [1], defined Allosauroidea Currie and Zhao 1994 as branch-based, including all theropods that are more closely related to *Allosaurus fragilis* than to either *Megalosaurus bucklandii* Mantell 1827 or Neornithes. While *Allosaurus* is one of the best-known Jurassic theropods, with thousands of bones collected since 1877, it also has a complex taxonomical history. *Allosaurus* is an abundant genus in the Upper Jurassic (Kimmeridgian, 157.3–152.1, Tithonian, 152.1–145 Ma), with a large chronostratigraphic and paleobiogeographic distribution, with fossils identified as *Allosaurus* in America and Europe and, arguably, in Africa [2]. Chure and Loewen, 2020 [3], considered three species to be valid: *A. fragilis* Marsh, 1877, and *A. jimmadseni* Chure and Loewen, 2020, in the United States

of America (U.S.A.) from the Morrison Formation and *A. europaeus* Mateus et al., 2006 in Portugal from the Lourinhã Formation.

Remains significantly diagnostic of *Allosaurus* were described from Andrés Quarry from Upper Kimmeridgian of Alcobaça Formation close to the village of Andrés, Leiria, West-Central Portugal, now deposited in Museu Nacional de História Natural e da Ciência, under the number MNHNUL/AND.001 [4], which includes part of the right quadrate, vertebrae and chevrons, dorsal ribs and gastralia, a partial pelvis, parts of the hind limbs, and indeterminate fragments, which were assigned to *Allosaurus fragilis* [4,5]. In 2005, new work in the same quarry revealed more material from the same level and believed to belong to the same individual, including the right quadrate and quadratojugal, both lacrimal bones, the right frontal, the right dentary, the posterior end of the right mandibular ramus, and a complete braincase. Additionally, a complete ilium belonging to a larger individual was also found. Both were identified as belonging to the American species *A. fragilis* [6].

In 2005, an isolated theropod maxilla (MG 27804 previously IPFUB Gui Th 4) was described by Rauhut et al. [7]. as a hatchling of *Allosaurus* from Kimmeridgian Late Jurassic Guimarota mine in Portugal. This specimen represents the first non-coelurosaurian theropod hatchling skull remains in Portugal. It is referred to as the *Allosaurus* genus with certainty but is not diagnostic at the species level. This specimen represents the earliest ontogenetic specimen and the oldest fossil record of this genus in Portugal [7].

Postcranial fossils were found in Late Jurassic strata of Cambelas (Torres Vedras, Portugal) in the Freixial Formation (upper part of the lower Tithonian–upper Tithonian), including caudal vertebrae, chevrons, tarsals, metatarsals, and phalanges. This specimen is reposited in Sociedade de História Natural de Torres Vedras (SHN), ALT-SHN.0019. These remains exhibit characteristics similar to those of *Allosaurus fragilis* from Andrés, suggesting that they may belong to the same taxon [8], but later were classified as a new taxon, *Lusovenator santosi*, in [9].

Mateus et al. [10] described new remains of this genus from the Lourinhã Formation (Figure 1), consisting of a partial skull and neck (ML415). They erected a new species, *A. europaeus*, characterized by "jugal contribution to the antorbital fenestra; a maxilla that is forked posteriorly and has a truncated ventroposterior process; a nasal bone with two pneumatic foramina, with the anterior foramen being twice the size of the posterior; a posteroventral projection of the jugal bone that is more than twice the posterior dorsal projection; no lacrimal–maxillary contact; a squamosal bone that contacts the quadratojugal bone by a sigmoidal suture and projects ventrally into the lateral temporal fenestra; a narrow lacrimal horn in lateral view; a large ventral projection of the postorbital bone; a rugose dorsal rim of the nasal bone; occipital condyles located above the squamosal–quadratojugal contact; the anterior tip of the quadratojugal bone located anterior to the lateral temporal fenestra; a subtle lateral lamina of the lacrimal bone, and a palatine bone that contacts the pterygoid dorsoposteriorly and the ventral tip of the postorbital bone reaches the lower rim of the orbit", according to Mateus et al. [10].

The validity of the species *A. europaeus* has been questioned by Malafaia et al., 2007, and Malafaia et al., 2010 [5,6]. It is stated that the original description is based on a set of characters falling within the morphological variability of *A. fragilis*, and it is possible that some features were misinterpreted. Evers et al., 2020 [11], stated that one of the distinguishing characters of the original description (the participation of the anterior process of jugal bone in the antorbital fenestra) is not valid, considering that this feature does occur in *A. fragilis*, contradicting the famous reconstructions by Madsen, 1976 [12].

The presence of this genus in both the Morrison and Lourinhã formations strengthens the link between the North American and Portuguese dinosaur faunas during the upper Kimmeridgian–Tithonian. The faunal similarities can also be seen in the appearance of

other taxa, such as the theropods *Ceratosaurus* and *Torvosaurus* [10] or the ornithischians *Stegosaurus* [13] and *Miragaia* [14], found in both countries. Therefore, the taxonomy of *Allosaurus* is important for the understanding of the paleobiogeography of dinosaurs during the Late Jurassic and is also important for contributing to our knowledge about the opening of the North Atlantic and its implications to the faunal interchanges between Europe and North America in the Late Jurassic.

2. Geological Context

The holotype of *Allosaurus europaeus*, ML415, was discovered on the beach of Praia de Vale Frades, within rockfall remains (Figure 1). Located in the west-central coast of Portugal in the Lusitanian Basin, in the Consolação sub-basin of the Lourinhã Formation, the formation is primarily composed of continental deposits, punctuated by localized marine incursion events [15]. The Lusitanian Basin is a rift basin that covers the western margin of the Iberian Peninsula, stretching from Porto to Lisbon and covering an area of 20,000 km^2, making it the largest Mesozoic basin in Portugal. It underwent four rifting episodes, one of which (Late Oxfordian to Early Kimmeridgian) culminated in the creation of complex fault-bounded and diapir-bounded sub-basins [16]. One of these is the Consolação sub-basin, which is flanked by the Berlengas Horst to the West, the fault zone controlled by the Caldas da Rainha, Bolhos, and Santa Cruz diapirs to the east, and the Nazaré fault to the north [17]. This sub-basin contains a significant number of outcrops along the coast, mainly composed of sediments of the Lourinhã Formation. The Lourinhã Formation is composed of five distinct members, namely, the Praia da Amoreira, Porto Novo, Praia Azul, Assenta, and Santa Rita members, with a thickness of approximately 700 to 800 m.
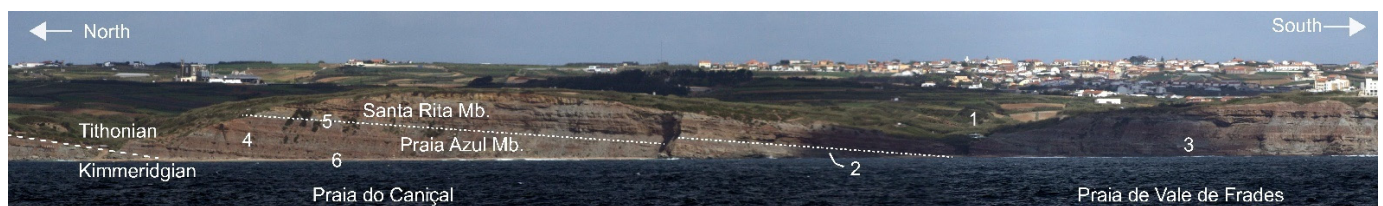
Figure 1. Cliffs of Lourinhã Fm. outcrops of Praia do Caniçal and Praia de Vale Frades, taken from ca. 39.278° N, 9.348° W, toward the east. 1. *Draconyx loureiroi* type-locality; 2. *Allosaurus europaeus* type-locality ML415 (top of Praia Azul Mb. or base of Santa Rita Mb.); 3. Tracheophytes in situ roots; 4. Theropod nest; 5. Plesiochelid; 6. *Lusognathus almadrava* Fernandes et al., 2023 type-locality.

Praia de Vale de Frades is a beach ("praia"), also known as "Vale Frades" and "Vale dos Frades", in the municipality of Lourinhã and parish (freguesia) of Lourinhã e Atalaia, bordered by Upper Jurassic cliffs that can reach 50 m above sea level.

The age is Lower Tithonian of Lourinhã Formation (Fm.), divided by two members: the top of Praia Azul Mb. and the base of Santa Rita Mb. (≃Bombarral Unit), divided by a ~50 cm-thick bioclastic brackish transgressive layer. The lithology is an intercalation between mudstone floodplains and sandstone channels, with occasional paleosol levels. Three fossil sub-localities can be recognized, as follows:

1. Praia de Vale de Frades north (top of Praia Azul Mb.). The fossil locality altitude varies between −1 and 10 m relative to sea level. The faunal list is:

    - Transgressive layer (last of Praia Azul Mb.), dominated by the bivalves *Jurassicorbula edwardi* (Sharpe, 1850), with some *Isognomon lusitanicus* and fragments of Plesiochelidae turtles, and charcoal fragments.
    - *Allosaurus europaeus* Mateus et al., 2006 (type specimen ML415), from the gray sandstone channel, 2–3 m below the guide transgressive layer.

- Camarasauridae sacral neural spine fragment (ML specimen, previously under ML415b).
- Dryomorpha pes track (ML1000), of very large proportions, 70 cm-long (Ornithopoda in Mateus and Milàn 2008) at the intertidal sandstone level, 39°16′30″ N, 9°20′09″ W, 0 m alt. (Praia Azul Mb.) [18,19]).
- Dacentrurinae (*Deltapodus* sp.) pes track (ML1342), probably attributable to *Miragaia longicollum*, in the same location and level as the previous one [19–21].

2. Vale de Frades (top of the cliff, Santa Rita Mb.), base of the sandstone channel at the road, cut at the coordinates 39°16′31″ N, 9°20′00″ W (~36 m alt.).

- *Draconyx loureiroi* Mateus and Antunes, 2003 (type specimen).
- Plesiochelyidae indet (specimen ML).

3. Praia de Vale de Frades south (new locality) is a terrestrial sandstone channel at 39°16′22″ N, 9°20′08″ W (3 m alt.), with Tracheophytes in situ roots and Lycopodiopsida megaspores (Santa Rita Mb.).

The outcrop present on the beach of Praia de Vale Frades has exposed two members, the top of Praia Azul Member and the base of the Santa Rita Member. Because the specimen was discovered within rockfall remains and the previously mentioned situation, it is difficult to know from which member ML415 comes from, although it has been considered from the Praia Azul Member by Mateus et al., 2006 [10], based on the stratigraphy of Hill 1989.

The Praia Azul Member consists of marls and mudstones with tabular and lenticular geometry and rare sandstone bodies with intense bioturbation, wave ripples, cross-bedding, and carbonated debris, from late Kimmeridgian to early Tithonian. The member is characterized by the presence of three distinct, laterally traceable, shelly units, developed in thick floodplain mud sequences [15]. The first shelly unit is located at the base of the member contacting the Praia da Amoreira and Porto Novo members with *Eomiodon securiformis* (Sharpe 1850) in situ. The second shelly unit is in the middle of the Praia Azul Member with *Isognomon lusitanicus* (Sharpe 1850), and the last one is at the top at the contact with the Santa Rita Member with a *Jurassicorbula edwarsi* (Sharpe 1850) community in situ. This unit is present at the beach Praia de Vale Frades, where ML415 was found [17]. The paleoenvironment of this member has been interpreted as a meandering fluvial system, a low-lying coastal plain connected with transitional systems, such as deltas with marine incursions [15].

The Praia Azul Member is rich in dinosaur fauna, with several holotypes established. The first dinosaur remains found in this member were those of *Lusotitan atalaiensis* [22], previously named *Brachiosaurus atalaiensis* by Peralta [18,19]. Other taxa were described three decades after this discovery, starting with the discovery of *Dinheirosaurus lourinhanensis* (holotype ML 414) in 1987 [23], found on the beach of Porto Dinheiro [24], followed by the discoveries of *Lourinhanosaurus antunesi* (holotype ML 370) [25], also found by Peralta, and the *Miragaia longicollum* holotype (ML 433) described in [26], found in the top unit of this member close to the village of Miragaia [14].

Other vertebrates can also be found, such as Plesiochelyidae, Pleurosternidae *Selenemys* Pérez-García and Ortega 2011, *Ophiussasuchus paimogonectes* López-Rojas et al. (2024), *Machimosaurus hugii* Von Meyer (1837), and *Hydodus lusitanicus* [15]. Micro-vertebrate remains show the occurrence of bony fishes, anurans, albanerpetontids, plesiosaurs, pterosaurs *Lusognathus almadrava* Fernandes et al., 2023, lizards, early snakes, small crocodylomorphs, and mammaliaforms. The Member also contains remains of some invertebrates, such as *Jurassicorbula*, *Isognomon*, *Eomiodon*, *Archaeomytilus*, *Protocardia gigantea* Schneider et al., 2010, *Juranomia calcybyssata* Fürsich & Werner 1989, and flora [15].

The Santa Rita Member of the Lourinhã Formation of the Consolação sub-basin is laterally equivalent to the Assenta Member of the Lourinhã Formation in the Turcifal sub-

basin and is limited at the base by the aforementioned shelly unit [15]. It is characterized by the alternation of cross-bedded sandstones and bioturbated mudstones with paleosols and frequent levels of pedogenic carbonate concretions. There are also levels with nodular and marly bioclastic limestones with ostracods and foraminifera. On the cliffs, bioturbations and loading features (soft sediment deformation) with recurrent slumps can be seen. The age of this member was determined as mainly early Tithonian to Berriasian using foraminifera, ostracods, and magneto-stratigraphy [15]. The paleoenvironment was interpreted in the equivalent Areia Branca member in [17] as a meandering river system within a greater floodplain environment.

The invertebrates in the Santa Rita member are characterized by the presence of dinocyst forms, a diverse assemblage of foraminifera, ostracods, and charophytes [17], with a diverse bivalve fauna [27]. Also, the authors of [14] stated that some stegosaurian remains previously discovered probably came from the Santa Rita Member, including some remains from *Miragaia longicollum* (MG 4863), including *Draconyx loureiroi* (holotype ML 357) in the Vale Frades region [28], but in younger deposits within the Santa Rita Member at the top of the cliff, contrary to what is stated in [29].

Even though we do not know the exact location of the holotype of *Allosaurus europaeus* ML415, nevertheless, since the second shelly unit defines the boundary of the Kimmeridgian–Tithonian, and both the Praia Azul and Santa Rita Members are represented in the beach area between the third shelly unit and above the second, it is assured with certainty that ML415 is Tithonian in age.

The principal objective of this study is to provide a comprehensive re-description and detailed anatomical analysis of *Allosaurus europaeus* ML415, including the partial skull, three cervical vertebrae, and several ribs, which represent the holotype specimen [10]. The secondary objective of this study is to discover, if possible, a new set of characters present in the specimen and compare them with those of other *Allosaurus* species using morphometric phylogenetic analysis. This was facilitated by mechanical preparation, photogrammetry, and comparative descriptions of the material.

3. Materials and Methods

The type specimen of *Allosaurus europaeus* ML415 consists of a caudal portion of the articulated skull, one fragment of the occipital condyle, three articulated cervical vertebrae, and several cervical ribs. In order to thoroughly study the specimen while minimizing the risk of damage, three 3D models of the fragile and heavy fossils (the skull and vertebrae) were created from photographs and using Agisoft Metashape 1.8.5 and 2.0.1 software. Canon EOS 450D and Nikon D3300 cameras were used with light rings to produce images for the 3D models.

The articulated vertebrae are almost fully exposed, and most of the contacts between the bones are all visible, so no further preparation was necessary. Despite the fact that all bone contacts of the skull were fully displayed in lateral view, this is not the case on the medial side, where the braincase was difficult to observe, whereas the medial and dorsal sides were broken, and its lateral left surface must be better preserved within the matrix as well as the pterygoid, ectopterygoid, and quadrate, which is also the case on the medial side of the lacrimal, jugal, postorbital, quadratojugal, and squamosal bones.

For general placement of *Allosaurus europaeus* ML415, two phylogenetic analyses were conducted, using the dataset by Eddy and Clarke, 2011 [30], which includes a total of 177 characters and 24 taxa (the original 22 plus ML415 and *Allosaurus jimmadseni*), as well as 51 characters from Carrano et al.'s dataset [2] that were added because they were informative to resolve the part of the tree that includes *Allosaurus* (plus *A. europaeus* and

A.jimmadseni). The final matrices and character list can be found at https://morphobank. org/permalink/?P5203, accessed on 1 May 2024.

A second analysis was conducted on *Allosaurus* using a new matrix that included only seven taxa. *Sinraptor dongi* Currie and Zhao 1994 was used as the outgroup. The analysis also included *Neovenator salerii* Hutt et al., 1996, *Allosaurus europaeus* ML415, *Allosaurus fragilis* USNM 4734 (neotype), *Allosaurus jimmadseni* (holotype and paratype), *Allosaurus* DINO 2560 [12], and the *Allosaurus* from Andrés (MNHNUL/AND.001, Portugal). This analysis utilized 48 characters that may be relevant to *Allosaurus*: 14 new ones (see the New Restricted Phylogenetic Analysis for *Allosaurus* Section), 4 taken from Carrano et al., 2012 [2], 24 from Eddy and Clarke, 2011 [30], and 6 are the "autapomorphies" provided by Chure and Loewen, 2020 [3]. Characters from other matrices that were not in-group-informative were not included. See the table with matrix and character lists in phylogeny restricted to *Allosaurus*, available at: https://morphobank.org/permalink/?P5203 (accessed on 1 May 2024).

The analysis was conducted using TNT 1.6 Beta, which is freely available at: www.lillo. org.ar/phylogeny/tnt/ (accessed on 1 May 2024) [31]. A heuristic search was performed, starting with 1000 replications of the Wagner tree, followed by TBR, retaining 10 trees per replication, with 10 random seeds. All characters were treated and assigned equal weight.

4. Systematic Paleontology

<div align="center">

Dinosauria Owen, 1842

Saurischia Seeley, 1887

Theropoda Marsh, 1881

Neotheropoda Bakker, 1986

Tetanurae Gauthier, 1986

Avetheropoda Paul, 1988

Carnosauria Huene, 1920

Allosauroidea Currie and Zhao, 1994

Allosauridae Marsh, 1878

Allosaurus Marsh, 1877

Allosaurus europaeus Mateus et al., 2006

</div>

Holotype: ML415 is comprised of two blocks and several separated fragments. The first block contains a partially articulated skull, with most of the left posterior bones preserved and part of the atlanto-axis complex, including three teeth. The fragments consist of one disarticulated angular, one articulated lacrimal bone with small pieces of nasal and maxilla, and several disarticulated rib fragments. The second block consists of three cervical vertebrae and their respective articulated left cervical ribs (Figure 2).

Type locality: Praia de Vale Frades, Lourinhã Municipality, central-west Portugal (ca. 39.27° N, 9.33° W).

Type horizon: Lourinhã Formation. The specific area from which the fossil was obtained is uncertain, but it is believed to be from either the uppermost light-grey medium-sandstone body at the top of the Praia Azul Member or the base of the Santa Rita Member. These levels differ by approximately five meters between them.

Age: Early Tithonian, Late Jurassic.

Revised diagnosis: *Allosaurus europaeus* exhibits the following unique set of characters (numbered as "Ch." after the second phylogeny analysis below, see Figure 3):

1. Lacrimal anterior projections contacting nasally, posteriorly, ventrally, and dorsally (i.e., the lateroposterior tip of the nasal projection projects ventrally to the lacrimal dorsoanterior projection; Ch. 1).

2. Lacrimal ventral ramus, lateroanterior vertical projection, restricted to the dorsal half of the antorbital fenestra (aof), and not continuous to the medial vertical ridge that borders the aof (Ch. 3).

3. Pterygoid contact with the quadrate ventral shelf of the pterygoid flange, with participation of the pterygoid in the fold that constitutes the shelf (Ch. 6; see Hendrickx et al., 2015 [32] for quadrate topology).

4. Pterygoid contact with the ectopterygoid, with prominent ventral projection and anterior notch (Ch. 7).

5. The maxilla ventroposterior end is step-like (nearly vertical contact; Ch. 8).

6. Postorbital, ventral termination of ventral ramus close to the ventral margin of the orbit and ventral to squamosal–quadratojugal contact (plesiomorphic, shared with *Sinraptor*, but is a local autapomorphy different from other *Allosaurus*; Ch. 10).

7. Cervical vertebrae, position of parapophyses on the centrum in the middle (Ch. 43; shared with *Neovenator*; Ch. 41).

8. Fourth and fifth cervical vertebrae, latero-anterior base of the neural spine with oblique-to-vertical subtle accessory lamina at the posterior end of the spinoprezygapophyseal lamina (best seen in lateral–dorsal views; Ch. 45).

9. Shape of postorbital contact with jugal sigmoidal bone (Ch. 46).
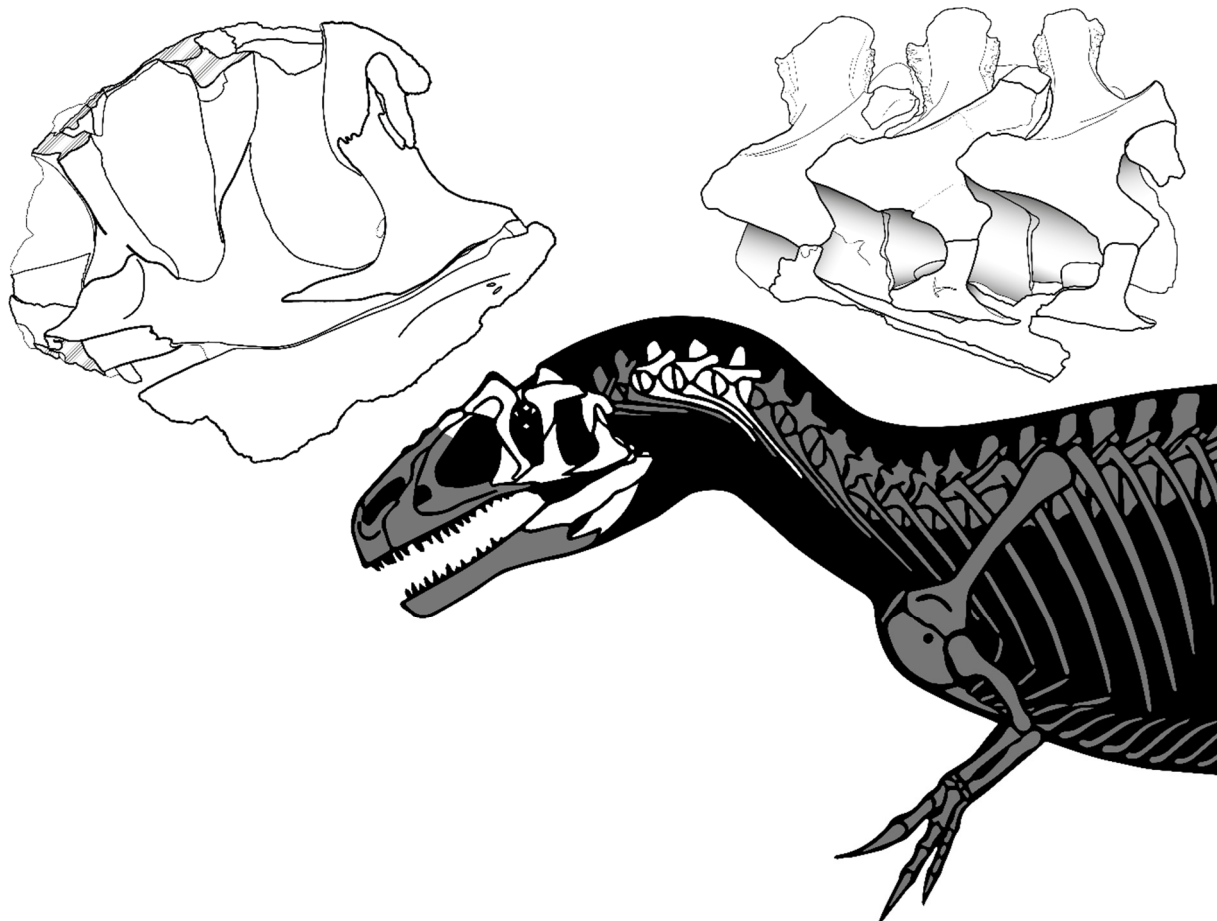
Figure 2. *Allosaurus europaeus* holotype ML415, found material.

Differentia (differential diagnosis): *Allosaurus europaeus* differs from *Allosaurus fragilis* in the pinched crest present on the dorsolateral edge of the nasal bone, in the very pronounced lacrimal horns (20% or more of the height in lateral view), in the sizes of the nasal pneumatic foramina (posterior larger than anterior), and in the very small accessory laminae present in the 4th and 5th cervical vertebrae.
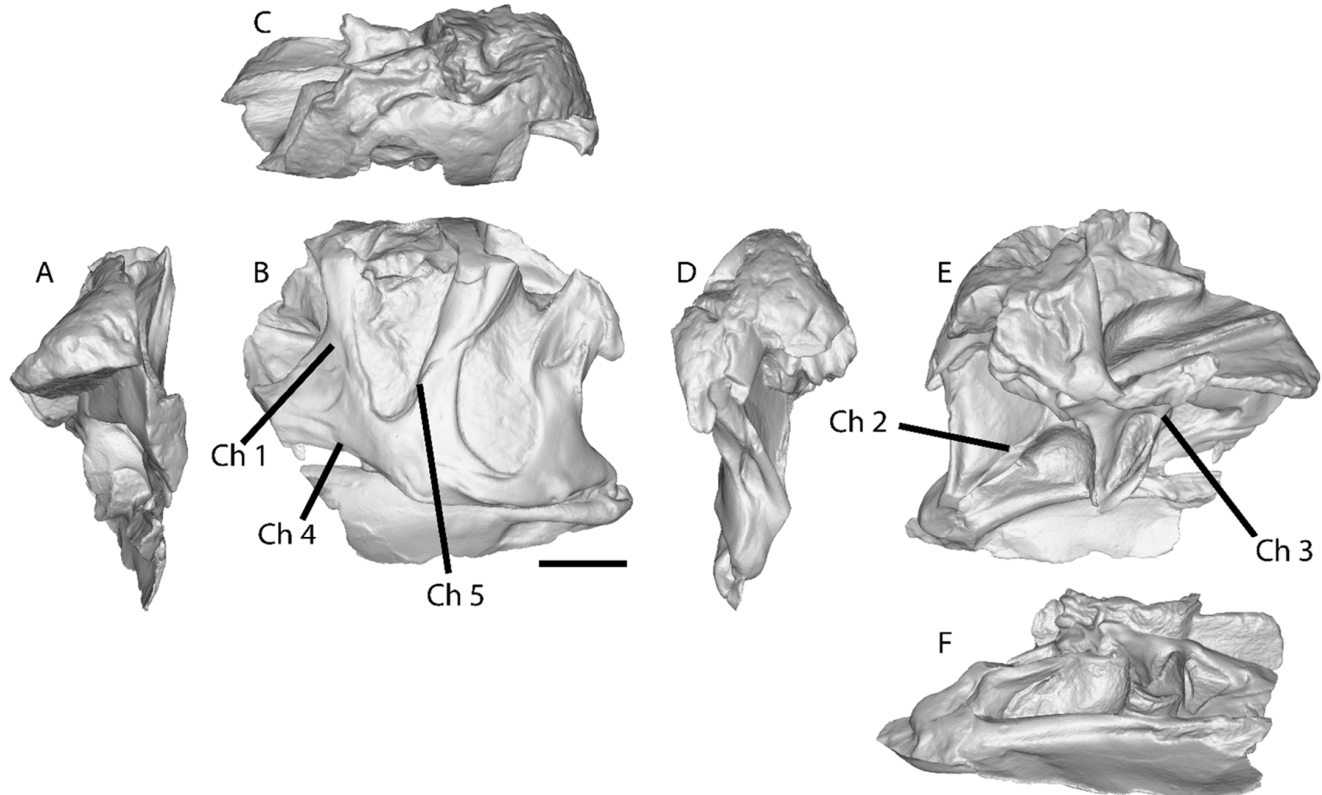
Allosaurus europaeus differs from *Allosaurus jimmadseni* in its curved jugal ventral margin, its sigmoidal jugal, and in the number of surangular posterior foramina.

Allosaurus europaeus differs from both *A. fragilis* and *A. jimmadseni* in its step-like maxilla ventroposterior end, in the lacrimal portion overlapping the nasal bone dorsally (when compared with DINO 2560, not preserved in USNM 4734), in the interrupted lacrimal latero-anterior vertical projection, in the postorbital sigmoidal contact with the jugal bone, in the ectopterygoid projection of the pterygoid (when compared with DINO 2560), and in the contribution of the pterygoid in the quadrate pterygoid flange fold (when compared with DINO 2560).

5. Description

5.1. General Description of the Skull and Mandible

The skull (Figure 3) was found in a sub-rectangular block that had been shaped and cut by modern erosion by the wind and sea. The dorsal surface, as well as the anterior surfaces of the palatines and pterygoids, have been lost due to erosion, but it is still possible to see the original outlines in the eroded surface. Around one-quarter of the articulated skull is preserved and in good condition, but it is broken and almost split in half from the medial axis and the snout. Most of the left side of the cheek region of the skull and some additional bones are present. This includes almost all bones of the dermatocranium from the left side, except the vomer, most of the chondrocranium, and some bones of the splanchnocranium and lower jaw. Although the cervical vertebrae are deformed, much of the skull appears intact, apart from a few bones, which will be further emphasized. The majority of the bones are exposed, but many of their surfaces are still covered by matrix or contacts. It is possible that entire bones are still hidden within it.

Figure 3. *Allosaurus europaeus* posterior portion of the skull ML415, (**A**) anterior view, (**B**) lateral view, (**C**) dorsal view, (**D**) posterior view, (**E**) medial view, and (**F**) ventral view. Ch. 1 to 5 indicate the phylogenetic characters 1 to 5, as indicated in Section 7.3. The 3D model of the skull: scale bar 10 cm.

In general, most contacts between bones are well defined and are not fused, making the task of contouring the bones easier. However, the areas where bones meet the broken surface are not so well defined, and some contacts are stained with old glue that has aged poorly, obtaining the same color as the surface where it was applied. This makes it difficult to distinguish sediment with oxidized iron from some of the bones. It is important to note that the interpretation of bones in this work, including their shape and description, was based on hours of work, visualizing the remains, and observing the 3D models and photographs, as well as comparing them to a casts, photographs, and drawings of *A. fragilis* and *A. jimmadseni*. It is possible that this interpretation may change in the future.

5.1.1. Major Cranial Fenestrae, Foramina, and Fossae

Here, most of the preserved major cranial fenestrae and fossae are described. However, some are present in the skull but poorly preserved and are too fragmented to deserve a detailed description, so they are not described in detail. These fenestrae and fossae are the anterior margin of supratemporal fossa, the foramen magnum (which has some matrix filling), and the dorsal margin of the external mandibular fenestra.

Antorbital fossa: Only two small portions of the antorbital fossa are preserved in ML415. The left is restricted to the posterior and ventral margins in the main skull, and the right to the dorsal margin of the right lacrimal bone.

The limit of left antorbital fossa is marked as a low, subtle ridge of the lacrimal ventral ramus and pneumatic recess of the jugal bone. The remain of this fossa presents a rounded "L" shape. The right antorbital fossa is restricted to the nasal dorsal rim and the lacrimal vacuity. The flexion between the lacrimal anterior ramus and its ventral ramus creates an acute angle of the fossa. This angle has a high intraspecific variability [33].

Since it is poorly preserved, we cannot assess its entire shape; nevertheless, by combining both fossae and according to previous reconstructions [3,10], it may suggest that it does not look so different in shape compared to other *Allosaurus* species. However, the ridge that delineates this fossa, as previously mentioned, is far less pronounced in this specimen compared to other *Allosaurus* species, creating a shallower fossa in the contact between the lacrimal and jugal bones.

Antorbital fenestra: Similar to the antorbital fossa, only the posterior and part of the ventral margins of the left antorbital fenestra and part of the dorsal margin of the right antorbital fenestra are preserved. By looking at the angle of these margins, it is indicated that these fenestrae would be large. The left has the shape of one-quarter of a circle, and the right has a similar shape to its corresponding antorbital fossa with an acute angle.

In line with the antorbital fossae, the analysis of the shape of the antorbital fenestrae was not feasible, but through the integration of both extant fenestrae and the observation of prior specimen reconstructions, we inferred that its morphology remained consistent with that of other *Allosaurus* species [3].

Orbital fenestra: The left orbital fenestra is almost complete, with only the dorsal margin missing in the ML415 specimen, and it is still filled with sediment. It is mostly marked by the lacrimal, jugal, and postorbital bones in its anterior, ventral, and dorsal margins, respectively. The orbit has an oval or elliptical shape, being dorsal-ventrally taller than the anterior–posterior border.

The shape of the orbit does not differ from other *Allosaurus* species. The ventral margin differs from others *Allosaurus* species by having contributions to the ventral ramus of both the lacrimal and postorbital bones.

The sclerotic ring can be found within the sediment of the orbit on its dorsal region. Despite that the ring presents a good preservation, some sclerotic elements are broken, and the ring has collapsed on itself with all the sclerotic elements squeezed together, rearranged in anterior–posterior orientation. These elements have a sub-rectangular shape and there are at least fourteen, which probably represent two quadrants of the sclerotic ring [3].

The position of the ring indicates that the eye would be in the similar position as other *Allosaurus* species in the dorsal-most part of the orbit [3,34].

Supratemporal fenestra: Only the left supratemporal fenestra is preserved in the specimen. This fenestra is broken in the dorsal and lateral regions bordered by the frontal, parietal, and squamosal bones, anteriorly, medially, and posteriorly, respectively. The incomplete fenestra almost has a sub-rectangular shape, but this may be due to the fact that it is fragmented, since all species of this genus have a sub-oval shape [3,12,35].

Lateral temporal fenestra: The left lateral temporal fenestra is broken in its dorsal region, being only bordered by the postorbital, jugal, quadratojugal, and squamosal bones. Half of the anterior margins are formed by the postorbital bone, dorsally, and jugal bone, ventrally, while half of the ventral margins are formed by the jugal bone, anteriorly, and the other half by the quadratojugal bone, posteriorly. The dorsal half of the posterior margin is composed of the squamosal bone, while the ventral half is formed by the quadratojugal bone. This fenestra has a squeezed and elongated sub-oval shape due to the tightening arising from the ventral process of the squamosal bone overlapping with the anterior aspect of the dorsal process of the quadratojugal bone.

The lateral temporal fenestra in *Allosaurus europaeus* is similar in shape to the fenestra of *A. fragilis* specimen USNM 4734 and appears to differ from *A. jimmadseni* and *A. fragilis* specimen DINO 2560, being more elongated. This difference between the two *A. fragilis* specimens may be due to the distortion and missing elements of the skull of USNM 4734.

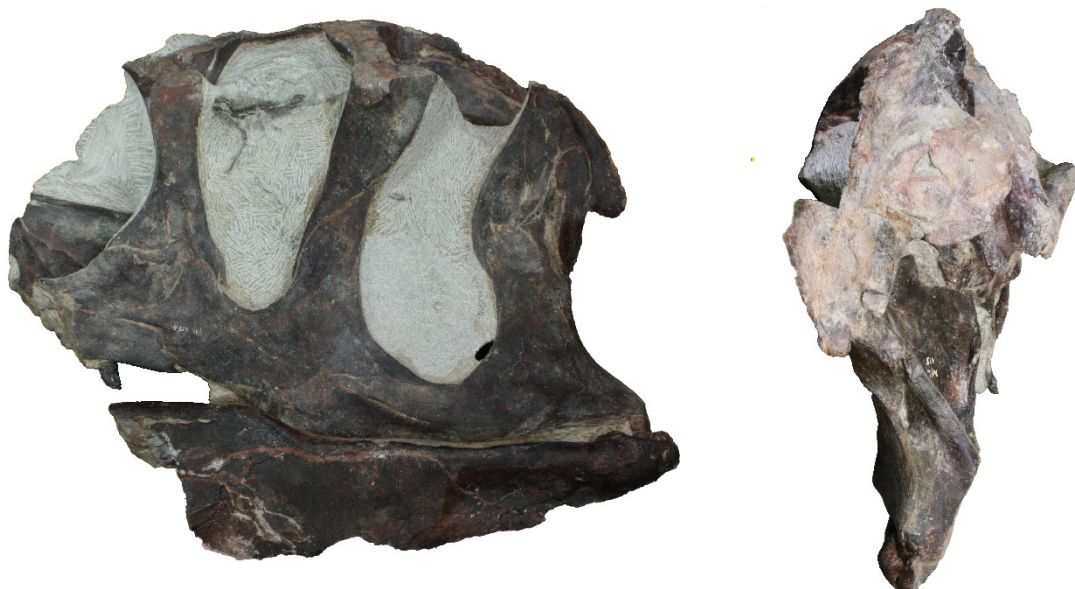Cranial bones are depicted in Figures 3–17.

Figure 4. *Cont.*

Figure 4. *Allosaurus europaeus* ML415 skull in lateral, posterior, medial, and anterior view, respectively. Scale: 10 cm.

5.1.2. Bones of the Dermatocranium

Maxillae: The specimen contains two fragments of two maxillae (Figures 3–9). The dorsal ramus posterior end of the right maxilla and the posterior body with three teeth of the left maxilla are preserved. The bones are almost entirely exposed, except for the contact surfaces.

For the left maxilla in medial view, two teeth are visible on its ventral margin. One of the teeth is complete and represents the last tooth of the maxilla. The other tooth is the second to last and is partially preserved, revealing only a small portion of its base, along with at least one interdental plate. Moving along this view, the maxilla has a triangular shape. Its posterior tip bends ventrally and posteriorly, reaching the hock process of the ectopterygoid. The dorsal margin of the structure makes contact with the palatine. A groove filled with sediment is present anteriorly to this contact.

The left maxilla, in the anterior view, displays an almost parasagittal section of the second tooth, and a third tooth is still in the process of emerging. The maxilla is 6.7 cm-long and 2.6 cm in height. The maxilla articulates with the jugal bone in a step-like outline.

The posterior terminus of the ascending ramus of the right maxilla articulates with the nasal bone in the dorsal direction and with the lacrimal bone in the posterior direction.

The articulation with the lacrimal bone is truncated and bifurcated, while the contact with the nasal bone is more linear, resembling a straight-bar contact. The maxilla has a sub-rectangular shape, oriented in a posterior–anterior direction. The body is fully encapsulated in the antorbital fossa, and the ventral margin participates in the antorbital fenestra. When viewed from the anterior view, the maxilla exhibits a profile reminiscent of an hourglass, with thicker dorsal and ventral margins and a relatively thinner middle section. The termination of the dorsal ramus of the maxilla of *A. europaeus* is similar to the types of *A. jimmadseni* where the posterior (dorsal portion in lateral view, without the skull roof) is clearly anterior to the nasal posterior end, but differs from DINO 2560, where it is at the same level or close (this is not preserved in USNM 4734). The maxilla also differs from *Sinraptor dongi* (IVPP 10600) [36], *A. fragilis* (USNM 4734 and DINO 2560), and *A. jimmadseni* (DINO 11541 and MOR 693) in the maxilla–jugal articulation, where it displays a step-like outline rather than acute/tapering.
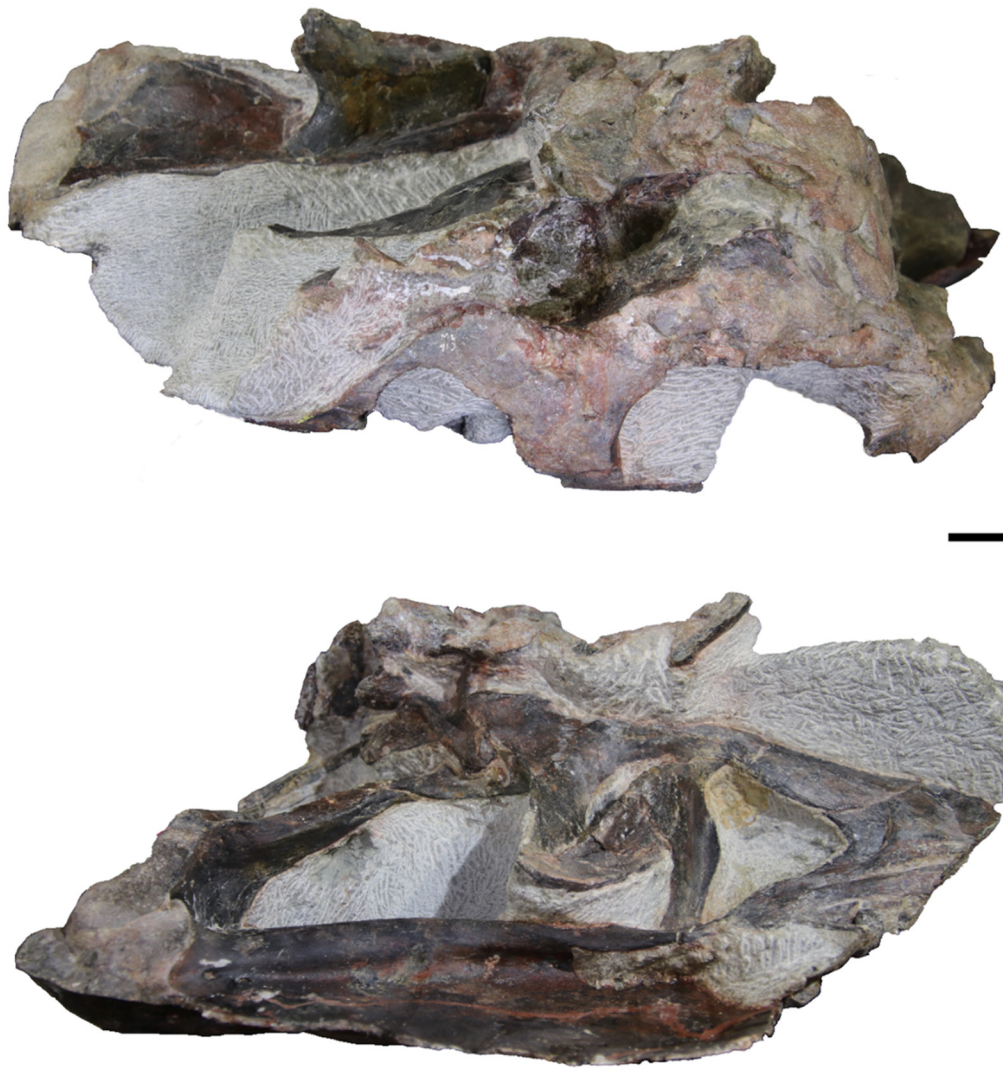
Figure 5. *Allosaurus europaeus* ML415 skull dorsal (**top**) and ventral (**bottom**) views, respectively., Scale: 10 cm.

Nasal: The nasal bone (Figures 6–8) is partially preserved, with only the posterior portion intact, while the medial and anterior portions are fractured. It is fully exposed, except for the ventral margin of the lateral side and part of the lateral–posterior margin, where it articulates with the ascending ramus of the maxilla and the lacrimal crest, respectively.

In anterior view, the nasal bone appears as a broad sheet that curves laterally to form a crest. In the lateral view, the nasal crest is more prominent and originates immediately after the junction with the lacrimal bone; when viewed dorsally, it almost merges with the lacrimal bone, into a single crest. Further, anteriorly, in lateral view, the nasal bone curves slightly medially to participate in what remains of the antorbital fossa. In this area, anteriorly, two pneumatic foramina are present, with different sizes. The posterior foramen has a sub-rectangular shape, while the anterior foramen is sub-triangular in shape. The ascending process of the maxilla prevents the nasal bone from bordering the antorbital fenestra. The nasal bone expands medially and posteriorly in dorsal view. The medial expansion would contact the right nasal, while the posterior expansion would contact the frontal. *Allosaurus europaeus* shares, with *A. jimmadseni* but not with *A. fragilis*, the presence of a tall parasagittal crest on the dorsolateral edge of the nasal bone, rather than pronounced dorsolateral rims. We assume, since due to the anterior cut of the nasal bone, the crest is still visible, that this crest was continuous up to the premaxilla. It also differs

from *A. fragilis* in the pneumatic foramina sizes, where the posterior is larger than the anterior, rather than the other way around. The nasal posterior termination in DINO 2560 differs from the rest, as previously mentioned, due to the fact that it ends at the same level or close to the posterior termination of the dorsal ramus of the maxilla.
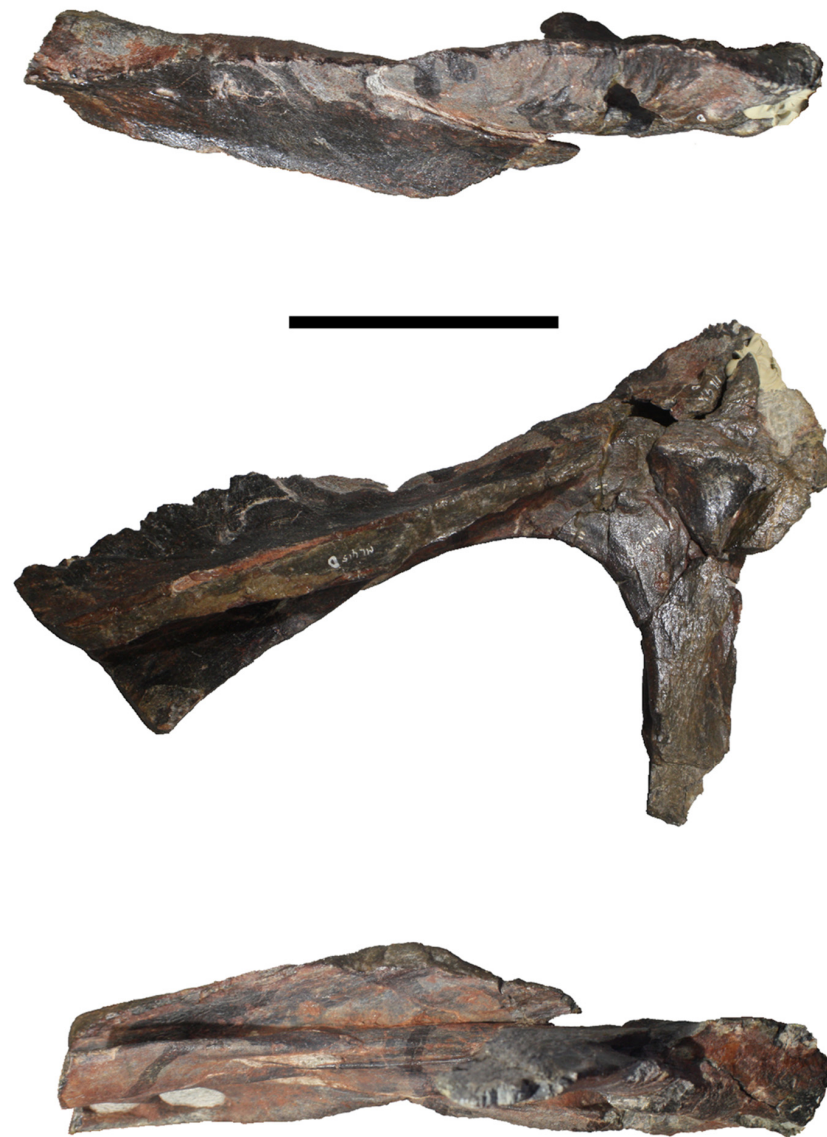

Figure 6. *Allosaurus europaeus* ML415 lacrimal bone articulated, respectively, with nasal and maxilla posterior ramus in posterior, lateral, and anterior views. Scale: 10 cm.

Lacrimal bones: The lacrimal bones (Figures 3–9) are present in the form of two fragments, one from the left lacrimal bone and one from the right lacrimal bone. Both lacrimal bones are broken, the right ventrally and the left dorsally. The vacuity of the right lacrimal bone is still partially hidden by the matrix, but the rest is fully exposed. The left lacrimal bone is exposed laterally, dorsally, and a bit anteriorly, with the rest still concealed by the matrix. The lacrimal crest of the right is slightly broken posteriorly and presents a pneumatic fossa in the middle of the lateral side.

The left lacrimal bone is represented by a ventral process that is still articulated to the skull. It has a smooth, thin, hourglass shape. Most of the ventral process contributes to the posterior margin of the antorbital fenestra as well as the anterior margin of the orbital fenestra, of which the latter is entirely composed of it. This happens due a long posterior process of this ramus that isolates the jugal bone from this margin.

The right lacrimal bone consists of an anterior process featuring a lacrimal crest and a small segment of the descending ramus. The posterior processes of the nasal bone and maxilla are still articulated to it. The anterior process attains its maximum length ventrally, measuring approximately 13 cm from the base of the descending ramus. This process terminates between the bifurcated ascending process of the maxilla anteriorly, while establishing dorsal contact with the nasal bone. The lacrimal crest ends posteriorly to this process, while also overlapping the nasal bone dorsally. The ventral process is not extended considerably ventrally due to a ventral fracture. Instead, it is reduced to a slim rectangular projection.

The lacrimal bone differs from *A. fragilis* (USNM 4734 and DINO 2560) and *A. jimmadseni* (DINO 11541 and MOR 693) in the ridge, limiting the antorbital fossa, where it is not continuous when it meets this ridge in the jugal bone, rather than a single continuous ridge.

Figure 7. *Allosaurus europaeus* ML415 dorsal, medial, and ventral views, respectively, of the right lacrimal, maxilla and lacrimal bones. Scale: 10 cm.

Frontal: Only the left frontal bone (Figures 3–5, 9 and 10) is preserved, broken dorsally and medially with a large posterior portion and two anterior fragments. The dorsal surface of the main body is eroded, cutting the natural surface of the bone. They are all still covered by matrix ventrally, with some surfaces of the small fragments also still hidden medially or laterally. The main body of the frontal bone is still articulated with the postorbital and prefrontal laterally and with the parietal bone and braincase posteriorly (the braincase is medial to the parietal bone). The most posterior small fragment is articulated medially to the short piece of the laterosphenoid and appears scattered within the matrix.

The main body of the frontal bone is a very thin arm anteriorly, which develops into a bulkier bone posteriorly. In the dorsal view, the articulation with the postorbital and parietal bones is truncated, whereas the articulation with the prefrontal bone is straight. In this view, a small foramen is present in the middle of its surface, which is filled with sediment. In the orbital fenestra, the frontal bone has a lateral concave margin, as well as the posterior margin in the supratemporal fenestra and a straight to medially convex medial surface. The lateral–anterior surface is reduced laterally to a very thin, blade-like margin. Posteriorly on the lateral surface, it is possible to see the contact between the parietal bone and the braincase, which is performed in an interdigitated way.

The small pieces are located more anteriorly compared to the main body of the frontal bone. The exposed fragments have a very thin, sheet-like shape. The most posterior fragment is still attached to the laterosphenoid and presents a straight profile. The most anterior fragment bends medially in its dorsal region, with the ventral–medial region represented by thick, sheet-like-shaped bone that shows a striated surface. This may be the contact surface with the right frontal bone, the inter-frontal suture, which is known in other allosauroids to be a posterior interdigitated contact [3].

Parietals: The parietal bones (Figures 3–5, 9 and 10) are broken and reduced to a small portion of the left parietal bone on the dorsal part of the skull. It contacts the frontal bone anteriorly, the braincase medially and ventrally, and the paraoccipital process of the occipital bone posteriorly.

The parietal bone has a sub-rectangular shape, broader antero-posteriorly than laterally–medially. It forms the dorsal lateral posterior margin of the specimen and contributes to the supratemporal fenestra. In this bone, there is a foramen with a posterior groove, which are both filled with sediment, in the lateral view close to the braincase and frontal contact. In comparison to McClelland, 1990 [37], this foramen is possibly the foramen for the vena capitis dorsalis, where in this specimen, the groove is posteriorly shorter, while the singular groove is potentially autapomorphic.
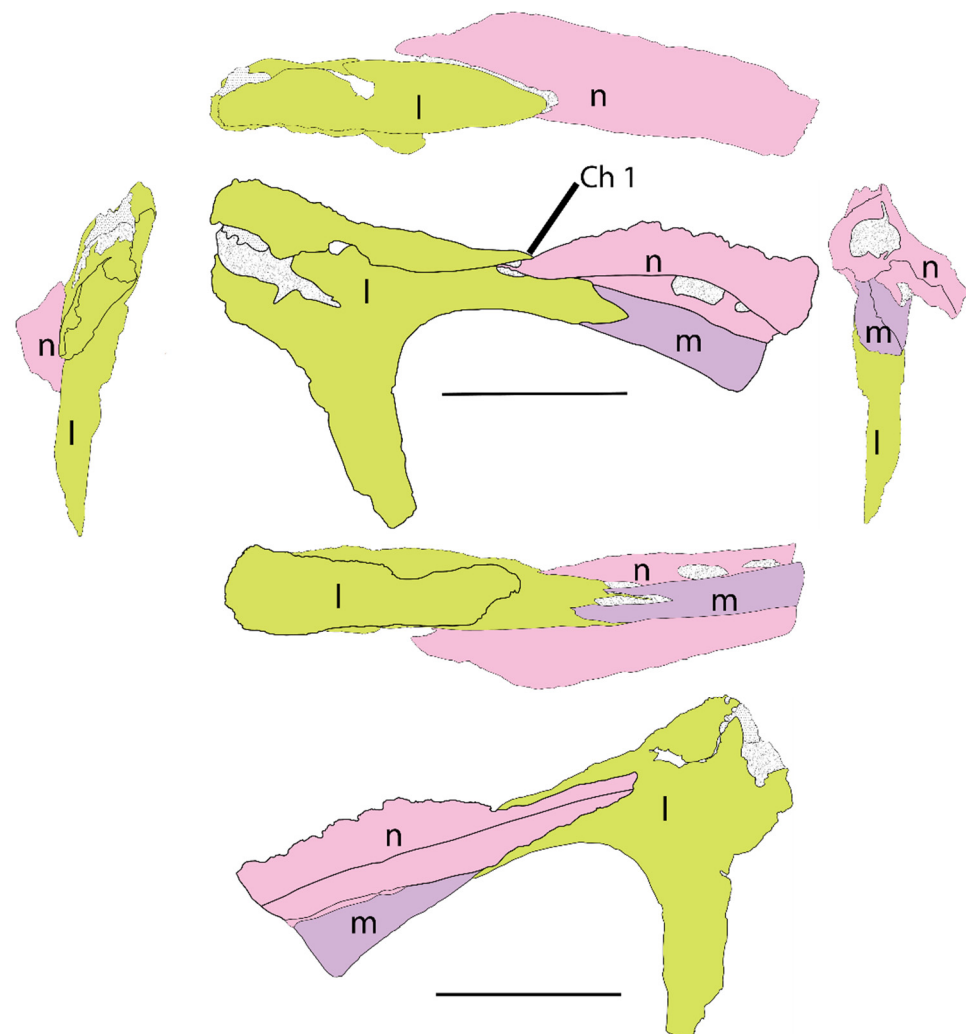
Figure 8. *Allosaurus europaeus* holotype ML415, incomplete right lacrimal, nasal, and maxilla posterior ramus bones in dorsal, posterior, lateral, anterior, ventral, and medial views, respectively. Scale: 10 cm. Osteological abbreviations: l, lacrimal; n nasal; m, maxilla; Ch. 1 indicate the phylogenetic character 1.

Squamosal: The left squamosal bone (Figures 3–5, 9 and 10) is broken dorsally, and it is reduced to its ventral region, where it contacts with the quadratojugal and quadrate bones. It also contacts with the paraoccipital process of the occipital bone medially, only seen in the dorsal view. The lateral surface is the most exposed surface, as most of the medial region is still covered in matrix. The fractured surface of the dorsal region is difficult to observe, as it is covered by an aged orange glue as well as the sediments, so that its perimeter is only visible by scraping with a tungsten pen. For this reason, it is difficult to tell if it contacts the parietal bone, but it does not appear to do so.

On the lateral view, the squamosal bone contacts the quadratojugal bone ventrally in the interdigitated format, as mentioned above, although anterior to this contact, there is a curved ventral process that excludes, anteriorly, the dorsal tip of the dorsal ramus of the quadratojugal bone from the lateral temporal fenestra. This ventral contact is performed in a straight way. The squamosal bone contributes to most of the posterior margin of the lateral temporal fenestra. Dorsal–posteriorly, the squamosal bone widens ventrally into the post-cotyloid process, which has a sub-circular-shaped tip and envelops the quadrate head.

In the dorsal view, the squamosal bone has a triangular shape, being wider anteriorly and tapering posteriorly.

Postorbital: The postorbital bone (Figures 3–5, 9 and 10) is eroded dorsally, with only the ventral process remaining, which is fully exposed laterally. The postorbital bone articulates with the frontal bone medially and forms a sigmoidal slight lap joint with the jugal bone ventrally. On the eroded dorsal surface, suture with the frontal bone is still visible, which presents a deep concave profile.

In lateral view, the ventral process of the postorbital bone extends anteroventrally along the dorsal process of the jugal bone, forming most of the posterior wall of the orbit. The posteroventral process forms a sigmoidal, comma-like posterior profile, producing a narrow tip. There is some evidence of light postorbital ornamentation directly behind the position of the eye, but this is largely eroded. The postorbital bone differs from *A. fragilis* (USNM 4734 and DINO 2560) and *A. jimmadseni* (DINO 11541 and MOR 693) in its ventral region, excluding most of the jugal bone from the posterior portion of the orbit, and it also differs from *Sinraptor dongi* (IVPP 10600) [36] and other *Allosaurus* species in its sigmoidal postorbital–jugal contact (rather than straight).

Jugal: The left jugal (Figures 3, 4 and 9) bone is mostly visible in its lateral view and remains fully articulated, maintaining contacts with the maxilla, quadratojugal, postorbital, and lacrimal bones. Most of these contacts are well preserved and observable, except for the medial contacts, which are concealed within the matrix. The hidden areas within the matrix include at least the medial contacts of the lacrimal and postorbital bones.

The jugal bone presents a dorsal ramus that connects to the ventral ramus of the postorbital bone. It also has two posterior projections designed to accommodate the quadratojugal bone. Additionally, it features an anterior sheet-like extension with a pneumatic recess.

The ventral posterior projection of the ventral posterior prong extends beyond the boundaries of the lateral temporal fenestra and almost contacts the quadrate.

The jugal bone contributes ventro–posteriorly to the antorbital fossa and fenestra. This was originally interpreted as a unique feature of *A. europaeus*; however, later interpretations contest that all species share this feature and that it was misinterpreted in previous descriptions [11]. The jugal bone also encloses the ventral and a small portion of the posterior margin of the orbital fenestra, as well as half of the anterior and approximately two-thirds of the ventral margin of the lateral temporal fenestra.

The preserved and visible contact between the jugal bone and maxilla occurs along the ventral surface of the jugal anterior projection and in a small anterior contact on the main body of the jugal bone. The contact in ML415 differs from the pattern observed in other

Allosaurus species, which is characterized by acute demarcation. In ML415, the demarcation is notably more step-like.

In terms of overall morphology, the jugal bone closely resembles the jugal bone observed in other species of *Allosaurus*, particularly resembling the jugal bone of *A. fragilis*, which both share the ventral curved outline [38].
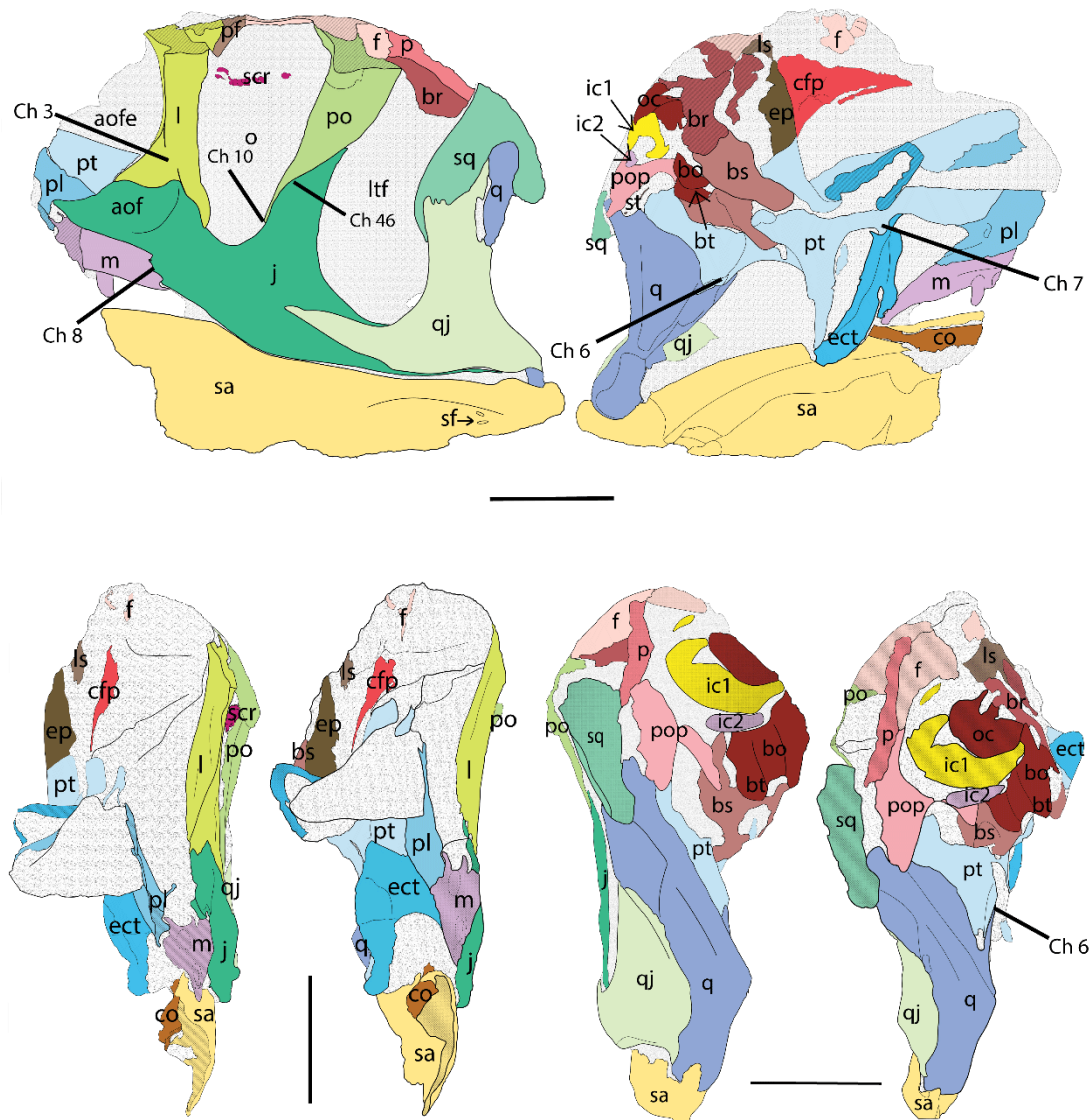
Figure 9. *Allosaurus europaeus* skull ML415, in lateral (**upper left**), medial (**upper right**), anterior (**lower left**), and posterior (**lower right**) views. Osteological abbreviations: aof, antorbital fossa; aofe, antorbital fenestra; bo, basioccipital; bs, basisphenoid; bt, basal tubera; br, braincase (including prootic); cfp, cultriform process of the parasphenoid; co, coronoid; ect, ectopterygoid; ep, epipterygoid; f, frontal; j, jugal; l, lacrimal; ls, laterosphenoid; ic1 and 2, intercentrum of atlas-axis; m, maxilla; o, orbit; oc, occipital condyle; p, parietal; pf, prefrontal; pl, palatine; po, postorbital; pop, paraoccipital process of the otoccipital; pt, pterygoid; q, quadrate; qj, quadratojugal; sa, surangular; sf, surangular foramina; sq, squamosal; st, stapes; ltf, laterotemporal fenestra; scr, sclerotic ring; Ch. indicate the phylogenetic character number. Scale bar equals 10 cm.

Quadratojugal: The left quadratojugal bone (Figures 3, 4 and 9) is fully exposed laterally, while medially it is mostly concealed by the quadrate contact or by matrix. In medial view, only part of the base of the anterior ramus is visible. In lateral view, the quadrate bone articulates to the jugal bone anteriorly and ventrally, the squamosal bone dorsally, and the quadrate bone posteriorly and medially.

The quadratojugal bone takes on a roughly boot-like or "L" shape in lateral view. The anterior process of the quadratojugal bone is notably elongated, extending to the midpoint axis of the postorbital ventral process. Little of the anterior process contributes to the ventral margin of the lateral temporal fenestra. The dorsal surface that forms the contact with the squamosal bone is ribbed and features a groove. Within this contact, at the posterior end of the dorsal surface, the quadratojugal bone presents a dorsal process that separates a considerable portion of the ascending ramus of the quadrate from the squamosal bone. This process establishes the dorsal–posterior contact with the quadrate bone, and its posterior view remains obscured by sediment. The quadratojugal bone forms the "L" shape in lateral view that is common in basal theropods and lacks a posterior process. The quadratojugal bone is similar to the condition found in *A. fragilis* and *A. jimmadseni*.
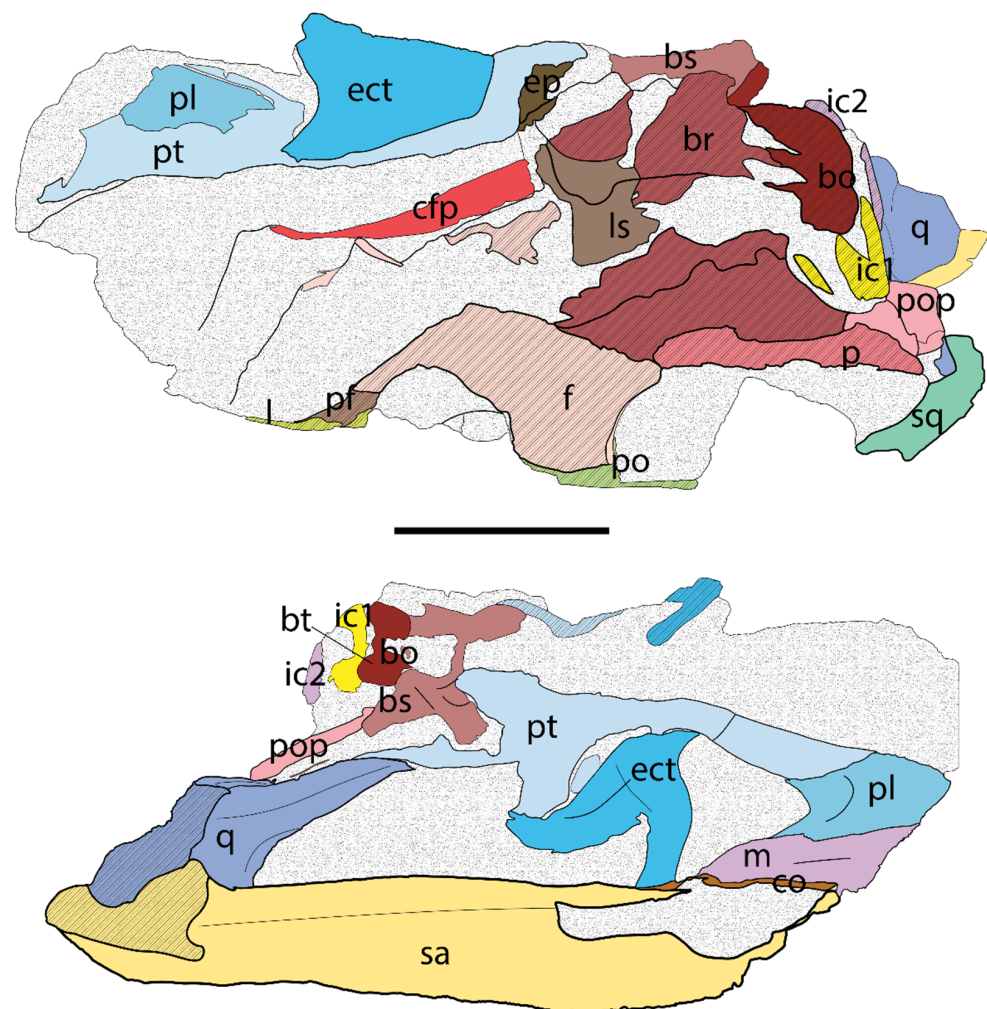

Figure 10. *Allosaurus europaeus* skull ML415, in dorsal (**upper**) and ventral (**lower**) views. Osteological abbreviations: bo, basioccipital; bs, basisphenoid; bt, basal tubera; br, braincase (including prootic); cfp, cultriform process of the parasphenoid; co, coronoid; ect, ectopterygoid; f, frontal; l, lacrimal; ls, laterosphenoid; ic1 and 2, intercentrum of atlas-axis; m, maxilla; p, parietal; pl, palatine; po, postorbital; pop, paraoccipital process of the otoccipital; pt, pterygoid; pf, prefrontal; q, quadrate; sa, surangular; sq, squamosal. Scale bar equals 10 cm.

Ectopterygoids: The ectopterygoid bones (Figures 3–5, 9 and 10) are both preserved but not fully exposed. Although the left ectopterygoid bone is relatively intact, despite several medial fractures, it is not fully exposed due to matrix obstruction on its lateral side. Both ectopterygoid bones remain in articulation with their respective pterygoids. In contrast, the right ectopterygoid bone is laterally fractured and deformed upwards,

resulting in its placement in a relatively posterior position compared to its left counterpart. This positioning causes a lack of symmetry between the two ectopterygoid bones.

The left ectopterygoid bone is oriented almost vertically and has a lateral hook process that runs ventrally and contacts the maxilla and jugal bone laterally. The main body contacts the pterygoid ventrally and overlaps the small ectopterygoid process of the pterygoid bone laterally at its dorsal tip. In the dorsal view, the right ectopterygoid bone shows a trapezoid outline with a concave anterior margin. In the medial view, it is still possible to observe the hook-shape process that would contact the right maxilla and jugal bone. The dorsal surface has a concave profile, which may be a result of the lithostatic deformation that the bone has suffered.
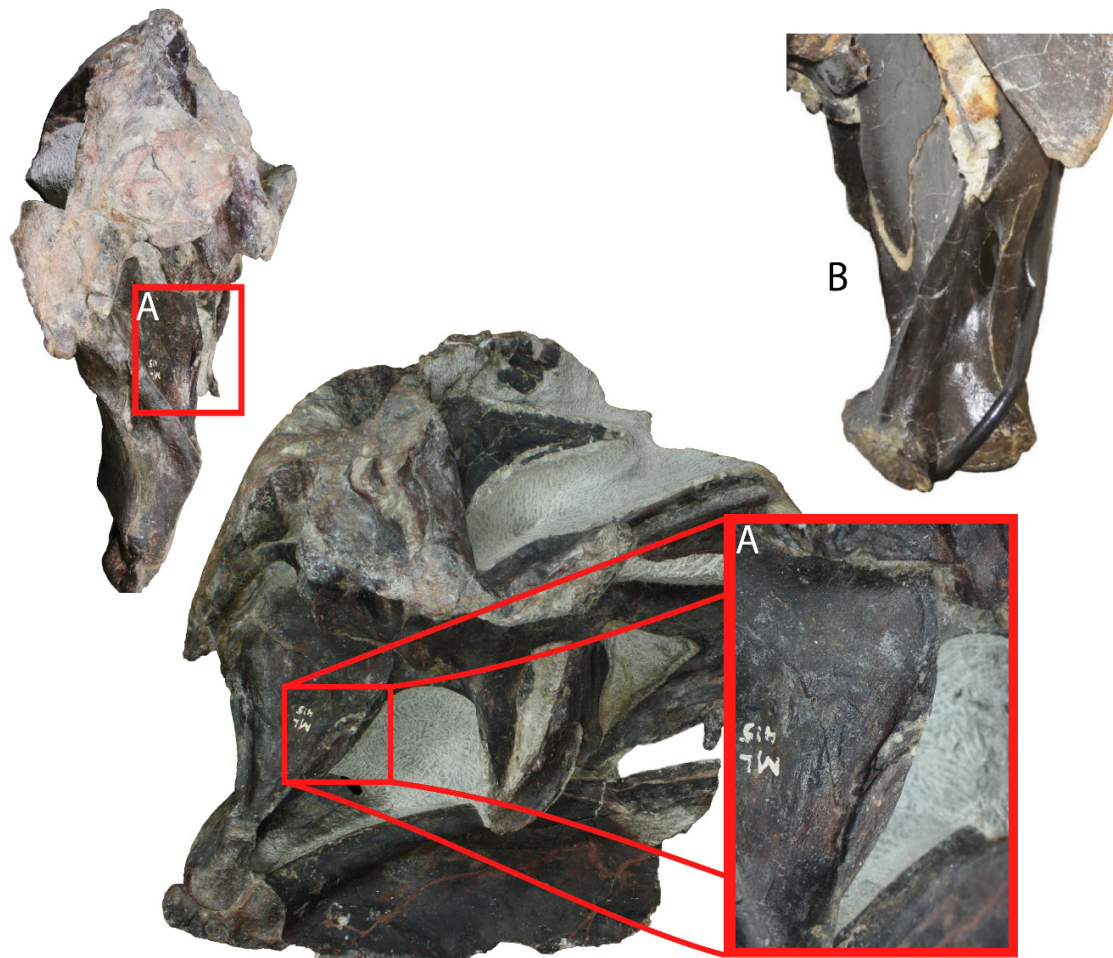
Figure 11. (**A**) *Allosaurus europaeus* ML415 quadrate shelf with pterygoid contribution in posterior and medial view. (**B**) Quadrate and pterygoid bone contact, with no contribution of the pterygoid bone to the quadrate shelf in *Allosaurus jimmadseni* paratype MOR 693 in posterior view, modified from [3].

Pterygoids: The pterygoid bones (Figures 3–5 and 11–15) are preserved from both the left and right sides, but their conditions differ. The left pterygoid bone is almost complete, apart from the palatal process, which is broken anteriorly. The right pterygoid bone is extensively fractured in various directions, except for the medial aspect, and it is mostly encompassed by the palatal process. The right pterygoid bone shows a lateral deformity, slightly elevated dorsally compared to the left pterygoid bone. This pterygoid bone is not exposed in its medial view, whereas the left pterygoid bone is not fully exposed in its lateral side, revealing only a portion of the anterior process, which articulates with the palatine bone.

The right pterygoid bone also articulates with the ectopterygoid and epipterygoid bones. It presents a triangular sheet-like shape, best seen in dorsal view, which expands anteriorly and tapers posteriorly, forming a concave profile dorsally into a lateral–dorsal ridge. Toward the posterior and lateral regions, the right pterygoid bone, in comparison with the left pterygoid bone, would have an expansion that would develop into the quadrate wing, which is broken, but still shows an observable contact with the basipterygoid process of the basisphenoid bone. Anteriorly and ventrally, the right pterygoid bone articulates with a small fragment of the right palatine bone.

The left pterygoid bone is a long anterior–posterior tripartite bone that is still fully articulated and contacts the quadrate, basisphenoid, ectopterygoid, and palatine bones. In the medial view, the palatal process has a machete-like shape with a convex anterior–ventral edge. Proceeding posteriorly, it develops a ventral concave process, partially covered by matrix, which contacts the ectopterygoid bone medially. This concave region corresponds to the ectopterygoid recess, and a remnant of this bone is present in sediment. Above the ectopterygoid bone, there is a small ventral process that covers the dorsal tip of the ectopterygoid bone, which is not mentioned in other specimens of *Allosaurus* (Figure 12). Posterior to the ectopterygoid process, the pterygoid bone bifurcates into two distinct processes, known as the quadrate wing and the basisphenoid process. Between these processes is an indentation known as the basipterygoid cotylus, which receives the basipterygoid process of the basisphenoid. The basisphenoid process terminates at the base of the basipterygoid process without extending significantly posteriorly. Conversely, the quadrate wing expands into a large sheet that overlaps the pterygoid flange of the quadrate. Along the ventral margin of this wing, there is a ridge that gradually curves posteriorly in a ventral–posterior direction and contributes to the formation of the quadrate shelf (Figures 11 and 15). The pterygoid bones from *A. europaeus* differ other *Allosaurus* species in the contribution of the pterygoid bone in the quadrate flange and the presence of the ventral process, both of which appear to be absent in *A. fragilis* (USNM 4734 and DINO 2560) and *A. jimmadseni* (DINO 11541 and MOR 693).
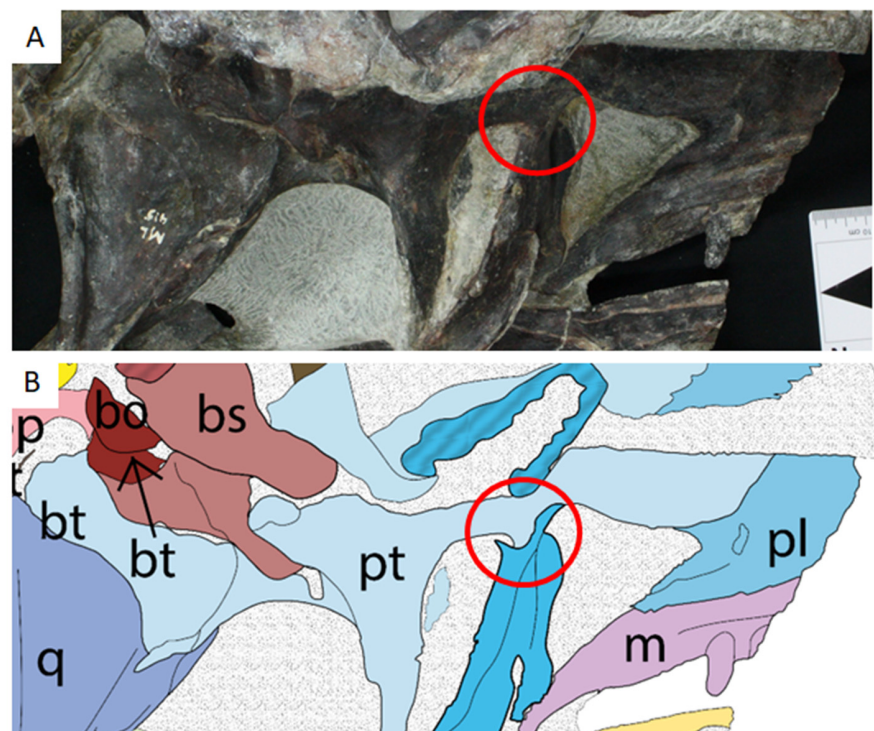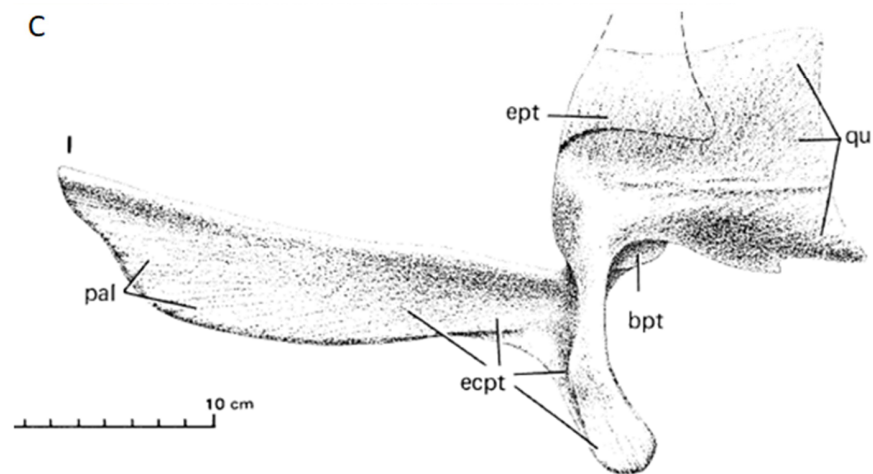

Figure 12. *Cont.*

Figure 12. Ventral ectopterygoid process of the pterygoid bone in *Allosaurus*. (**A**) Pterygoid bone from the medial view of *Allosaurus europaeus* ML415. (**B**) Drawing of the pterygoid bone medial view from *Allosaurus europaeus* ML415 from Figure 2. (**C**) compare with the pterygoid bone in lateral view from *A. fragilis* adapted from [12] (Osteological abbreviations: bo, basioccipital; bs, basisphenoid; bt, basal tubera; bpt, basiopterygoid articulation; ecpt; contact with ectopterygoid; ept, contact with epipterygoid; l, lacrimal; m, maxilla; p, parietal; pl, palatine; pt, pterygoid; pal, contact with palatine; q, quadrate; qu, contact with quadrate.

Palatines: The palatine bones (Figures 3–5, 9 and 10) are broken in their anterior regions but they remain articulated with their respective pterygoid bones in their posterior region. The left palatine bone is substantially preserved, whereas the right palatine bone is reduced to a fragment of its posterior extent. The left palatine bone is still occluded laterally by matrix at its posterior end and dorsally–medially at its anterior tip. The right palatine bone is exposed laterally but remains hidden medially.

The remains of the right palatine bone are limited to a paper-thin bone that overlaps the palatal ramus of the right pterygoid bone. In the dorsal view, this palatine bone has a sub-rectangular shape.

In contrast, the left palatine bone articulates with the maxilla and is visible from a medial perspective. Following this view, the posterior margin of this bone bifurcates to accommodate both the maxilla and the pterygoid bones. The posterior and posterior–dorsal margins have a concave contour, with the latter being the receiving site for the palatal ramus of the pterygoid bone. The ventral margin, where it contacts with the maxilla, is straight. However, the anterior margin is fractured and exhibits a diagonal break. In the lateral perspective, the palatine bone shows a squamous connection with the pterygoid palatal ramus towards the posterior region. Anteriorly, a ridge forms a dorsal process with a ventral anterior tip at the base, while the anterior section of the dorsal part is broken. Posteriorly, the base of this process diverges from the pterygoid bone and extends laterally. Unfortunately, the presence of sediment covering the rest of the structure limits further observations. However, it is possible that the palatine bone could interact with the jugal bone [37].

5.1.3. Bones of the Chondrocranium

Laterosphenoid: The laterosphenoid bone (Figures 3–5, 9 and 10), from what is observed, is a small remnant piece above the prootic bone. It is broken on almost all surfaces except the anterior. The anterior surface is not completely exposed, as the rest is still hidden in the matrix. Not much can be said about this bone, it is barely visible, and it is identified this way due to its location and shape, which look like it would be the base of the lateral process.

Prootic: The prootic bone (Figures 3–5, 9 and 10) is poorly preserved and incomplete. The bone is fractured dorsally and laterally, with the medial side hidden within the matrix. The remains that are considered to be the prootic bone are from the right lateral side and are interpreted as such because of their position in relation to other specimens of the genus. It has an inverted and elongated water-drop shape in lateral view. No definitive marks can be seen, except for the ventral region, which bears a resemblance to the crista prootica. The surrounding sediments may potentially represent the filling of the foramina of the prootic bone, but in the absence of appropriate classification, it is not justified to identify it definitively as such.

Parasphenoid: The parasphenoid bone (Figures 3–5, 9, 10 and 13) remains partially concealed, but its main body is visible. It appears to be relatively intact, with the lateral right side exposed.

Its ventral–anterior margin is concave, and the dorsal–anterior margin is mainly straight. It has a blade-like morphology that tapers toward the anterior end. Two pneumatic recesses are present at the base of the parasphenoid, one at mid-length and one dorsally.

At the anterior tip, there is an apparent presence of a posterior–ventral projection. However, it is uncertain whether this represents a true process or a fractured portion that originates from the tip or, alternatively, if it is a sediment-filled groove within the ventral region. Considering the lack of knowledge regarding such a process in this particular genus, and even among theropods, it is most likely indicative of a fractured piece [3].

Basisphenoid: The basisphenoid bone (Figures 3–5, 9 and 10) exhibits excellent integrity, except for on the lateral surfaces, where on the right side, the basipterygoid process is fractured in half, and the attachment site for the ilio-costalis cervicus muscle is disrupted. The dorsal region and lateral right side are exposed, where the left side is hidden within the matrix.
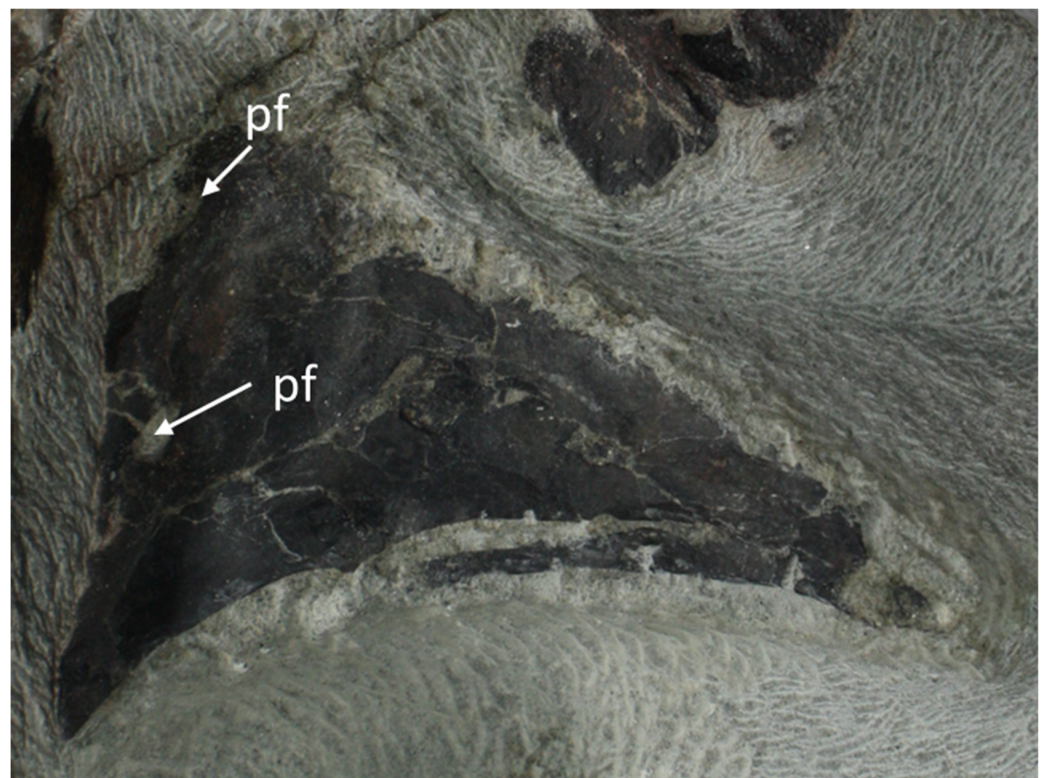
Figure 13. Lateral view of the right parasphenoid bone of *Allosaurus europaeus* ML415; pf, pneumatic foramina.

In general, its morphology does not differ from that of other *Allosaurus* species. It is connected to the basioccipital from the sides and separated posteriorly only by grooves. Two grooves separate the basal tubera and the ilio-costalis cervicus muscle process and two separate the basal tubera and the base of the basipterygoid process. The basipterygoid process from the left side is still articulated to the basisphenoid process of the pterygoid bone.

The basioccipital and the basisphenoid bones form a box in the ventral base of the braincase with a deep recess in the center, the basisphenoid recess. This recess is excavated medially and its position on the midline is between the basal tubera and the basipterygoid process.

Basioccipital: The basioccipital bone (Figures 3–5, 9 and 10) is broken along the right lateral surface of the basal tubera and on the dorsal aspect of the occipital condyle. The majority of the basal tubera is exposed, while the occipital condyle remains hidden in its medial region. The integrity of the occipital condyle is partially compromised, with approximately 50% of its structure remaining intact and connected to the persistent elements of the atlanto-axis complex. The neck of the condyle is largely obscured by matrix, although some fragments are visible on the right lateral side.

The occipital condyle is obstructed by its attachment to the atlanto-axis complex; however, by tracing a distinct dark semi-sub-elliptical line, its outline can be delineated. In terms of morphology, the condyle has a subspherical shape and contains an anterior central cavity, which is filled with sediment, and this may correspond to remnant of the foramen magnum. It should also be noted that the estimated maximum diameter of the condyle is approximately 5.60 cm. The angle formed between the neck of the occipital condyle and the basal tubera measures approximately 90° degrees, indicating a right angle.

The posterior surface of the basioccipital bone is a slightly concave configuration in a lateral–medial orientation. The distance between the extremities of each basal tubera is approximately 2.55 cm, while the span from the mid-groove of the basal tubera to the neck of the condyle is around 6.14 cm. The basal tubera is formed by the basioccipital bone in the medial part and entirely formed by the basisphenoid bone in the lateral part, separated by a lateral longitudinal groove.

5.1.4. Bones of the Splanchnocranium

Stapes: The stapes (Figures 4 and 14) is difficult to preserve due to its fragile nature, making it prone to breakage and dislocation. A bone fragment is present between the articulation with the basipterygoid process and the basisphenoid process of the pterygoid, which may be the stapes. However, upon closer observation, it becomes apparent that the fragment is too thick and located in an unusual position to be the stapes. Although, there is a laminar bone fragment resembling the stapes located below the paraoccipital process and above the quadrate bone, which is a more probable location.
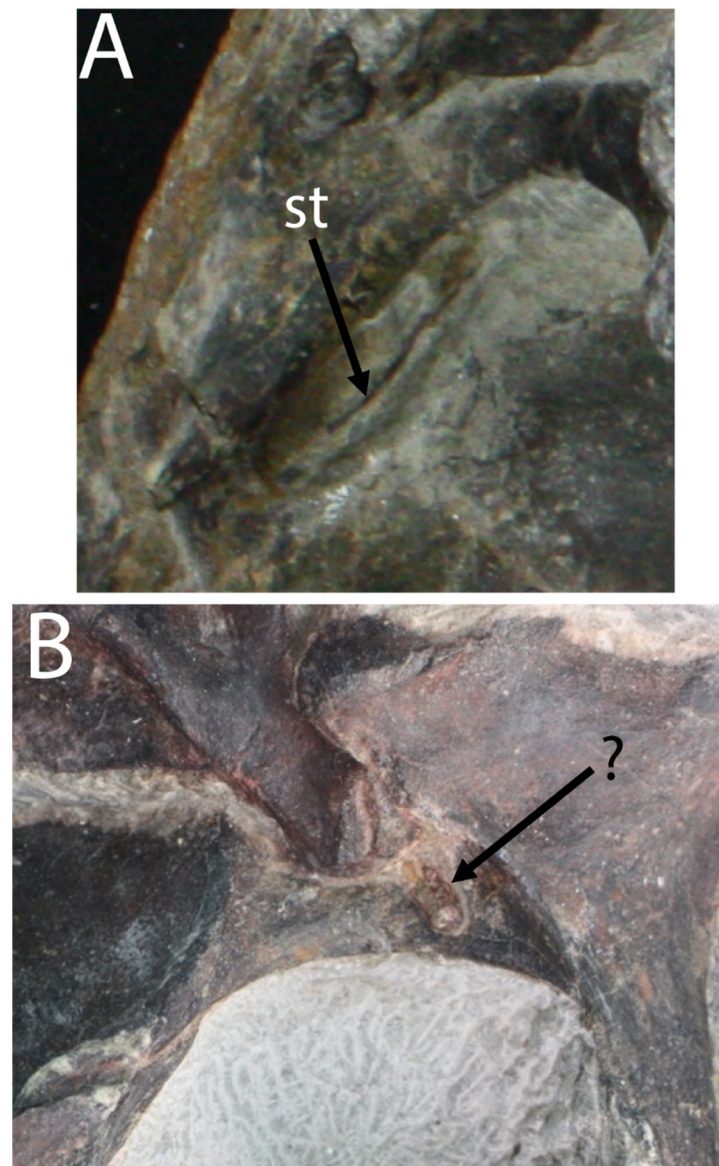
Figure 14. *Allosaurus europaeus* ML415, (**A**) stapes location (st, stapes) and (**B**)? indicates an unknown bone.

The preserved stapes, from the left side, appears to be broken and not fully exposed. It does not contact any other fragments and consists of two thin cylindrical fragments, one larger at approximately 2.90 cm in length and the other smaller at 2.40 mm in length.

Epipterygoid: The right epipterygoid bone (Figures 3–5, 9 and 10) is not complete, with fragmentation in the posterior and dorsal regions. However, it does not seem to be deformed and is still articulated with the pterygoid bone and braincase. The left is not visible in the specimen, but since the quadrate flange of the left pterygoid bone is completely intact, it may still be concealed in the matrix. Morphologically, it is a laminar bone, with a blade profile that is thicker anteriorly and thinner posteriorly. The articulation with the pterygoid bone is hindered, probably due to the fusion of these two bones.

Quadrate: The quadrate bone (Figures 3–5, 9, 10 and 15) in the specimen is the left one and it is broken medially. The mandibular articulation is roughly broken through the intercondylar sulcus, with the medial condyle and the entocondyle completely broken, and the lateral condyle and the ectocondyle partly broken [32]. The dorsal portion of the quadrate bone is roughly covered by the matrix or by the quadrate ramus of the pterygoid and paraoccipital process of the occipital and squamosal bones. Only the posterior, medial,

and lateral portions of the quadrate head are exposed. This cotylus is articulated within the squamosal bone and it is partly enveloped medially by the paraoccipital process of the occipital bone, representing the most dorsal part of the quadrate bone. The quadratojugal bone excludes the quadrate bone from the lateral surface of the skull, except for the quadrate head ascending ramus and part of the ectocondyle ventral to the articulation with the surangular bone.

Figure 15. *Allosaurus europaeus* specimen ML415 anteromedial view: quadrate shelf with pterygoid contribution.

In the posterior view, the quadrate bone exhibits the presence of a posterior fossa and posterior fenestra. Both the quadrate and quadratojugal bones contribute medially and laterally, respectively, to this fenestra. This view shows two prominent ridges: the quadrate ridge, originating from the dorsal region of the entocondyle, and extending to near the base of the quadrate head, and a second ridge that begins lateral–dorsally to the quadrate ridge and smoothly ends at the point of articulation between the quadrate head and the squamosal bone. The configuration of these ridges appears as a nearly continuous shaft; however, it is divided by a deep groove that extends laterally–ventrally, reaching the quadrate foramen.

From the quadrate ridge, a dorsal–anterior expansion resembling a sheet-like structure emerges and contacts with the pterygoid bone. This expansion is recognized as the pterygoid flange of the quadrate bone and has been designated as such by Hendrick et al., 2015 [32]. The quadrate bone also curves medially along the anterior–ventral border of the pterygoid flange, forming a ridge. The ridge extends posteriorly from its dorsal apex, creating a shelf for the quadrate wing of the pterygoid bone. The posterior expansion of this ridge persistently extends into the pterygoid quadrate wing.

A distinct section of the quadrate shaft and quadrate head is visible when examined laterally. The quadrate bone has a ventrally twisted, sub-rectangular shape. A large part of the quadrate structure either articulates with the quadratojugal and squamosal bones or is concealed within the matrix. Establishing anterior contacts with both bones proves to be a complex process, mainly due to the extensive matrix covering. Nonetheless, the evidence

suggests that the ascending process of the quadratojugal bone restricts the quadrate from making anterior contact with the squamosal bone. It extends above the point where the quadratojugal and squamosal bones meet, but it does not go beyond the lateral temporal fenestra. The quadrate bone is similar to the other quadrates of *Allosaurus* species [12].

5.1.5. Dermal Bones of the Lower Jaw

Surangular: The surangular bone (Figures 3–5, 9 and 10) is the largest bone preserved, although it is incomplete, with some portions broken, including the anterior, ventral, medial, and posterior regions. It remains articulated to the quadrate bone dorsally in the posterior region, and the coronoid bone medially in the anterior region. The remaining glenoid fossa of the surangular bone contacts the ectocondyle of quadrate bone since all are cut medially. Deciphering the contact with the coronoid bone is difficult since it is filled with fractures and covered with matrix. However, the contacts of the bones can be seen on the anterior broken surface.

In medial view, there is a surangular ridge on the dorsal region that starts at the articulated region of the quadrate bone and smooths out to the coronoid articulation. This ridge is the most robust part of this bone. A ventral groove is present on the surangular ridge, which becomes smoother toward the posterior and thickens toward the anterior. The anterior part is still filled with sediment. Below this ridge, the surangular bone is paper-thin and very fragile, hence the fractures present on this piece.

In the lateral view, there is a prominent ridge on the dorsal–posterior region that starts at the quadrate articulation zone and becomes smoother toward the mid-length. Below it, anteriorly, is a deep groove, followed by two small surangular foramina. Based on the position and articulation of the bone, we can assume that the specimen died with its mouth closed or partially closed. The surangular bone in *A. europaeus* differs from *A. jimmadseni* and *A. fragilis* USNM 4734, as it has two surangular foramina instead of one, which is also present in *A. fragilis* (DINO 2560) and *Sinraptor dongi* [36].

Angular: The angular bone (Figure 16 is fairly complete, only broken at the anterior end and some parts of the posterior end. It is now disarticulated but was found semi-articulated with the surangular bone. Due to its fragile nature, this bone is filled with fractures throughout its body, even in the thicker parts, where the fractures are thicker. These thicker fractures may be the result of the previous preparation phase when the specimen was found.

It is a long bone with a paper-thin plate at the posterior end, truncating and thickening anteriorly. From the anterior region, the dorsal edge has a pronounced posterior concave curvature until it reaches the midpoint, where it forms an apex in height. Beyond this apex, the dorsal margin continues smoothly with a posteriorly concave contour, with the ventral vertex extending posteriorly to a greater length. The ventral margin has a smooth, concave, almost straight edge. The angular dorsoposterior rims in *A. europaeus* and *A. jimmadseni* are deeper at mid-length than in *A. fragilis* DINO 2560 (in USNM 4734, it is unknown).

Coronoid: The coronoid bone (Figures 3–5, 9 and 10) is fractured ventrally and anteriorly, it looks slightly deformed, and it is affected posteriorly by a large fracture. The posterior end is still hidden in the matrix. It is still articulated with the surangular bone; in fact, it is difficult to distinguish it with clarity, but on the anterior surface of the fracture it is possible to see that there are two bones separated by sediment and, following the suture line, it is possible to limit it.

It is a thin bone with a prismatic shape at the posterior end, which widens ventrally–anteriorly into a small plate bone of about 3 mm in thickness.

Figure 16. *Allosaurus europaeus* ML415 angular bone, medial and lateral views, respectively. Scale: 10 cm.

Figure 17. Posterior most maxillary tooth of *Allosaurus europaeus* ML415. (**A**) The mesial surface and (**B**) the distal–lingual surface.

5.1.6. Dentition

Maxillary teeth: There are at least three partial teeth (Figure 17) present in the ML415: the last tooth of the maxilla (the most distal), the second to last tooth, and the third to last. The dental enamel is still intact on these teeth. The second and third to last teeth are limited to small fragments, with the second having a small piece of the crown cut and with an exposed root, and the other still within the maxilla. The last tooth is almost complete, with a broken apex and fully emerged.

The final tooth measures approximately 1.8 cm in length from the base to apex when viewed laterally. It has a d-shaped cross-section and a triangular shape, when viewed from lateral or medial view. The apex is curved distally, and the distal surface is serrated with denticles, while the mesial surface is smooth. Observing the denticles can be challenging due to the fragmentary surface of the tooth, which makes it difficult to determine where they start. Nevertheless, these denticles are unified as a single blade that starts at the base of the crown and ends at the apex of the tooth. They have a sub-rectangular shape with a convex operculum and shallow interdenticular slit. The interdenticular spaces are big enough and are often being filled with sediment, making it impossible to visualize the interdenticular diaphysis. At the base of the crown, the tooth has a fracture from where it has broken on a few occasions.

The second to last tooth, the remnant of the crown, is cut in a way that resembles a distorted, distally triangular shape. From the anterior view, it shows sub-elliptical shaped rings, with a lighter color in the center and a darker color at the border. The root of the tooth is also visible, but it does not extend very deep into the maxilla. Between the first and second teeth, there is a small interdental plate in the medial view.

In the anterior view, there is a sub-elliptical remnant that resembles a tooth located anterior–dorsally to the second tooth. This tooth is deep within the maxilla and has not emerged, making it an undeveloped tooth, representing the third to last tooth of the maxilla.

These represent the last three tooth positions of the maxilla, corresponding to positions 14, 15, and 16, when compared to the most complete skulls with 16 maxillary tooth positions of *A. fragilis* [12].

5.2. Description of the Cervical Vertebrae and Ribs

From the mid-cervical region (Figures 18–22), the only fossils preserved are the fairly complete fourth, fifth, and sixth, and one piece of the third and one from seventh cervical vertebrae, as well as several rib fragments. They were found in perfect articulation in a subspherical beach boulder, cut and shaped by the sea erosion. The vertebrae were at the core of the boulder and were almost completely preserved. The posterior portion of the sixth cervical vertebra was partially lost by the erosion. The fourth vertebra was also articulated to a portion of the third cervical centrum, showing a full degree of disarticulation. The third and seventh are represented by a small piece of the cotyle and the pre-zygapophyses, respectively.

Figure 18. *Allosaurus europaeus* of ML415 cervical vertebrae block during the preparation process.
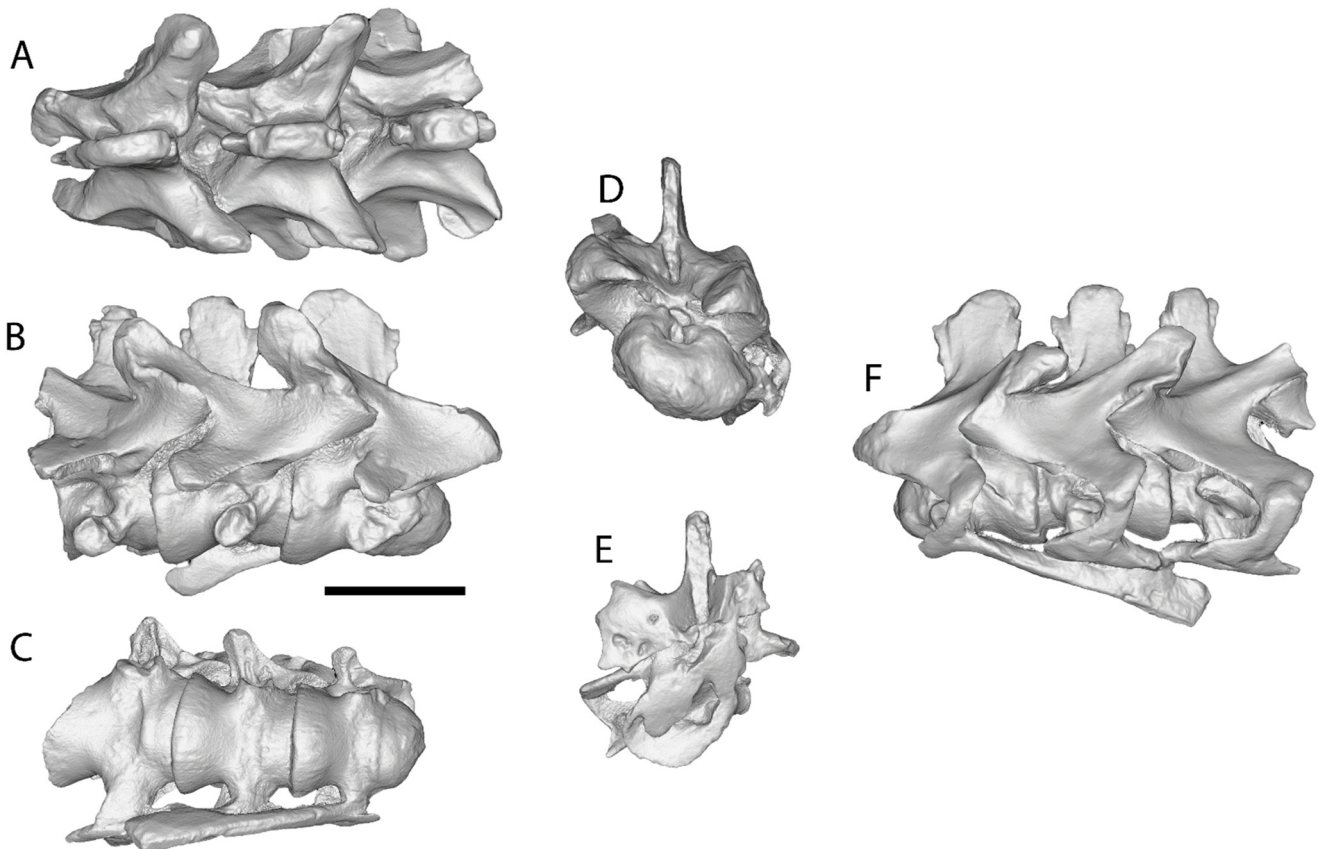
Figure 19. *Allosaurus europaeus* ML415, 4th, 5th and 6th cervical vertebrae and ribs (**A**) dorsal view, (**B**) lateral right view, (**C**) ventral view, (**D**) anterior view, (**E**) posterior view, and (**F**) lateral left view. Scale: 10 cm.

Figure 20. *Allosaurus europaeus* ML415: 4th, 5th and 6th cervical vertebrae and ribs in lateral left, posterior, and anterior views, respectively. Scale: 10 cm.

The surface preservation is excellent, but some lateral shear deformation is visible, with the right side being raised relative to the left side, possibly due to lithostatic pressure. The fossil was nearly fully prepared and was thus visible from all sides.

This section is interpreted as the 4th, 5th, and 6th cervical vertebrae when compared to *Allosaurus fragilis* in Gilmore, 1920 [35], and Madsen, 1976 [12], based on the anterior–posterior length of the neural spine, the prominence of the epipophyses and interspinous scars, and the relative sizes between the vertebrae. The left cervical ribs remained fully articulated to the vertebrae, suggesting that this was the side on which the body lay, which by being covered earlier, could better preserve the articulation. The individual probably had the right side more exposed after death. However, the tips of the epipophyses on the left side are eroded dorsally, whereas those on the right are more complete. The right side is also better preserved than the left, where fractures are more common. This may indicate that the left side was the side that was eroded and exposed to the elements after diagenesis.

Compared to the vertebrae of ML415 resembling the fourth, fifth, and sixth cervical vertebrae described in the osteology of *Allosaurus fragilis* [12], in the interspinous ligament scar, it is much more developed and robust on the fourth, fifth, and sixth cervical vertebrae of ML415, but this character varies among specimens, including SMA 0005, USNM 4734, MOR 693, and CLDQ material. These distinguishing features are less prominent in other vertebrae. For instance, the first vertebra of ML415, identified as the fourth in sequence, cannot reasonably be considered as the third vertebra. Similarly, the third vertebra of the specimen, classified as the sixth, cannot be equated with the seventh. This differentiation is based on the presence of a relatively concealed interspinous scar ligament on the anterior aspect of the third vertebra, as well as on both the anterior and posterior aspects of the

seventh vertebra. Additionally, the neural spine of the seventh vertebra is medial–laterally thicker. In contrast, the neural spine of vertebrae, such as the eighth and ninth, is less developed and dorsal–ventrally shorter. In addition, the triangular piece that connects the apophyses has two laminae: the spinoprezygapophyseal and spinopostzygapophyseal, instead of the usual single prepostzygapophyseal, with the epipophyses connected to the neural spine and not the pre-zygapophyses. However, the ML415 cervical vertebrae do have two differences. Firstly, the centrum is wider from side to side than it is tall from top to bottom. Secondly, the parapophyses are located in the middle of the centrum, a condition seen in *Neovenator*, which was not observed in *A. fragilis* by Madsen, 1976 [12], where the centrum is as tall as it is wide and the parapophyses are located anteriorly.

The separately described cotyle has a distinct shape that confirms its origin from the third cervical vertebra. This is due to the presence of a suture line observed on the fourth cervical vertebra that corresponds in shape to that of the cotyle. The preserved fragment of rib, including the tuberculum and capitulum, is unequivocally identified as a cervical rib due to its positional alignment with these elements, along with the unique ventral–posterior trajectory of the rib shaft characteristic of cervical ribs.

Atlanto-axis complex: The atlanto-axis complex (Figures 3–5, 9 and 10) is preserved in the specimen, and is still articulated with the occipital condyle. The specimen is limited to two sub-ellipse atlas and one sub-rectangular axis intercentrum remains, as well as one sub-rectangular epipophysis and one sub-triangular unidentified remain, which may be from the axis.

The intercentrum of the atlas articulates directly with the occipital condyle, while the remaining intercentrum of the axis articulates ventrally with this piece of the atlas. An unidentified remnant is located on the left lateral side of the atlas. The epipophysis, located anteriorly to the atlas intercentrum, is isolated and situated to the left of the occipital condyle.

The remains of this complex were initially believed to be the occipital condyle due to their appearance as a single fragmented bone, which would suggest a very large condyle. However, upon closer inspection of the original surface of the specimen, a dark line can be observed between these remains that marks the contour of the occipital condyle, separating it from the rest of the remains.

Fourth cervical vertebra (Cv4): The fourth cervical vertebra (Figures 19–22) is complete and almost fully exposed, as it is attached to the fifth vertebra, and the posterior axis is not visible. The tip of the left epipophysis is eroded.

The centrum is a strongly opisthocoelus and has an oval condyle, best seen in anterior view, as it is wider transversely, with a transverse diameter of 7.9 cm, than it is tall dorsoventrally, with approximately 4.31 cm in diameter. The posterior margins of the centrum are thicker than the anterior margins to accommodate the posterior vertebra, yielding an ear plug profile in ventral view. The neural canal lies above the condyle and below the baseline of the pre-zygapophyses and has an oval shape, although this time it is wider dorsoventrally, with a diameter of approximately 2.3 cm and transverse diameter of 1.3 cm. The spinoprezygapophyseal fossa is wider dorsoventrally than transversely. The neural arch is located at mid-length of the centrum and its neural spine is located immediately above it at mid-length. The neural arch is broader than the centrum, with both diapophyses and postzygapophyses exceeding the lateral limits of the centrum.

The centrum is about 12.0 cm in length. In the lateral views, the parapophyses are in the middle of the centrum, which distinguishes them from other *Allosaurus* species (this may be due to lithostatic distortion). In the ventral view, the centrum has a relatively flat surface and shows longitudinal striations in the ventral posterior margin. A smooth transverse crest borders the anterior condyle between the parapophyses. The parapophyses are prominent, being about one-fifth the length of the centrum. They have a sub-circular

outline in lateral view, with concave surfaces and antero-dorsally raised rims. The rims protrude laterally and stand out from the surface of the centrum. The right exposed parapophysis has a renniform profile and it is dorsoventrally broader. The left side is probably similar but is not visible, as it is still connected to the cervical rib by the capitulum, just as the left diapophysis is connected to the rib by the tuberculum. The lateral facets of the centrum have a single elongated cavity, the pleurocoels, located at mid-length, just below the neural arch and dorsally posterior to the parapophyses. These pleurocoels are present in all cervical vertebrae of the ML415 specimen.

The apophyses, such as the prezygapophyses, the postzygapophyses, epipophyses, and diapophyses, are connected in a single structure with several laminae. This structure has a triangular shape that resembles the tip of an arrow, with the prezygapophyses representing the apex and the remaining vertices constituted by the postzygapophyses, with epipophyses and diapophyses. This characteristic shape is observed consistently across all the examined vertebrae.

The prezygapophyses, postzygapophyses, epipophyses, diapophyses, and the neural spine are positioned above the centrum. The facets of the zygapophyses are planar. The distance between the prezygapophyses and the epipophyses is approximately 17.5 cm and to the diapophyses is around 9.1 cm. The prepostzygapophyseal laminae are very evident, with a smooth crest, and the most prominent laminae are prezygapophyseal–diapophyseal laminae, although the right lamina is smoother and lateromedially thicker than the left side.

The prezygapophyses are positioned below the level of the base of the neural spine and above the centrum condyle. In the anterior view, they appear medially bent, due to the deformation, with their articular facets almost facing each other medially and with their symmetry between them disrupted. Two fossae are located below each prezygapophysis and above the centrum condyle. The right fossa is almost cylindrical in shape and is partially obscured by the base of the prezygapophysis. The left fossa is exposed and has a more sub-circular shape. This difference may be due to deformation applied to the vertebrae.

The diapophyses are positioned near the center of the centrum in an anteroposterior orientation, with their tips oriented posteroventrally. They have a rounded end with a sub-rectangular body. The left diapophysis is still attached to the rib by the tuberculum. Both have an anterior–posterior fracture at its base. On their ventral surface, there is a smooth medial–lateral lamina, with a small fossa located anterior to it.

The postzygapophyses are long, extending slightly beyond the posterior margin of the centrum. The articular surfaces of the postzygapophyses face ventrally and connect to the prezygapophyses of the fifth vertebra. Their articular facets are lateromedial and slightly inclined medially. The epipophyses are longer posteriorly than the postzygapophyses, and the distance between them is 15.0 cm. Their shape, when viewed dorsally, is that of an irregular pyramid, with the apex pointing posteriorly. On the right side, in the dorsal view, there is a small, deep, sub-elliptical cavity between the prezygapophyseal–epipophyseal lamina and the neural spine, just below the shallow ridge of the neural spine. This cavity is not present on their counterparts of left side.

The height of the neural spine is equal to that of the centrum, measuring 8.5 cm from the tip to the base at the same level as the prezygapophyses. It is approximately 1.1 cm-thick at the top and 7.3 cm in anteroposterior length. The neural spine is laterally compressed with the tip of the dorsal spine, having a sub-rectangular outline when viewed dorsally, and it is subrounded and bends posteriorly, when viewed laterally. The scars of the interspinous ligament are visible on the anterior and posterior surfaces below the dorsal tip. It expands antero-posteriorly from the top of the base of the neural spine and terminates at the base of the tip. Shallow ridges parallel to the neuroprezygapophyseal lamina are present on each side of the anterior base of the neural spine, just below the scars. The presence of the

aforementioned scars has implications for which cervical vertebrae they are. According to Madsen, 1976 [12] not all cervical vertebrae have these scars. At the base of the neural spine, immediately below the anterior interspinous ligament, there is a shallow ridge parallel to the neuroprezygapophyseal lamina. This cervical vertebra differs from other *Allosaurus* in the position of the parapophyses, which is in the middle of the centrum, and the presence of the accessory lamina parallel to the neuroprezygapophyseal lamina.
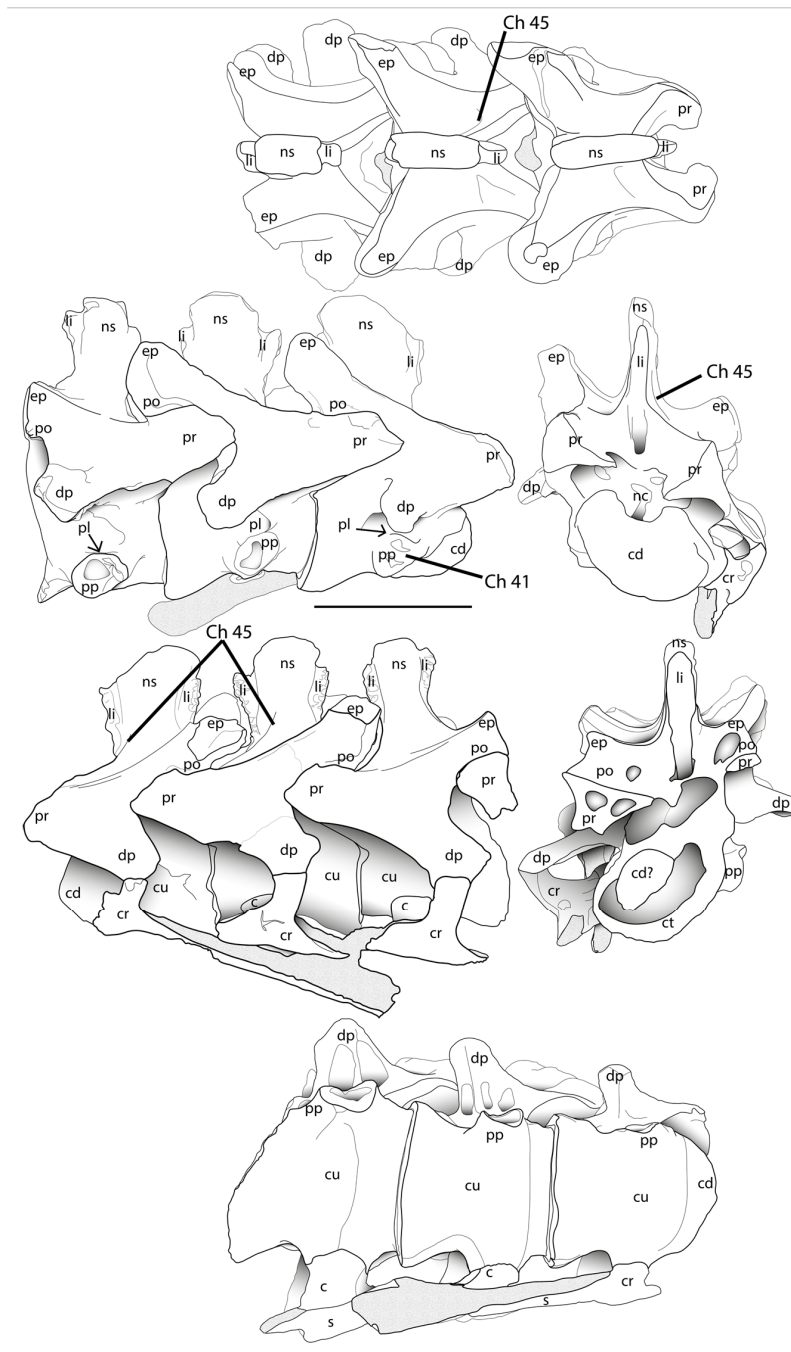

Figure 21. *Allosaurus europaeus* ML415: dorsal, ventral, and other lateral views, respectively, of the cervical vertebrae. Scale: 10 cm.

Fifth cervical vertebra (Cv5): The fifth cervical vertebra (Figures 19–22) is almost fully complete and exposed as it articulates between the fourth and sixth cervical vertebrae, where the axial views are limited. The vertebra has an articulation to the left rib, and the left epipophysis tip is eroded. The parapophysis of the left side is also articulated to the rib by the capitulum. The prezygapophyses are better preserved than in the fourth vertebra, with the articular surface still connected to the postzygapophyses of the fourth.

The centrum is also strongly opisthocoelous, with the anterior convexity well nested into the previous vertebra and an ear plug profile. The parapophyses differ from those of the fourth vertebra, being more sub-elliptical, dorsoventrally broader, and more prominent, especially

in lateral view. They are also concave with raised rims antero-dorsally. The pleurocoels are in a similar position to those of the fourth vertebra, but in this vertebra, the cavities of the pleurocoels are deeper ventrally and medially. Similar to the previous vertebra, the ventral surface of the centrum displays a flat surface with longitudinal striations at the ventral posterior margin and a subtle transverse crest bordering the anterior condyle between the parapophyses. Posterior to the pleurocoels, the neurocentral suture is best visible and is deeper than the fourth. The neural arch is similar to the previous vertebra position in the mid-length of the centrum, with its neural spine located above it in the mid-length.

Figure 22. *Allosaurus europaeus* ML415: dorsal, lateral right, anterior, lateral left, posterior, and ventral views, respectively, of the cervical vertebrae. Scale: 10 cm. Osteological abbreviations: c, capitulum; cd, condyle; cr, cervical rib; ct, cotyle; cu, centrum; dp, diapophyses; ep, epipophyses; li, interspinous ligament; nc, neural canal; ns, neural spine; pl, pleurocoel; po, postzygapophyses; pp, parapophyses; pr, prezygapophyses; s, shaft. Ch. indicate the phylogenetic character number.

The diapophyses are simple, being anterior–posteriorly wider than dorsoventrally taller, with two shallow ventral laminae. The prezygodiapophyseal laminae are the most prominent laminae, which are fused to the centrozygapophyseal laminae. Similar to the fourth the prezygapophyses, the postzygapophyses, epipophyses, diapophyses, and the neural spine are above the centrum, and zygapophyses also have planar facets. The main axis of the diapophyses projects lateral–posteriorly and are antero-posteriorly thicker than the fourth. The zygapophyses are broad and robust, with a strong and prominent epipophyses. There is a dorsal project prezygapophyseal–epipophyseal ridge.

The neural spine is shorter anterior–posteriorly than the fourth, measuring 7.0 cm from scar to scar. At the tip of the dorsal spine, the neural spine is still laterally compressed, with a sub-rectangular outline in the dorsal view. The lower two halves of the neural spine have prominent interspinous scars, which are more developed anteriorly than posteriorly. In lateral view, the neural spine tip outline is sub-rounded and does not bend posteriorly. At the base of the neural spine, there is a potentially unique shallow ridge parallel to the neuroprezygapophyseal lamina. This cervical vertebra differs from other *Allosaurus* in the position of the parapophyses, which is in the middle of the centrum, and the presence of the accessory lamina parallel to the neuroprezygapophyseal lamina.

Sixth vertebra (Cv6): The sixth vertebra (Figures 19 and 20) is deformed and broken in the posterior section; however, it is still well-preserved enough to allow for a description. Due to the deformation and cut of the fossil, the vertebra has an asymmetrical profile. On the right side, it appears shorter than the other vertebrae, but this is not the case on the left side, where the posterior side is more complete. Therefore, the posterior cut plane is not completely orthogonal with the main axis. As a result of this cut, the postzygapophyses, epipophyses, and the right diapophysis are incomplete and broken. The condyle is well fitted in the cotyle of the fifth vertebra, making the anterior surface impossible to observe.

The centrum has a maximum length of 9.5 cm when measured from the left side. It is wider toward the posterior and has a similar shape to the previous vertebrae. From the ventral view, the smooth transverse crest can also be observed among the parapophyses, where it is most prominent in all vertebrae, making the concavity in the ventral face more anteriorly deep compared to the fourth and fifth vertebrae.

In the posterior view, the broken concave cotyle reveals that the centrum is camerate, as well as the internal structure of the postzygapophyses, which has phylogenetic implications. Above the cotyle, there is a deformed neural canal that is tilted to the right side. Fragments of the prezygapophyses of the seventh vertebra are still attached to the broken postzygapophyses, with the left piece revealing the camerate internal structure. Despite being broken, it is possible to observe the tip of the prezygapoepipophyseal laminae of the epipophyses sticking out.

The parapophyses are larger and more robust, particularly noticeable in ventral and lateral views, compared to the other cervical vertebrae. This is due to the posterior increase in size of the ribs. The left parapophysis still has the cervical rib articulated. The parapophyses maintain the same renniform profile as the others, but in lateral view, there is a deeper cavity with raised rims that projects laterally and stands out from the centrum surface. The pleurocoels are situated directly above the parapophysis and are more medially positioned compared to the previous cervical vertebrae.

The prezygapophyses extend almost 4 cm forward from the centrum length and are deeply articulated anteriorly into the postzygapophyses of the fifth vertebra. The total distance from the tip of the prezygapophysis to the top of the postzygapophysis is 17.5 cm. The centrozygapophyseal laminae are more prominent than those of the other vertebrae, and the prezygodiapophyseal fuses to this lamina as well.

The neural spine is less wide in the anterior–posterior direction when compared to the fourth and fifth vertebrae. Its maximum size is 5.4 cm in anteroposterior length and 3.0 cm-thick at the top of the tip. When viewed dorsally, it is less laterally compressed, affording the tip profile a square belt-buckle shape. The concavity in the posterior surface at the bottom of the neural spine, between the two postzygapophyses, is the deepest of all vertebrae. The interspinous scars are present and are more anterior–posteriorly prominent compared to the fourth cervical vertebra but less compared to the fifth cervical vertebra. On the dorsal surface of the lateral right side, there is a small cavity located posteriorly between the neural spine and the prezygapophyseal process. This cavity differs from the one found in the fifth cervical vertebra in terms of location and depth, but both may have originated from deformation since they are not present in their respective left counterparts. This vertebra lacks the autapomorphic shallow ridge found on the previous vertebrae dorsal surface, at the base of the neural spine, below the anterior interspinous ligament of the neural spine. This cervical vertebra differs from other *Allosaurus* in the position of the parapophyses, which is in the middle of the centrum rather than anterior.

Cotyle of Cv 3: The cotyle of the third vertebra is reserved to a small piece with good preservation, with concavity of the cotyle, in the posterior view, filled by sediment with some vestigial fragments of the condyle of the fourth vertebrae.

This is a small fragment of the right side of the edge of the cotyle. It has a comma shape in anterior or posterior view, with greater thickness in the dorsal area. It still has the central neural suture present in the anterior extremity located in the dorsolateral region.

Three main bodies of cervical rib (Figures 19, 20 and 22) fragments are still connected to the left side of the cervical vertebrae. The three ribs have a similar shape, but the ribs from the fifth and sixth vertebrae are more alike than the fourth. The rib from the fourth vertebra has a more complete shaft, whereas the other ribs have broken shafts at their bases, and their main bodies become progressively larger posteriorly. The rib from the fifth vertebra has an anteroposterior fracture in the base of the tuberculum.

In the lateral view, the rib from the fourth vertebra has a T-shape, with the head pointing anteriorly and the stem (shaft) directed posteriorly. It is connected to the parapophysis and diapophysis by the capitulum and the tuberculum, respectively. An anterior–ventral projection is presented laterally to the capitulum. This projection is also present on the other articulated ribs, but they are more anteriorly oriented and projected compared to the fourth cervical rib. The shaft of this rib extends posteroventrally and is longer than the vertebra itself, measuring 21 cm from the most anterior part of the shaft to the tip. It surpasses the next vertebra by a small amount, although it is broken, so it is unclear where it ends. The base of the shafts increases in robustness along the posterior ribs, giving the impression that shafts may be longer compared to the shaft of the rib from the fourth cervical.

Cervical rib fragments: There is one cervical rib (Figure 23) isolated and disarticulated, with fairly good preservation, except for the poor medial surface. It measures 8.5 cm in length, with a 7.0 cm separation between the capitulum and the tuberculum. The capitulum has a sub-elliptical shape and is well developed, but it is poorly preserved, with some sediment adhering to it. It is abruptly separated from the rib and has a cone with a sub-spherical base, medially shaped. The radius of the capitulum measures approximately 3.3 cm in the dorsoventral direction, with a smaller radius extending antero-posteriorly. An anterior–dorsal process is visible in lateral proximity to the capitulum in anterior view. Additionally, a cavity can be observed between the tuberculum and capitulum. The tuberculum is not well developed and likely connected to the diapophysis with a weak connection. It is elongated and dorsally tapered. In lateral view, there is a depression in the proximal zone of the shaft. The preserved length of the shaft is approximately 6.0 cm and

has a sub-cylindrical elliptical profile, with a medial surface filled with sediment. Based on the thickness of the tuberculum, this rib is likely from the third or fourth cervical vertebra.
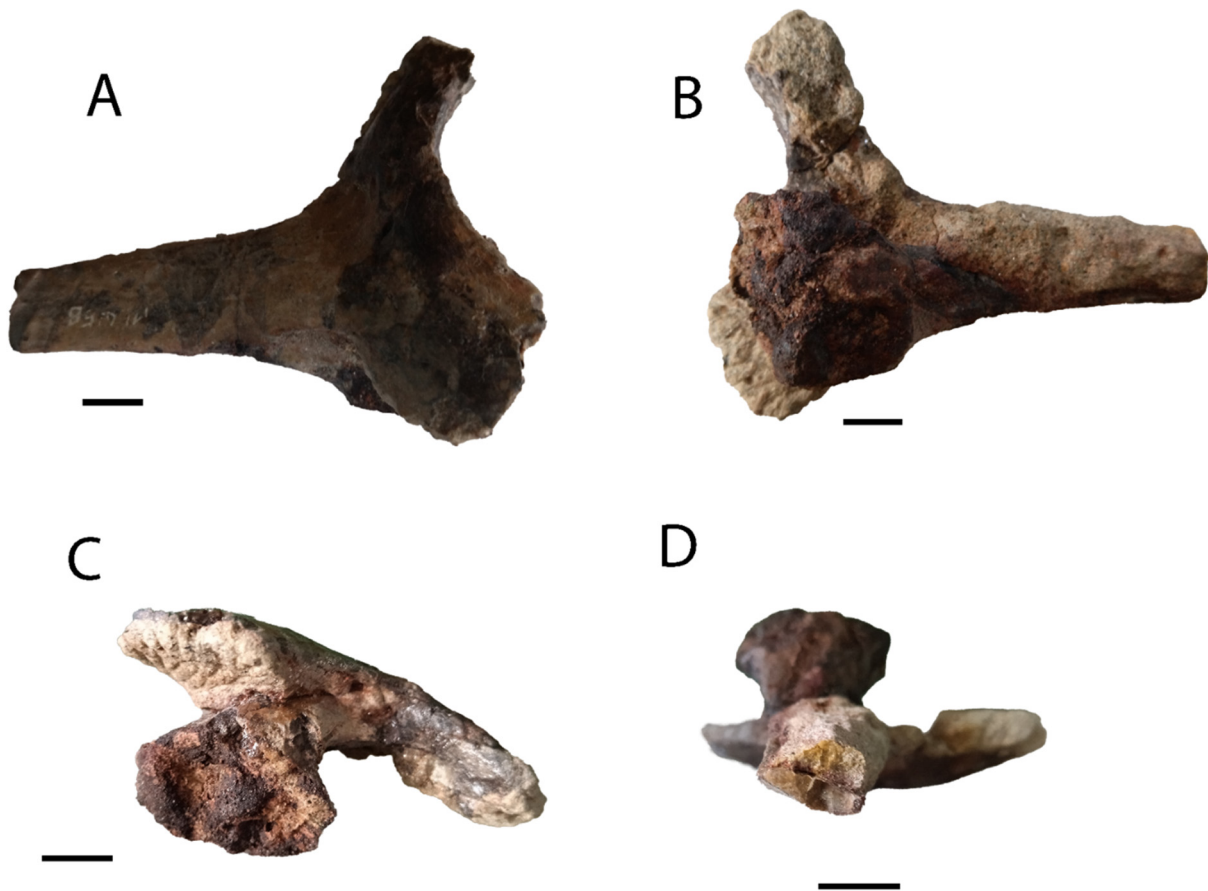
Figure 23. *Allosaurus europaeus* ML415: right cervical rib remains of the third or fourth cervical vertebrae. (**A**) Lateral view, (**B**) medial view, (**C**) anterior view, and (**D**) posterior view. Scale: 1 cm.

There are another six rib fragments, five of which are similar in size and shape. They are sub-cylindrical in cross-section, elongated, and taper along the body, with one side thicker than the other. These fragments may belong to a theropod, likely *Allosaurus* due to its size and slender build. The sixth fragment differs from the others and is more parallelepiped in the cross-section. It was originally thought to be from the dorsal rib. The fragment contains iron oxides and gypsum that are not present in any of the other fragments. This suggests that the fragment is from a different fossil and does not belong to the specimen.

6. Discussion

6.1. Validity of Other Allosaurus and Allosaurus-like Species

The holotype of the dubious species *Allosaurus atrox* Marsh 1878 (YPM 1890) was found in the middle Morrison Formation of southern Wyoming and originally described as "*Creosaurus atrox*", described a year after the first *Allosaurus* description by Marsh [34,38]. Later, in a monography on USNM 4734 by Guilmore, 1920 [35], he referred to the "*Creosaurus atrox*" species as pertaining to the same genus of *Allosaurus* (referring to his *Antrodemus*) and to a different species, the *A. atrox*, although he assumed that a more in-depth study of it was needed to validate the species. Paul, 1988 [39], stated that *A. atrox* (where DINO 2560 was previously referred to this taxon) is differentiated from *A. fragilis* with a bigger and more rectangular skull, with less triangular preorbital horns. In an in-depth analysis

by Chure, 2000 [34], on the clade of Allosauridae, he mentions that distortion has altered the contacts of some elements, resulting in an erroneous reconstruction of the skull of the specimen USNM 4734, which made some researchers believe that *A. fragilis* had a highly convex and short snout. It is also stated that in the context of lacrimal horn, there two morphotypes, one high and triangular core and one lower and round core, both of which morphs are considered as showing interspecific variation. If this short snout were true, it would probably be reflected in the angle between the anterior and ventral rami of the lacrimal bone compared to "*A. atrox*", which is not the case. Therefore, Chure, 2000, and Chure and Loewen, 2020 [3,34], considered *A. atrox* synonymous with *Allosaurus fragilis*.

Dalman et al., 2014 [40], described a new species, the *Allosaurus lucasi* (holotype: YPM VP 57589 and YPM VP 57726), found in the uppermost sediments of McElmo Canyon on the Brushy Basin Member at the top of Morrison Formation, southwest of the city of Cortez, which are Kimmeridgian to Tithonian age. The material of the holotype includes a fragmentary partial skeleton of an adult consisting of cranial, dental, and postcranial elements. The specimen includes the posterior end of the right dentary and part of the right splenial belonging to a juvenile. This species is characterized by a strongly reduced length of the premaxilla, short and deep maxilla, quadratojugal bone with reduced jugal bone process and quadrate bone process, the ventral margins of the rostral quadratojugal ramus and the quadrate process of the quadratojugal bone form a single line, and the lateral condyle of the tibia is strongly removed posteriorly, whereas in *Allosaurus fragilis* and *Saurophaganax maximus*, the condyle is more centered and occupies almost half the length of the tibial head. Chure and Loewen, 2020 [3], considered this nomen dubium, which refers to either *Allosaurus fragilis* or are *Allosaurus* species indeterminate. We agree that it is *Allosaurus* sp., as is later discussed.

Allosaurus is one of the oldest theropod names, coined by Marsh in 1878. Therefore, many named taxa fell into this genus, which worked as a taxonomical wastebasket. That includes some discussed here, together with other allosaurids (specimen numbers and locations after PBDB):

Allosaurus fragilis Marsh 1878

The type is YPM 1930, undiagnostic isolated bone. Its type locality is Felch Quarry 1, Garden Park (YPM), which is in a Kimmeridgian/Tithonian channel sandstone/claystone in the Morrison Formation of Colorado. It has been proposed to be replaced by the neotype USNM 4734 [38,41], which we support.

Allosaurus lucasi Dalman 2014 (*nomen dubium*)

Since the species is set on characters in too-fragmentary material, some of which, such as the premaxilla and jugal bone, have a high morphological variation in *Allosaurus fragilis* [33,42], it was considered a *nomen dubium* by Chure and Loewen, 2020 [3].

Labrosaurus ferox Marsh, 1884 (Figure 24)

Type USNM 2315, a dentary. Its type locality is Felch Quarry 1, Garden Park (YPM), which is in a Kimmeridgian/Tithonian channel sandstone/claystone in the Morrison Formation of Colorado. It has strange dentary due to a diastema-like gap and is very projected posteroventrally. The "diastema" may be pathological, but the specimen deserves a new study.
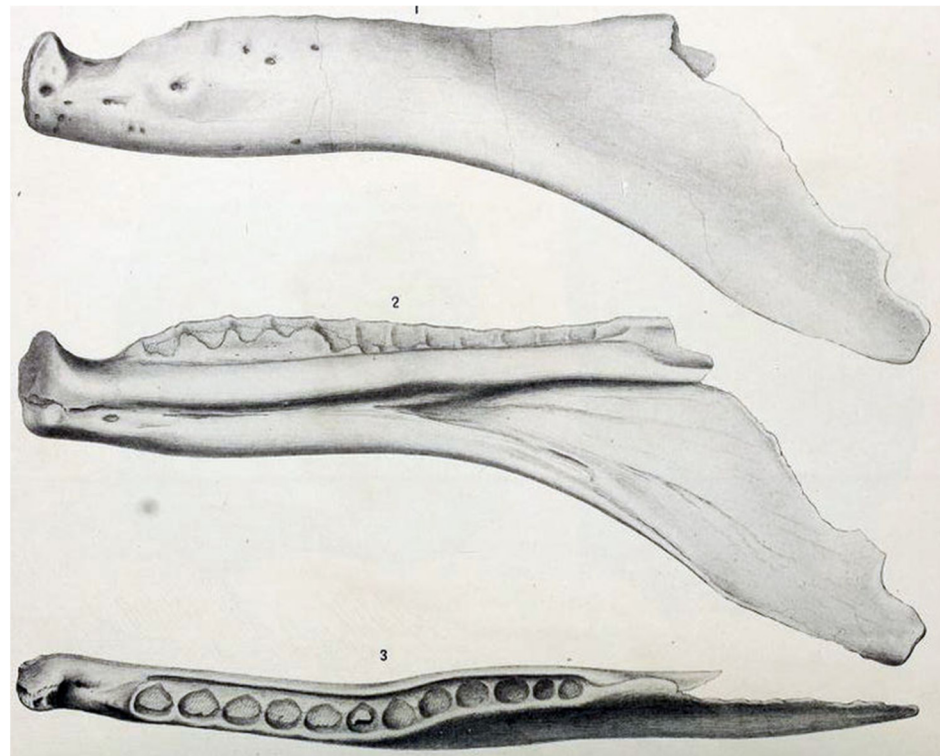
Figure 24. Dentary of the holotype of *Labrosaurus ferox*, adapted from Guilmore, 1920 [35] in 1—lateral, 2—medial and 3—dorsal views.

"*Allosaurus*" *tendagurensis* Janensch, 1925 (incerta sedis)

Type: Tibia from Tendaguru, Tanzania (MB.R.3620). Probably carcharodontosaurian or megalosaurid [43,44].

*Allosaurus lucaris* (Marsh 1878), originally *Labrosaurus*.

Type YPM 1931, dorsal vertebra. Its type locality is Quarry 3, Como Bluff (YPM), which is in a Kimmeridgian/Tithonian wet floodplain mudstone in the Morrison Formation of Wyoming. Chure, 2000 [34], considered that there is nothing in the specimen to warrant specific separation, so it is a junior synonym of *A. fragilis*.

Apatodon mirus Marsh, 1877 *Nomen dubium* (Dinosauria incertae sedis)

Type: Weathered vertebra, too fragmentary for a proper identification and has been lost [34].

Allosaurus atrox (Marsh 1878), originally *Creosaurus*. Possibly valid (Figure 25).

Type YPM 1890, a partial skeleton, including teeth, ilium, metapodial, pedal phalanges, and vertebrae. Its type locality is Quarry 1, Como Bluff (YPM), which is in a Kimmeridgian/Tithonian wet floodplain claystone in the Morrison Formation of Wyoming. It is unclear if this species is valid or a junior synonym of *Allosaurus fragilis*. *A. atrox* was considered a junior synonym by Chure, 2000, and Chure and Loewen, 2020 [3,34].
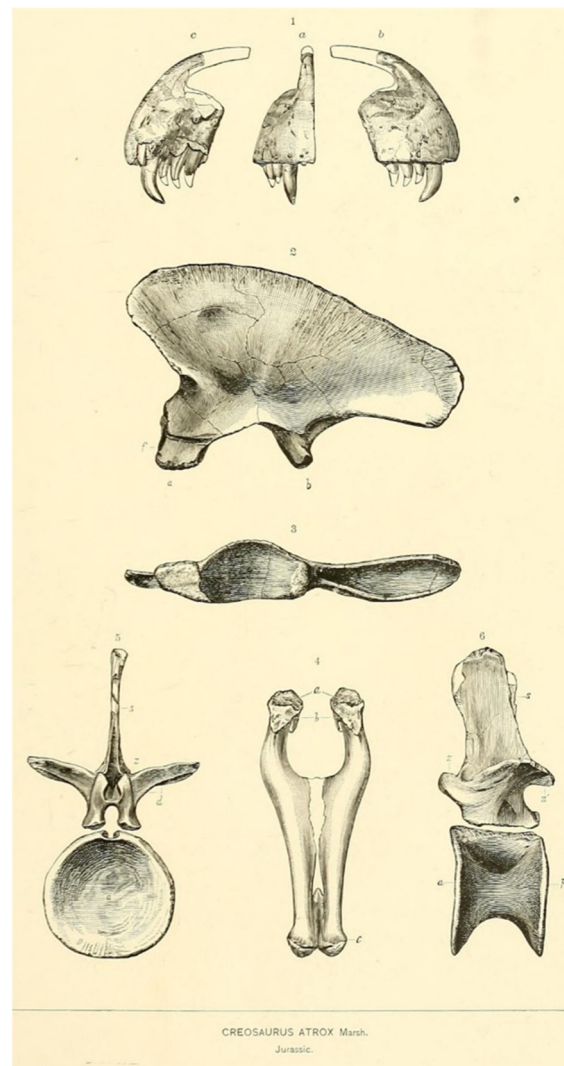
Figure 25. *Allosaurus* sp. Ilium type of *Creosaurus atrox* Marsh 1878. Original figure by Marsh, 1878. Public domain.

Epanterias amplexus Cope, 1878

Type is AMNH 5767: three vertebrae, a coracoid, and a metatarsal. Its type locality is Cope Quarry III, Cope's Nipple, which is in a Tithonian dry floodplain mudstone in the Morrison Formation of Colorado. New analysis on this specimen needs to be performed to test the validity.

Laelaps trihedrodon (Cope, 1877) *Nomen dubium*

Type AMNH (lost), a mandible. Its type locality is Cope Quarry I, Cope's Nipple, which is in a Kimmeridgian/Tithonian dry floodplain mudstone in the Morrison Formation of Colorado. Chure, 2000, considered it to be *Allosaurus* sp.

Antrodemus valens (Leidy, 1870) Leidy, 1873 (originally *Poekilopleuron*)

Holotype USNM 218, a set of vertebrae. Its type locality is Middle Park (USNM 218), which is in a Kimmeridgian/Tithonian Pond horizon in the Morrison Formation of Colorado. Gilmore, 1920 [35], compared *A. fragilis* material and found it to be conspecific, and proposed that the law of priority should prevail, suggesting that *A. fragilis* should be a junior synonym of *Antrodemus valens*. Madsen, 1976 [12], proposed the opposite: that *Atrodemus valens* should be a junior synonym of *A. fragilis*, since it is a well-known and established name, which we support.

Camptonotus amplus Marsh, 1879

Type YPM VP.1879, a pes from Morrison Fm. In 2015, a new reanalysis was conducted on the right pes of the holotype material of *Camptonotus amplus* Marsh, 1879, the YPM VP.1879, which was referred to in the ornithopod genus as the *Camptosaurus* Marsh, 1885, as well as the partial skull with a few postcranial bones, YPM VP.1892, which is stated to belong to the same individual [45]. It is suggested that the cranial material is similar to *Allosaurus* and the YPM VP.1879 is probably an allosaurid that is referred to as ?*Allosaurus amplus* (Marsh, 1879), but the validity of the latter depends on further evaluation of variation in the pes of *Allosaurus*. Galton et al., 2015 [45], considered it as probably an Allosaurid. Further information on the range of variation in the pes is needed.

Saurophaganax maximus (Chure, 1995), originally nomen nudum *Saurophagus maximus* Stovall, 1941

Also considering that for the debatable species *Saurophaganax maximus,* its bones are mostly postcranial bones, with almost no overlapping bones to the specimen ML415, with the exception of the postorbital and quadrate bones, which are not complete. Since the quadrate bone is fairly similar to *Allosaurus*, it is possible to compare the two.

The diagnostic arguments suggested by Chure, 1995 [46], for *Saurophaganax maximus* seem solid, and the species is seen here as a valid genus and species, but it was not the focus of this work, and more work needs to be performed, i.e., including it in a specimen-based analysis. Its type locality is Stovall's Pit 1, Kenton (OMNH V92), which is in a Kimmeridgian/Tithonian wet floodplain mudstone/sandstone in the Morrison Formation of Oklahoma.

6.2. Ontogeny and Size Comparisons

Regarding ontogenetic development, no histological study has been conducted. However, a few observations suggest an adult stage, but not senescent, mainly based on fused bone criteria [47]: fused neural–centrum suture (between the neural arch and the centrum) in the cervical vertebrae, and well-fused braincase and occipital region, with visible sutures. The individual was within the upper range known for adult *Allosaurus*. Due to the incomplete condition of ML415, the comparable measurement is the posterior end of the base of the last teeth to the most posterior point of the quadratojugal bone, which are the following: 36 cm in DINO 2560, 33 cm in USNM 4734, 29 cm in DINO11541, 31 cm in MOR693, and 35 cm in ML415. These values were calculated from photos using the given scale of the published figures. DINO 2560 is considered to have been about 12–13 m long ([12] pag. 5); therefore, based on this measurement, it is reasonable to classify the Portuguese species as being within the 10–12 m range.

6.3. Taphonomy

The holotype specimen of *A. europaeus* ML415 was found in three separate rounded boulders on the beach, which had been eroded by the elements in the beach environment (Figure 26). The skull is generally well preserved, although the anterior and dorsal surfaces show signs of modern erosion, suggesting that at least these surfaces were exposed after fossilization and diagenesis. The left posterior–lateral side of the skull is relatively complete and fully articulated. The broken medial region does not imply necessarily that the skull was in situ with the left side down, since this may have happened during modern erosion on the beach. The atlanto-axis complex remains articulated with the occipital condyle and show signs of modern erosion. It is likely that the skull and cervical vertebrae were articulated prior to beachward erosion of the cliff.
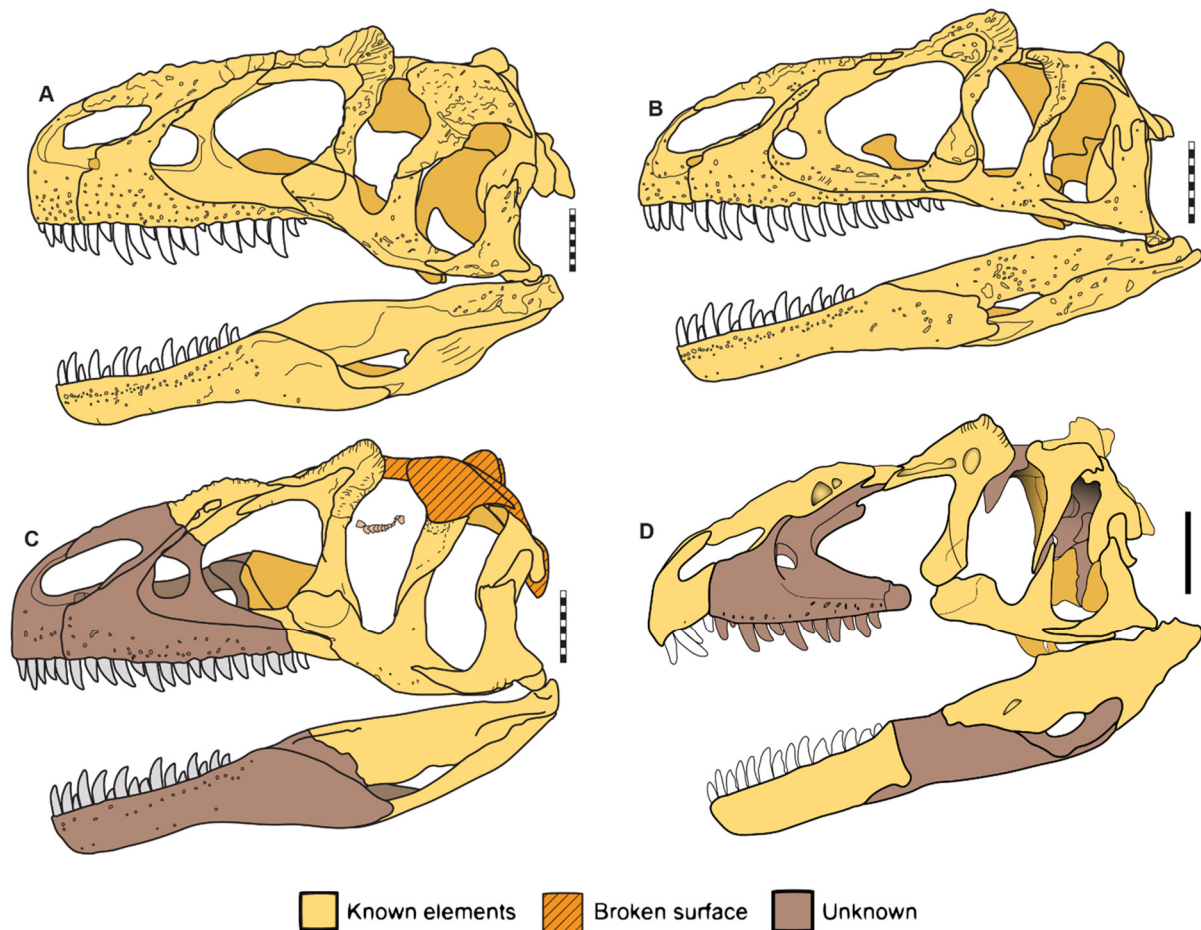
Figure 26. *Allosaurus europaeus* ML415 skull with the angular bone in the preparation process.

The cervical vertebrae are fully articulated, with the ribs on the left side, suggesting that the body was originally deposited left-side-down. The fragments of the seventh vertebra articulated to the Cv 6 shows that that this cervical vertebra was also articulated with the rest of the anterior cervical vertebrae. However, it appears that the posterior region of the Ce 6 and dorsal tips of the epipophyses on the left side of the cervical vertebrae suffered from modern erosion. This suggests that, at least for the vertebrae, the left side was exposed to the elements during erosion on the beach.

It is likely that the body was initially laid on its left side in a fully articulated position. The right (or up) side may have been partially exposed, resulting in some disarticulation and possible breakage due to scavenging or erosion, before being buried completely. After fossilization and diagenesis, differential erosion during modern exhumation on the cliff face and along the beach caused further disarticulation and differential exposure, resulting in the present erosion on the bone surfaces (Figures 9, 10, 20 and 26).

6.4. Comparisons of Allosaurus europaeus ML415

The skull of ML415 is identified as belonging to the genus based on the presence of a high, mid-laterally compressed dorsal projection on the diagnostic posterior–dorsal lacrimal surface, as diagnosed by Carrano et al., 2012 [2]. When comparing the skull to other specimens of this genus, it is evident that ML415 is more similar to the *A. fragilis* species than to *A. jimmadseni*, especially in relation to the proposed neotype specimen USNM 4734 on the lateral aspect. This is mainly due to the jugal bone shape, which both specimens share, with a curved ventral outline (Figure 27).

Figure 27. *Allosaurus* species skull in lateral view, scale 10 cm. (**A**) *A. fragilis* DINO 2560, (**B**) *A. jimmadseni* DINO 1154, (**C**) *A. europaeus* ML415, and (**D**) interpretation of the new reconstitution of *A. fragilis* USNM 4734. (**A**–**C**) Modified from Chure and Loewen, 2020 [3].

Upon analysis of other published *Allosaurus* specimens from Portugal, only the specimen of Andrés [6] and Guimarota (MG 27804 previously IPFUB Gui Th 4) [7] have overlapping material with ML415. However, the Guimarota material is limited to a single hatchling maxilla, which is not very useful for comparison with the ML415 specimen. This is due to the fact that the maxilla is ontogenetically different and not fully present in the *A. europaeus* specimen, and without skull articulation context, there is a risk of erroneous interpretation.

The Andrés (MNHNUL/AND.001) specimen has not been described or adequately figured out. The lacrimal bones appear similar, except for the lacrimal recesses, where the Andrés specimen shows two pneumatic foramina and ML415 shows one. The quadrate bones are similar in both specimens, but the ventral shelf appears to be projected medially (in Andres) rather than bent posteriorly, suggesting that the pterygoid bone may not contribute to the shelf. Additionally, the angle between the ventral shelf and quadrate ridge is more acute in ML415 than in Andrés MNHNUL/AND.001. Further study is necessary to suggest a taxonomic difference between these other Portuguese specimens and *A. europaeus*.

Comparing the cervical vertebrae of ML415 with other known large theropods of this age, the vertebrae of genus *Allosaurus* are the closest match. *Ceratosaurus* Marsh, 1884, for example, has amphiplatyan cervical vertebrae, with a flat anterior end of the centrum and a concave posterior end, which is completely different from ML415ML415 cervical vertebrae [48]. In *Lourinhanosaurus antunesi* [25], the cervical vertebrae are opisthocoelus, such as those of ML415. However, the characteristic median keels on the ventral surface

are absent from the vertebrae of the *A. europaeus* specimen [25]. The cervical vertebrae of *Torvosaurus gurneyi* [49] were not found, so it is impossible to compare them [12,49].

7. Phylogeny

7.1. General Phylogenetic Analysis

Based on the diagnosis of the genus of Carrano et al., 2012 [2], as was previously mentioned, the specimen of *Allosaurus* europaeus ML415ML415 is well diagnosed as *Allosaurus* because of the presence of a high, mid-laterally compressed dorsal projection on the diagnostic posterior–dorsal lacrimal bone surface. To test this in a phylogenetic way, the analysis using the data matrix of Carrano et al., 2012 [2], and Eddy and Clarke, 2011 [30], was used.

Here, 51 characters provided by Carrano et al., 2012 [2], which we considered useful for distinguishing *Allosaurus* species and could be scored for ML415, were added to the base matrix of 177 characters from Eddy and Clarke, 2011 [30]. The specific characters added were: 31–34, 40, 43, 46, 47, 51, 53–56, 59, 66, 68, 72, 74–81, 83, 84, 91, 92, 95–99, 110, 112, 113, 115–117, 132, 170–178, and 180 of Carrano et al., 2012 [2], and they were included as incremental characters, numbered 178 to 228. The matrix resulting from the analysis contains 228 characters (177 + 51) and 24 terminal taxa (22 from the original data matrix, plus *Allosaurus europaeus* ML415ML415 and *A. jimmadseni*, scored by us).

The resulting scoring of *A. europaeus* ML415 and *A. jimmadseni*, into Eddy and Clarke's matrix [30] with Carrano et al.'s [2] 51 additional characters, is as follows:

ML_415

??????????????10??0?12?1?1110?00000????0?0?00????0???0010???100?????1110 0????00??0?1???????0???????1???1011012??????????????????????????????????????? ???????????????????????11002012211000011020000000000100111111111111001010

'*Allosaurus_jimmadseni*'

10?01?210?1?011100000120101?10?00000?000100?000100100100010?101000?01111100? 00?0??0001100000?101?1101?01?1101??1??? ???????????????????????110020[01]2011000111020000000000010011?[01]111011100?1010

The complete matrix and character description are available at https://morphobank.org/permalink/?P5203, accessed on 1 May 2024. The matrix was run using TNT [31], as described in the Methods Section.

The phylogenetic analysis resulted in 52 trees, with a best score of 418 and a consensus tree showing a polytomy placing ML415 and *A. jimmadseni* as sister taxa of *Allosaurus fragilis* based on the following genus synapomorphies:

1. Ch. 7: Maxilla, promaxillary fenestra, lateral exposure is present, but completely obscured by the lateral lamina of the ascending ramus in *A. fragilis* and *A. jimmadseni* and unknown in *A. europaeus* (Ch. 7 from Eddy and Clarke, 2011 [30]).

2. Ch. 33: Jugal bone, lateral view, relative heights of quadratojugal prongs, the dorsal prong is shorter or equal in height in all species of *Allosaurus* (Ch. 33 from Eddy and Clarke, 2011 [30]).

3. Ch. 36: Jugal bone, lateral view, accessory pneumatization of the antorbital fossa is absent or shallow, shared across *Allosaurus* species (Ch. 36 from Eddy and Clarke, 2011 [30]).

4. Ch. 47: Prefrontal bone, medial view, shape of frontal bone articular surface is triangular in *A. fragilis* and *A. jimmadseni*, unknown in *A. europaeus* (Ch. 47 from Eddy and Clarke, 2011 [30]).

5. Ch. 55: Parietal bone, posteriorly placed, knob-like dorsal projection, form is absent or very low (0) in *A. fragilis* and *A. jimmadseni*, and is unknown in *A. europaeus* (Ch. 55 from Eddy and Clarke, 2011 [30]).

6. Ch. 84: Palatine bone, pneumatic recess, form is absent or small in all *Allosaurus* species (Ch. 84 from Eddy and Clarke, 2011 [30]).

7. Ch. 185: Lacrimal bone, horn morphology has a triangular horn across all *Allosaurus* species (Ch. 185, 47 from Carrano et al., 2012 [2]).

This set of synapomorphies support a monophyletic *Allosaurus* genus, comprehending *A. fragilis*, *A. jimmadseni*, and *A. europaeus*. The Portuguese ML415 is nested within *Allosaurus* with some level of certainty, but the matrix does not differentiate at the species level. The analysis was performed on the Carrano et al., 2012 [2] dataset plus *A. euroapeus* and *A. jimmadseni*. The resulting scoring of *A. europaeus* ML415 and *A. jimmadseni* in the matrix of Carrano et al., 2012 [2] is as follows:

"Allosaurus_europaeus"

??????????????????0??????????1100??101200002020002111000 00???????1???1?020 0000020011???000?101001?0?0?????11111?111?0???????????11?111?000000000?????????? ???????????0111100101?0??? ?? ???????????????????????????????????

"Allosaurus_jimmadseni"

00001000000100011?000000021111110001101 2000020&12000211100100 00100111100011 0200000020011011000?001001?0?02???2?11110111110 0010??00201101111110000 1000?1020 0100?1???1?1100010?1?? ?? ???

This analysis resulted in 2916 trees with 1027 steps, with a strict consensus that all *Allosaurus* taxa and *Saurophaganax maximus* are paired together in a polytomy. This result confirms that ML415 is well nested within *Allosaurus*. The phylogenetic position of *A. europaeus* remains unresolved at the species level. To determine the species validity and distinctions, a new matrix was constructed with a new set of characters, which are discussed further. The file was analyzed with TNT, where the ML415 is nested within the *Allosaurus* genus.

7.2. Discussion of Phylogenetic Characters

The data matrix by Eddy and Clarke, 2011 [30], was chosen, as it is the most recent phylogenetic analysis data focused on the Allosauroidea clade, with a particular emphasis on cranial material, considering that the *Allosaurus europaeus* specimen is mainly composed of cranial bones.

Some taxa of Carrano et al.'s [2] data matrix do not overlap with the taxa of the Eddy and Clarke [30] matrix, since these taxa are only tyrannosauroids (*Dilong* and *Tyrannosaurus*) and, as they were not the focus of this work and for time-saving purposes, their scores were marked as unknown ("?"). See full matrix at https://morphobank.org/permalink/?P5203, accessed on 1 May 2024.

It is important to note some remarks regarding the scoring. The Eddy and Clarke [30] matrix score is based on the analysis of BYU 571/8901, which consists of a fragmented and deformed skull, atlanto-axis complex, and several postcranial materials, as well as BYU 683/9466, which is a fragmented skull, both of which are considered *A. fragilis* according to Chure and Loewen, 2020 [3]. Also, for the specimens CM 1254 and 11843, with a premaxilla, two teeth, postcranial material, and a cranium (only partially prepared), with several parts

belonging to a young individual, respectively, both specimens are *A. fragilis* according to McIntosh, 1981 [50]. OMNH 780, as a claw of *Saurophaganax maximus* [34], and UUVP (multiple) specimens were probably the same that Madsen [12] based his illustrations. The scoring of the characters of Carrano et al., 2012 [2], was based only on *A. fragilis*, as *A. jimmadseni* was not published at the time and *A. europaeus* was not scored. Cranial characters for *A. fragilis* were scored from DINO 2560, USNM 4734, and disarticulated CLDQ material in the UMNH VP collection [2].

The score for the characters of *A. jimmadseni* was mostly based on Chure and Loewen, 2020 [3], regarding the holotype and paratype, except for some postcranial characters that were based on the known specimen of this species, SMA 0005, scored from direct observations and personal photographs.

It is also noted that for the cervical vertebrae character 110 (from Eddy and Clarke, 2011 [30]), the posterior articular surface of the mid-cervical centra width is 20% broader rather than taller in *A. europaeus*, and this may be due to the deformation.

In the analysis of the dataset by Carrano et al., 2012 [2], the score of *A. jimmadseni* was based on the published material from Chure and Loewen, 2020 [3]. The original *Allosaurus* score was considered for *A. fragilis*, in which only three characters were updated. The characters 51 and 52 pertain to the jugal bone contribution to the antorbital fenestra and fossa and its pneumatic features, respectively. According to Evers et al., 2020 [11], these characters were previously misinterpreted by other researchers, and they are present in all *Allosaurus* species. Additionally, character 118 was revised because it was originally scored as "2". Although the character only has two states, the score of "1" was given to this character. This appears to be an oversight by the original authors. The final matrices are available at morphobank.org (https://morphobank.org/permalink/?P5203, accessed on 1 May 2024).

7.3. New Restricted Phylogenetic Analysis for Allosaurus (Table 1)

The construction of the second analysis of the specimen-based matrix with *Allosaurus* in-group species was necessary since the previous matrix did not solve at the species level. To accomplish this, a search was conducted to identify the closest taxa to *Allosaurus*, one more basal to function as an outgroup, and the other more derived. Upon observation of Carrano et al.'s [2] phylogeny, the *Sinraptor dongi* and *Neovenator salerii* taxa were chosen as outgroup and derived taxa because they are well known and the closest taxa to *Allosaurus*. In this way, some characters from Carrano et al., 2012 [2], and Eddy and Clarke, 2011 [30], that both these taxa do not share with *Allosaurus* were chosen, as well as some that may be unique to some specimens of *Allosaurus* (characters: 7, 15, 30, 33, 36, 41, 47, 62, 64, 65, 69, 77, 78, 84, 87, 94, 95, 96, 99, 110, 127, 141, 157, and 166 from Eddy and Clarke, 2011 [30], and 40, 132, and 173 from Carrano et al., 2012 [2]).

Some diagnostic characters of *A. jimmadseni* were also added since they may be unique to these species based on the diagnosis of Chure and Loewen, 2020 [3], which are:

1. Maxila, lateral aspect, medioventral wall of the maxillary antorbital fossa: smooth (0); a row of neurovascular foramina (1) (Ch. 36).
2. Maxilla: straight posteroventral jugal ramus of maxilla, where it articulates with jugal bone (0); curved (1) (Ch. 37).
3. Laterodorsal margin of nasal bone "pinched" into the low crest, continuous from premaxilla to lacrimal bone: absent (0); present (1) (Ch. 38).
4. Posterior portion of the dorsal surface of nasal bone, cup-shaped, producing a median peak in the region of nasofrontal contact: absent (0); present (1) (Ch. 39).
5. Lacrimal horns: absent or reduced (0); pronounced (as in *Allosaurus fragilis* [12]) (1); very pronounced (20% or more in the lacrimal bone height, in lateral view) (2) (Ch. 40).

6. Jugal bone with a relatively ventral margin: straight-to-slightly-curved outline in dorsal view (0); curved sinosoidal (1) (Ch. 41).

Initially, it was planned to introduce these new characters to the initial matrix. However, due to limited time, it was not possible to code all those taxa. As one of the main focuses of this work was to resolve this taxon at the species level, a particular genus-restricted matrix was created. Following the careful observation of specimens through illustrations, photographs, and 3D models, new characters were created that may be unique to some specimens. The primitive condition was set according to the score of these characters in *Sinraptor dongi* (characters -1, 2, 3, 4, 5, 6, 7, 8, 9, 44, 45, 46, 47, and 48, see the matrix at https://morphobank.org/permalink/?P5203, accessed on 1 May 2024).

1. Lacrimal anterior projections contacting the lacrimal bone portion overlapping nasal bone dorsally: Contacts posteriorly, ventrally, and dorsally (i.e., the lateroposterior tip of the nasal bone projects ventral to the lacrimal dorsoanterior projection). It is seen in both *A. europaeus* and USNM 4734 specimens, it is unknown in *Allosaurus* of Andrés since the publish lacrimal bone is disarticulated, and in other specimens, the lacrimal bone contacts only posteriorly and ventrally to nasal bone—NEW (Ch. 1).

2. Lacrimal vacuity is single in *Sinraptor dongi* [36], *A. europaeus*, and DINO 2560 and clearly divided by a vertical strut in *Allosaurus* of Andrés and in USNM 4734. *A. jimmadseni* share both states. This character may not be significant since Carpenter, 2010 [33], states that this characteristic is within the intra-specific variation—NEW (Ch. 2).

3. Lacrimal ventral ramus lateroanterior vertical projection is restricted to the dorsal half of the antorbital fenestra (aof) and not continuous to the medial vertical ridge that borders the aof in *A. europaeus*. In pictures published of *Allosaurus* of Andrés lacrimal bone, it is hard to observe, but it seems similar to ML415, so it is considered that these share the same characteristic. Nevertheless, with further detailed study of the Andrés specimen, this may be subject to change. For the other specimens of *Allosaurus* and *Sinraptor dongi* [36], this is continuous. In *Neovenator salerii*, the lacrimal bone is not reported. If proven to be true in Portuguese taxa, it may represent an autapomorphy—NEW (Ch. 3).

4. Nasal and dorsal ramus of maxilla: posterior end (dorsal portion in lateral view, without the skull roof) in DINO 2560, and the nasal bone and maxilla dorsal ramus end are at the same level or close, whereas on the other taxa, the nasal bone end is clearly posterior to the maxilla dorsal ramus—NEW (Ch. 4).

5. Nasal pneumatic foramina size in USNM 4734: the anterior foramen is larger than the posterior, but in *A. europaeus* and *A. jimmadseni*, the posterior foramen is larger than the anterior, while in DINO 2560 it is not applicable (no foramina present, single foramen, or two of the same size, score "?")—NEW (Ch. 5).

6. Pterygoid bone contact with the quadrate ventral shelf of the pterygoid flange (see Hendricks et al., 2015 [32], for topology) is unique and autapomorphic in *A. europaeus* due to the participation of the pterygoid bone in the fold that constitutes the shelf—NEW (Ch. 6).

7. Pterygoid bone contact with the ectopterygoid is autapomorphic in *A. europaeus*, with prominent ventral projection and anterior notch—NEW (Ch. 7).

8. Maxilla ventroposterior end is autapomorphic in *A. europaeus*, with a step-like, nearly vertical contact—NEW (Ch. 8).

9. Dentary, the posterior end is bifurcated in *A. jimmadseni*, potentially autapomorphic for this taxon, whereas in DINO 2560, it is single pointed, but it is not known in *Neovenator salerii* and other specimens of *Allosaurus*—NEW (Ch. 42).

10. Nasal bone proportions (total length/maximum width measured at the anterior-most end of prefrontal) are 9 or less in *Sinraptor dongi* and in *A. fragilis* (USNM 4734) but 10 or more in *A. jimmadseni* and in DINO 2560. In *A. europaeus* it is unknown, and in Andrés, the nasal bone is not reported—NEW (Ch. 43).

11. The angular dorsoposterior rim (contact with surangular bone)/minimum depth at mid-length is 5 or more (1) in *A. europaeus* and *A. jimmadseni*. This condition is unknown in USNM 4734 since it is not preserved, and in the Andrés specimen, the angular bone is not reported. In *Sinraptor dongi* and in DINO 2560, it is 4 or less (0)—NEW (Ch. 44).

12. For the 4th and 5th cervical vertebrae, the latero-anterior base of the neural spine with oblique-to-vertical subtle accessory lamina at the posterior end of the spino-prezygapophyseal lamina (best seen in lateral–dorsal views) is autapomorphically present in ML415 but not in other taxa, and it is not reported in the Andrés specimen. (1)—NEW (Ch. 45).

13. The shape of postorbital bone contact with the jugal bone is sigmoidal, with a clear, curved outline, whereas in *A. fragilis* (USNM 4734 and DINO 2560) and *A. jimmadseni* (types), it is straighter—NEW (Ch. 46).

These characters are the result of hours of work based on several observations through the in-person observation of the ML415 specimen of *A. europaeus*, analysis of several published works, and examination of photographs provided of the specimens. It is important to note that these characters may be subject to change pending future studies and a detailed published description of the Andrés specimen. In sum, the resulting character list and scoring distribution is as shown in Table 1.

Table 1. Phylogenetic characters used in the analysis and the scoring distribution (0 = plesiomorphic state, 1 or 2 apomorphic state, ? = unknown state).

	Sinraptor dongi	*Neovenator salerii*	*Allosaurus europaeus* ML415	*Allosaurus fragilis* USNM4734	*Allosaurus jimmadseni* types	*Allosaurus fragilis* DINO 2560	*Allosaurus* Andrés
1. Lacrimal bone anterior projections contacting nasal lacrimal bone contacts only posteriorly and ventral to nasal (0); lacrimal bone portion overlapping nasal dorsally: contacts posteriorly, ventrally, and dorsally (i.e., the lateroposterior tip of the nasal bone projects ventral to the lacrimal dorsoanterior projection) (1). NEW	0	?	1	?	0	0	?
2. Lacrimal vacuity absent (0); single (1); clearly divided by a vertical strut (2). NEW	0	?	1	2	1/2	1	2
3. Lacrimal ventral ramus lateroanterior vertical projection: continuous to the medial vertical ridge that borders the aof (0); restricted to the dorsal half of the aof and not continuous to the medial vertical ridge that borders the aof (1). NEW	0	?	1	0	0	0	1

Table 1. *Cont.*

	Sinraptor dongi	*Neovenator salerii*	*Allosaurus europaeus* ML415	*Allosaurus fragilis* USNM4734	*Allosaurus jimmadseni* types	*Allosaurus fragilis* DINO 2560	*Allosaurus* Andrés
4. Nasal and dorsal ramus of maxilla, posterior end (dorsal portion in lateral view, without the skull roof) and nasal end clearly posterior to maxilla dorsal ramus (0); nasal and maxilla dorsal ramus end at the same level or close (1). NEW	0	0	0	?	0	1	?
5. Nasal pneumatic foramina size: anterior foramen larger than posterior (0); posterior foramen larger than anterior (1); scored "?" when not applicable (no foramina present, single foramen, or two of the same size). NEW	0	?	1	0	1	?	?
6. Pterygoid bone contact with quadrate ventral shelf of pterygoid flange (see Hendricks et al., 2015 [32], for topology): no participation of pterygoid bone (0); with participation of pterygoid bone in the fold that constitutes the shelf (1). NEW	?	?	1	?	0	0	?
7. Pterygoid bone contact with the ecpt: continuous (no obvious ventral projections) (0); with prominent ventral projection and anterior notch (1). NEW	0	?	1	?	0	0	?
8. Maxilla ventroposterior end: acute/tapering (ventroposteriorly inclined) (0); step-like (nearly vertical contact) (1). NEW	0	0	1	0	0	0	?
9. Cervical vertebrae, posterior articular face of mid-cervical centra, width: approximately as broad as tall (0); at least 20% broader than tall (1). (Ch. 110 [22]: p. 62, modified from [20]: p. 53)	0	0	1	0	0	0	?
10. Postorbital, ventral termination of ventral ramus: close to ventral margin of the orbit and ventral to squamosal–quadratojugal bone contact (0); dorsal to ventral margin of orbit and at same height or dorsal to squamosal–quadratojugal bone contact (1). (Ch. 41, modified from [21]: p. 7)	0	?	0	1	1	1	?
11. Nasal, development of dorsolateral surfaces: none, nasals low and dorsally convex (0); pronounced dorsolateral rims, sometimes with lateral crests (1); tall, parasagittal crests (2); inflated and forming a hollow midline crest (3). (Ch. 40)	0	1	2	1	2	1	?
12. Maxilla, promaxillary fenestra, lateral exposure: absent, no fenestra (0); partially or fully exposed (1); present, but completely obscured by the lateral lamina of the ascending ramus (2). (Ch. 7, modified from [22]: p. 6; ordered)	1	0	?	?	2	2	?
13. Maxilla, curvature of posterior ramus: straight (0); curved, ventral deflection does not surpass ventral margin of largest maxillary tooth (1); curved, ventral deflection equal to or surpasses ventral margin of largest maxillary tooth (2). (Ch. 15, modified from [12]: p. 32; ordered)	0	?	?	?	1	1	?
14. Lacrimal bone, suborbital process along posterior margin of ventral ramus: absent (0); present (1). (Ch. 30, modified from [12]: p. 79)	1	?	0	0	1	0	0
15. Jugal bone, lateral view, relative heights of quadratojugal bone prongs: dorsal prong shorter or equal in height (0); taller (1) than ventral prong. (Ch. 33)	1	?	0	0	0	0	?

Table 1. *Cont.*

	Sinraptor dongi	*Neovenator salerii*	*Allosaurus europaeus* ML415	*Allosaurus fragilis* USNM4734	*Allosaurus jimmadseni* types	*Allosaurus fragilis* DINO 2560	*Allosaurus* Andrés
16. Jugal bone, lateral view, accessory pneumatization of the antorbital fossa: absent or shallow (0); extensive, invaginated recess (1). (Ch. 36, modified from [22]: p. 28; [21]: p. 12)	1	?	0	0	0	0	?
17. Prefrontal, medial view, shape of frontal bone articular surface: triangular (0); rounded (1). (Ch. 47).	1	?	?	?	0	0	?
18. Braincase, supraoccipital, width of dorsal expansion: less than twice the width (0); more than twice the width (1) of the foramen magnum. (Ch. 62, wording modified from [13]: p. 97; [45]: p. 13).	1	?	?	0	0	0	0
19. Braincase, angle between occipital condyle and basal tubera: perpendicular, at or near 90° (0); acute (1). (Ch. 64, wording modified from [13]: p. 99; [45]: p. 7).	1	?	0	0	0	0	0
20. Braincase, shape of occipital condyle: subspherical (0); dorsoventrally compressed (1). (Ch. 65, wording modified from [45]: p. 15)	1	?	0	0	0	0	0
21. Braincase, form of trigeminal foramen (cranial nerve V) exit: single (0); fully split (1). (Ch. 69, wording modified from [13]: p. 108)	0	?	?	?	1	?	?
22. Pterygoid, medial view, fossae penetrating the quadrate and ectopterygoid rami: absent (0); present (1). (Ch. 77)	1	?	0	?	0	0	?
23. Pterygoid bone, medial view, angle of medial process with respect to angle of vomeropalatine ramus: parallel or subparallel (0); rotated dorsally by at least 30° (1). (Ch. 78)	1	?	0	?	0	0	?
24. Palatine bone, pneumatic recess, form: absent or small foramen (0); large fossa with one or more foramina (1). (Ch. 84)	1	1	0	?	0	0	?
25. External mandibular fenestra, lateral view, maximum anteroposterior length of fenestra relative to length of mandible: greater than 15% (0); less than 15% (1). (Ch. 87, modified from [21]: p. 38)	0	?	?	1	1	1	?
26. Splenial bone, medial view, mylohyoid foramen: present, completely enclosed by splenial (0); present, opens anteroventrally (1); absent (2). (Ch. 94, modified from [12]: p. 239)	0	?	?	?	1	1	?
27. Angular bone, posterior termination: posterior or ventral to surangular foramen (0); anterior to surangular foramen (1). (Ch. 95, wording modified from [12]: p. 233)	1	?	0	0	0	0	?
28. Surangular bone, dorsoventral depth over the external mandibular fenestra: less than half the depth of the mandible (0); more than half the depth of the mandible (1). (Ch. 96, [22]: p. 56, modified from [20]: p. 47).	0	?	1	1	1	1	?

Table 1. *Cont.*

	Sinraptor dongi	*Neovenator salerii*	*Allosaurus europaeus* ML415	*Allosaurus fragilis* USNM4734	*Allosaurus jimmadseni* types	*Allosaurus fragilis* DINO 2560	*Allosaurus* Andrés
29. Prearticular bone, mylohyoid foramen: absent or fails to perforate anteroventral margin of prearticular (0); present, foramen height less than half the dorsoventral height of prearticular above foramen midline (1); (Ch. 99; ordered)	0	?	?	1	1	1	?
30. Anterior caudal vertebrae, ventral surface: shallow groove (0); distinct sunken groove (1); robust ventral ridge (2). (Ch. 127, wording modified from [9]: p. 120; [10]: p. 128)	1	2	?	?	?	0	?
31. Scapulocoracoid, notch between scapular acromion process and coracoid bone: absent (0); present (1). (Ch. 141, [22]: p. 94; wording modified from [1]: p. 68)	0	?	?	1	?	1	?
32. Pubis, pubic boot size relative to pubic length: less than 50% (0); 50–60% (1); greater than 60% (2). (Ch. 157, [22]: p. 80; wording modified from [20]: p. 51; ordered)	0	0	?	1	?	1	1
33. Tibia, lateral condyle: confluent with cnemial crest anteriorly in proximal view (0); strongly offset from cnemial crest by incisura tibialis (1). (Ch. 166, [9]: p. 204; [10]: p. 200)	0	?	?	1	?	1	?
34. Maxila, lateral aspect, medioventral wall of the maxillary antorbital fossa: smooth (0); a row of neurovascular foramina (1).	0	?	?	?	1	0	?
35. Maxilla posteroventral jugal ramus of maxilla, where it articulates with jugal bone: straight (0); curved (1).	0	0	1	1	0	1	?
36. Nasal, laterodorsal margin of nasal bone pinched into a low crest, continuous from premaxilla to lacrimal bone: absent (0); present (1).	0	?	1	0	1	0	?
37. Posterior portion of dorsal surface of nasal bone, cup-shaped, producing a median peak in the region of nasofrontal contact (Chure and Loewen 2020: pp. 20 and 22): absent (0); present (1).	0	0	?	0	1	0	?
38. Lacrimal horns (Chure and Loewen 2020: pp. 20 and 22): absent or reduced (0); pronounced (as in *Allosaurus fragilis* Madsen 1976) (1); very pronounced (20% or more the lacrimal bone height, in lateral view) (2).	0	?	2	1	2	1	2
39. Jugal bone with relatively ventral margin: straight-to-slightly-curved outline in dorsal view (0); curved sinosoidal (1).	0	?	1	1	0	1	?
40. Surangular bone, number of posterior surangular foramina: one (0);. two (1) (Ch. 132, Carrano et al., 2012, [2])	1	?	1	0	0	1	?
41. Cervical vertebrae, position of parapophysis on centrum: anterior (0); middle (1). (Ch. 173, Carrano et al., 2012, [2])	0	1	1	0	0	0	?
42. Dentary, posterior end bifurcated (0); single pointed (1). NEW	0	?	?	?	0	1	?

Table 1. *Cont.*

	Sinraptor dongi	*Neovenator salerii*	*Allosaurus europaeus* ML415	*Allosaurus fragilis* USNM4734	*Allosaurus jimmadseni* types	*Allosaurus fragilis* DINO 2560	*Allosaurus* Andrés
43. Nasal proportions (total length/maximum width measured at the anterior-most end of prefrontal): 9 or less (0); 10 or more (1). NEW	0	1	?	0	1	1	?
44. Angular: dorsoposterior rim (contact with surangular bone)/mininum depth at mid-length: 4 or less (0); 5 or more (1). NEW	0	?	1	?	1	0	?
45. 4th and 5th cervical vertebrae, latero-anterior base of the neural spine with oblique-to-vertical subtle accessory lamina at the posteror end of the spinoprezygapophyseal lamina (best seen in lateral–dorsal views): absent (0); present (1). NEW	0	0	1	0	?	0	?
46. Postorbital contact with jugal bone: straight (0); sigmoidal (1). NEW	0	?	1	0	0	0	?

This matrix can be adapted for a TNT file format, read by TNT software, by copying it into a .txt file, as follows:

xread

46 7

Sinraptor_dongi 00000?0000010111111101110010010000000001000000

Neovenator_salerii ???0???00?10??????????1??????2?0??0?0???1?1?0?

Allosaurus_europaeus_ML415 11101111102??000??00?000??01??????11?2111??111

Allosaurus_fragilis_USNM4734 ?20?0??0011??000?000????1?011?111?1001100?0?00

Allosaurus_jimmadseni__types_ 0[12]00100001221000000010001101 1????1011200011?0

Allosaurus_dino2560 0101?000011210000000?00011011011101001110 11000

Allosaurus_andres ?21?????????0???000??????????1?????2????????

;proc /;

;

The resulting file was then uploaded to TNT and the analyses were run. Alternatively, the matrix, character list, and supplementary images are available at: https://morphobank.org/permalink/?P5203, accessed on 1 May 2024.

8. Phylogenetic Results and Discussion

The outcomes derived from the matrix, which confines the taxonomic scope to the genus level, showed one parsimonious tree with 59 steps. In this tree (1), *A. europaeus* paired with *Allosaurus* of Andrés, with Ch. 2 as a synapomorphy, which is very plausible in terms of paleobiogeography and biochronology since both are from Portugal and have a similar age. Consequently, this configuration represents the most plausible scenario (Figure 28).

The single parsimonious tree (58 steps, CI 0.879, and RI 0.563) placed *A. europaeus* and the Andrés specimen together, and both as sister taxa of *A. jimmadseni*. The synapomorphies list is as follows:

*Neovenator*: Ch. 41 (Bootstrap clade support value: 40)

Allosaurus genus: Ch. 24 and 32 (Bootstrap clade support value: 26)
Allosaurus_fragilis USNM4734: Ch. 40 and 43
A.jimmadseni + *A. europaeus*: Ch. 5, 11, 36, and 44 (Bootstrap clade support value: 21)
*Allosaurus_jimmadseni_*(types): Ch. 40
Allosaurus europaeus ML415: Ch. 3 (Ch. 1, 3, 6, 7, 8, 41, and 46 if OTU Andrés is removed)
(Bootstrap clade support value: 14).
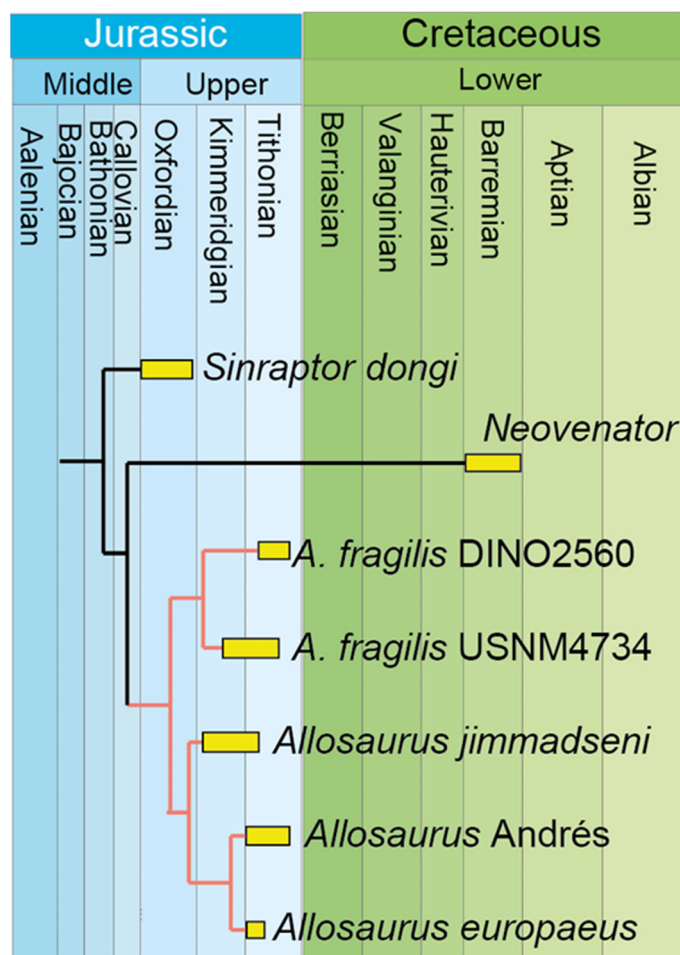
Figure 28. Relationship of *Allosaurus* calibrated chronologically with hypothetical geochronology dispersion of *Allosaurus* species based on *Allosaurus*-focus matrix (46 characters × 7 OTU), resulting in a single most parsimonious tree.

According to what was discussed previously, two characters are subject to debate: character 2, primarily due to observed intraspecific variation in the lacrimal bone, as seen by Carpenter, 2010 [33], and character 3, which presents challenges in its observation based on the available published photographs. It should be noted that there is some uncertainty in the coding of character 3 for the Andrés specimen. Analyses were conducted removing Ch. 2 and recoding Ch. 3 as unknown ("?"), or removing both.

After excluding the character 2, the analysis produced a single tree with 56 steps. This resulting tree is identical to tree 1 from the previous analysis, with the Andrés specimen positioned as the sister taxa to *A. europaeus*. In the fourth analysis, if character 3 was unknown ('?') in the Andrés specimen, the result was too unstable, creating 6 trees with 59 steps. This yielded a consensus tree with a polytomy between all *Allosaurus* specimens. This suggests that the Andrés specimen does not have a sufficient amount of data. If both characters were removed (fifth analysis), this resulted in 3 trees with a best score of 55. In this scenario, a polytomy was still present in the consensus tree, reinforcing more that the

Andrés specimen does not have sufficient information to resolve it. The importance of providing a detailed description of this specimen cannot be overstated, as it may provide crucial information for understanding this significant Jurassic genus.

If the Andrés specimen was removed or this specimen and character 2 were removed from the matrix, the tree became fully resolved in 58 or 56 steps, respectively, with a similar result to the original analysis.

More autapomorphic characters for *A. europaeus* were identified (1, 3, 6, 7, 8, 41, and 46) if the Andrés specimen was removed from the dataset. The characters 10 and 45 were not identified as synapomorphies due to the plesiomorphic condition in *Sinraptor dongi* (local autopomorphy) and the missing data on *A. jimmadseni*-type specimens, respectively. They were provisionally considered autapomorphic pending further verification. Consequently, *Allosaurus europaeus* is proposed to be recognized as a valid and distinct species.

On the other hand, the specific classification of the Andrés specimen remains inconclusive. The most probable scenario, supported by paleogeographic distribution and tree 1, suggests that Andrés should be classified as *A. europaeus*. It is important to note that the assignment of characters for *Allosaurus* from Andrés relies on existing published works, which offer limited descriptive details. Further descriptions may lead to different outcomes and conclusions. Additionally, a thorough examination of *Allosaurus* from Andrés, particularly involving postcranial characters, in future publications could potentially alter these results.

9. Cleaning the *Allosaurus* Wastebasket in Europe and Asia

The genus *Allosaurus* is considered a wastebasket, a term coined by Steven Jay Gould in a 1985 paper to classify organisms that fit nowhere else, but in paleontology is often applied to taxa that have received poorly supported attributions from very incomplete fossils, tentative field identification, or superficial taxonomic study. These attributions affect the databases because they may erroneously or misleadingly extend the biogeography and chronology of taxa. In Europe, *Allosaurus* fossils have been reported from Portugal, France [51], England [52], and Germany [53,54]. The Portuguese specimens (Andrés, Praia de Vale Frades, and Guimarota [4,6,7,10]) are discussed above, and the classification as *Allosaurus* is well supported.

Outside of Portugal and the U.S.A., the best-supported study showing the presence of *Allosaurus* is provided by Wings et al., 2016 [53], who showed, based on multivariate and cladistic analyses, that three teeth (GZG.V.010.334, NLMH106235a, and NLMH16416a) from the Upper Kimmeridgian of Tönniesberg and Kahlberg in Lower Saxony, Germany, are indeed *Allosaurus* sp.

Other specimens are more problematic. Diedrich, 2011 [54], also reported a tooth crown with serrated carinae from the Early Kimmeridgian of the Bruns Quarry, Wiehengebirge, Germany. Although the age and geography are consistent with *Allosaurus*, the claim is not supported by anatomical data and the images do not allow any further conclusion than that of Theropoda indet.

The teeth from the Berriasian of Grotte des Huguenots and Saléve, France, were attributed to *Allosaurus* sp. [51], but lack detailed anatomical features (morphology of denticles and enamel) to support such an attribution. The distal carina is centrally positioned and not strongly labially deflected, as in *Allosaurus*, indicating that it cannot be attributed to this genus. The visible features (weak labiolingual compression, position, and extension of the carina) allow attribution possibly to Avetheropoda indet. In the Late Berriasian/Aptian of England, the authors of [52] reported tracks from the Chilton Chine, Isle of Wight, to *Allosaurus* (*Antrodemus* in the original), but the genus cannot be distinguished from the tracks

alone, and the age is inconsistent with the known chronology. We reject this attribution and reclassify it as Theropoda indet.

In the Late Cenomanian to Early Turonian of the Mifune Group, Kamimashik, Kumamoto, Japan, the authors of [55] reported vertebrae, femur, tibia, and teeth of *Allosaurus* sp. If this was correct, it would be the youngest *Allosaurus*. However, the femur is remarkably similar to the contemporaneous *Segnosaurus galbinensis* shown in [56], namely, the dorsally projecting femoral head, with a well-defined neck, hemispherical femoral head, well separated from the greater trochanter, and a reduced trochanter. Therizinosaurs have been independently reported from the same fossil site [57]. Therefore, we attribute to *Segnosaurus* sp. the Mifune vertebra, femur, tibia, and teeth previously assigned to *Allosaurus.*

As result of this cleaning of the *Allosaurus* wastebasket in Europe and Asia, the known distribution of the *Allosaurus* genus is restricted to the United States (Late Kimmeridgian to Late Tithonian), Portugal (Late Kimmeridgian to Early Tithonian), and Germany (Late Kimmeridgian).

10. Paleobiogeography and Biochronology

In the Kimmeridgian and Tithonian, the Atlantic Ocean was already forming on the North Hemisphere, with Eurasia already separated from the North American continent. At this time, Europe consisted of a group of islands, including Iberia [58,59]. The supercontinent Gondwana was still present but was starting to split. Although the Morrison and Lourinhã formations are separated by sea, they share major clades of dinosaurs, indicating a fauna exchange between North America and Iberia. The *Allosaurus* genus is also included in this exchange [60,61].

According to the Paleobiology Database (PBDB), available at paleobiodb.org, the fossil record of this genus is found between the Kimmeridgian and Tithonian ages of the Late Jurassic. The *A. jimmadseni* species is from the Salt Wash Member in the Morrison Formation (Kimmeridgian) in Utah and the lower part of the Brushy Basin Member of the Morrison Formation below the "clay change" in Wyoming and South Dakota, except for at Dry Mesa Quarry, which occurs only two meters above the "clay change". This clay change marks the abrupt transition from predominantly non-smectitic clays below to predominantly smectitic clays above and is an important marker in about the middle or upper middle part of the formation [62].

The holotype and the neotype of the American species *A. fragilis*, YPM 1930, and USNM 4734, respectively, come from Felch Quarry 1, north of Canon City, Colorado, of the Morrison Formation [12,35,63], which is equivalent to the Salt Wash Member from the Morrison Formation and probably the top part, since the "clay change" is just above this quarry [64]. The specimen DINO 2560 (UUVP 6000) is from the Brushy Basin Member in the Carnegie Quarry from the Morrison Formation [34] as well as the Cleveland-Llyod Dinosaur Quarry specimens.

According to Kirkland et al., 2020 [65], the Salt Wash Member is lower and older than the Brushy Basin Member in the Morrison Formation. The Salt Wash Member is of Kimmeridgian age, whereas the Brushy Basin Member is of Tithonian age [3,65,66]. *A. jimmadseni* shows temporal distribution ranges within Kimmeridgian of 157.3 to 152.8 Ma, according to Chure and Loewen, 2020 [3], while *A. fragilis* is abundant in Tithonian. The geochronological relation [63,64] between the quarries shows that *A. jimmadseni* is the earliest species of the genus and that the specimens from Cleveland-Lloyd and DINO 2560 are the one of the youngest of the North Americanoccurences. Maidment, 2024 [67], stated that both *A. fragilis* and *A. jimmadseni* are partly contemporaneous, with different geographical distributions and with almost no overlap, where *A. fragilis* was found more south and east of Morrison Basin and *A. jimmadseni* was found further north and west.

The specimen from Andrés Quarry was found in the fluvial deposit unit, referred to as the Bombarral Formation, also known as the "Grés Superiores" unit, which is partially equivalent to the Alcobaça Formation in the northern sector of the Lusitanian Basin [6]. This unit is mainly of Tithonian age, except for its lowermost levels, which may be of Upper Kimmeridgian age [6]. Although the specific member of the Lourinhã Formation is unknown, it is possible to assume, with some level of certainty, that the Portuguese species *A. europaeus* comes from the early Tithonian age rocks of the Lourinhã Formation present in Vale Frades Beach. This is congruent with the diverse vertebrate fauna in Andrés Quarry, which is most likely from the Tithonian age as well [6,68].

The Guimarota specimen is from the Kimmeridgian stage of the Late Jurassic period. It appears to be the earliest record of this genus in Portugal. However, it is not sufficiently diagnostic at the species level [7], which may be misleading. Nevertheless, it suggests that dispersal may have occurred during the Kimmeridgian.

A. jimmadseni is the oldest species within the *Allosaurus* genus in North America. However, the type of *A. jimmadseni* and Guimarota maxilla are equivalent in age—Late Kimmeridgian. Therefore, it is unclear which occurrence is the oldest, and the biogeographic origin of the genus remains uncertain. It is possible that *Allosaurus* originated in both North America and Europe. However, the Allosauridae is absent from Europe in the Late Middle Jurassic until the Kimmeridgian, despite the occurrences of theropods being numerous on this continent, contrary to North America. There is no evidence for *Allosaurus* ancestry in Europe in Callovian, Oxfordian, and Kimmeridgian. The absence of Allosauridae in the European Middle Jurassic record seems to indicate a true absence, whereas in North America, there seems to be a bias resulting from the lack of fossiliferous outcrops. On the other hand, the diversity hotspot of *Allosaurus* is clearly in North America, suggesting that the genus originated and proliferated first in North America, as the hotspot genetic diversity is normally associated with the origin of the species (Vavilov center of origin [69]). This, however, has never been tested for genus-level and deep-time vertebrate paleontology.

Hypothetically, *Allosaurus* originated in North America and dispersed at least once into the European archipelago during or before the Late Kimmeridgian. The Iberia–North America similarity in species and potential land connections has been discussed since 1895 [70], and for dinosaurs [4,13,61,71]. Brikiatis, 2016 [72], suggested a terrestrial connection prior to or at the Late Kimmeridgian–Early Tithonian. This connection, which matches the age of the specimen, may have facilitated the exchange of fauna between the two continents.

11. Conclusions

In sum, it is concluded that:

1. The specimen of theropod dinosaur ML415, holotype of *Allosaurus europaeus* Mateus et al., 2006, is composed of cranial and cervical bones, with revealed additional elements, including the atlas-axis, coronoid bone, new dental remains, and rib fragments.
2. A specimen-based analysis of *Allosaurus* confirmed a monophyletic genus, composed of three valid species: *A. fragilis* (USNM 4734 as neotype), *A. europaeus* (ML415), and *A. jimmadseni*.
3. *Allosaurus atrox*, *A. amplus*, and *A. lucasi* holotypes do not have distinct autapomorphies and, therefore, are considered nomina dubia.
4. A single parsimonious tree, with 58 steps, placed *A. europaeus* ML415 and the Andrés specimen MNHNUL/AND.001 as sister taxa, supporting that the Andrés specimen is *A. europaeus*.

5. *A. jimmadseni* is closer to both Portuguese specimens than it is to *A. fragilis*. This confirms the validity of the species *A. europaeus*.
6. The origin of the *Allosaurus* genus appears to be rooted in North America. The dispersal of *Allosaurus* into Europe (no later than Late Kimmeridgian) was after the phylogenetic split between *A. jimmadseni* and *A. europaeus*, and before the split between *A. europaeus* ML 451 and Andrés MNHNUL/AND.001.
7. The previously reported *Allosaurus* sp. from the Cenomanian of Japan is attributed to *Segnosaurus* sp. The *Allosaurus* genus is restricted to the United States (Late Kimmeridgian to Late Tithonian), Portugal (Late Kimmeridgian to Early Tithonian), and Germany (Late Kimmeridgian).

References

1. Rauhut, O.W.M.; Pol, D. Probable Basal Allosauroid from the Early Middle Jurassic Cañadón Asfalto Formation of Argentina Highlights Phylogenetic Uncertainty in Tetanuran Theropod Dinosaurs. *Sci. Rep.* **2019**, *9*, 18826. [CrossRef]
2. Carrano, M.T.; Benson, R.B.J.; Sampson, S.D. The Phylogeny of Tetanurae (Dinosauria: Theropoda). *J. Syst. Palaeontol.* **2012**, *10*, 211–300. [CrossRef]
3. Chure, D.J.; Loewen, M.A. Cranial Anatomy of *Allosaurus jimmadseni*, a New Species from the Lower Part of the Morrison Formation (Upper Jurassic) of Western North America. *PeerJ* **2020**, *2020*, e7803. [CrossRef] [PubMed]
4. Pérez-Moreno, B.P.; Chure, D.J.; Pires, C.; Marques Da Silva, C.; Dos Santos, V.; Dantas, P.; Póvoas, L.; Cachão, M.; Sanz, J.L.; Galopim De Carvalho, A.M. On the Presence of *Allosaurus fragilis* (Theropoda: Carnosauria) in the Upper Jurassic of Portugal: First Evidence of an Intercontinental Dinosaur Species. *J. Geol. Soc.* **1999**, *156*, 449–452. [CrossRef]
5. Malafaia, E.; Dantas, P.; Ortega, F.; Escaso, F. Nuevos Restos de *Allosaurus fragilis* (Theropoda: Carnosauria) Del Yacimiento de Andrés (Jurásico Superior; Centro-Oeste de Portugal). In Proceedings of the V Encuentro de Jóvenes Investigadores en PaleontologíaAt, Cuenca, Spain, 18–21 April 2007.
6. Malafaia, E.; Ortega, F.; Escaso, F.; Dantas, P.; Pimentel, N.; Gasulla, J.M.; Ribeiro, B.; Barriga, F.; Sanz, J.L. Vertebrate Fauna at the *Allosaurus* Fossil-Site of Andrés (Upper Jurassic), Pombal, Portugal. *J. Iber. Geol.* **2010**, *36*, 193–204. [CrossRef]
7. Rauhut, O.W.M.; Fechner, R. Early Development of the Facial Region in a Non-Avian Theropod Dinosaur. *Proc. R. Soc. B Biol. Sci.* **2005**, *272*, 1179–1183. [CrossRef]
8. Malafaia, E.; Ortega, F.; Escaso, F.; Silva, B.; Ramalheiro, G.; Dantas, P.; Moniz, C.; Barriga, F. Análisis Preliminar de Un Nuevo Ejemplar de *Allosaurus* Del Grupo Lourinhã (Jurásico Superior de Torres Vedras, Portugal) A Preliminary Account of a New *Allosaurus* Individual from the Lourinhã Group (Upper Jurassic of Torres Vedras, Portugal). *Actas De Las IV Jorn. Int. Sobre Paleontol. De Dinosaur. Y Su Entorno Salas De Los Infantes* **2008**, 243–251.

9.   Malafaia, E.; Mocho, P.; Escaso, F.; Ortega, F. A New Carcharodontosaurian Theropod from the Lusitanian Basin: Evidence of Allosauroid Sympatry in the European Late Jurassic. *J. Vertebr. Paléontol.* **2020**, *40*, e1768106. [CrossRef]

10.   Mateus, O.; Walen, A.; Antunes, M.T. The Large Theropod Fauna of the Lourinhã Formation (Portugal) and Its Similarity to That of the Morrison Formation, With a Description of a New Species of *Allosaurus*. *Paleontol. Geol. Up. Jurass. Morrison Form. Bull.* **2006**, *36*, 123.

11.   Evers, S.W.; Foth, C.; Rauhut, O.W.M. Notes on the Cheek Region of the Late Jurassic Theropod Dinosaur *Allosaurus*. *PeerJ* **2020**, *2020*, e8493. [CrossRef] [PubMed]

12.   Madsen, J.H. *Allosaurus fragilis: A Revised Osteology Utah Department of Natural Resources*, 1993rd ed.; Utah Geological Survey: Salt Lake City, UT, USA, 1976; Volume 109.

13.   Escaso, F.; Ortega, F.; Dantas, P.; Malafaia, E.; Pimentel, N.L.; Pereda-Suberbiola, X.; Sanz, J.L.; Kullberg, J.C.; Kullberg, M.C.; Barriga, F. New Evidence of Shared Dinosaur across Upper Jurassic Proto-North Atlantic: *Stegosaurus* from Portugal. *Naturwissenschaften* **2006**, *94*, 367–374. [CrossRef]

14.   Costa, F.; Mateus, O. Dacentrurine Stegosaurs (Dinosauria): A New Specimen of *Miragaia longicollum* from the Late Jurassic of Portugal Resolves Taxonomical Validity and Shows the Occurrence of the Clade in North America. *PLoS ONE* **2019**, *14*, e0224263. [CrossRef]

15.   Mateus, O.; Dinis, J.; Cunha, P.P. The Lourinhã Formation: The Upper Jurassic to Lower Most Cretaceous of the Lusitanian Basin, Portugal – Landscapes Where Dinosaurs Walked. *Ciências Terra-Earth Sci. J.* **2017**, *19*, 75–97. [CrossRef]

16.   Gowland, S.; Taylor, A.M.; Martinius, A.W. Integrated Sedimentology and Ichnology of Late Jurassic Fluvial Point-Bars—Facies Architecture and Colonization Styles (Lourinhã Formation, Lusitanian Basin, Western Portugal). *Sedimentology* **2018**, *65*, 400–430. [CrossRef]

17.   Taylor, A.M.; Gowland, S.; Leary, S.; Keogh, K.J.; Martinius, A.W. Stratigraphical Correlation of the Late Jurassic Lourinhã Formation in the Consolação Sub-Basin (Lusitanian Basin), Portugal. *Geol. J.* **2014**, *49*, 143–162. [CrossRef]

18.   Mateus, O.; Milàn, J. Ichnological Evidence for Giant Ornithopod Dinosaurs in the Upper Jurassic Lourinhã Formation, Portugal. *Oryctos* **2008**, *8*, 47–52.

19.   Milán, J.; Mateus, O. Fra Strandbred Til Museum På Syv Dage–Historien Om et Gigantisk Dinosaur Fodspor. *Varv–Bl. Med Ældste Nyheder* **2003**, 8–14. [CrossRef]

20.   Mateus, O.; Milàn, J.; Romano, M.; Whyte, M.A. New Finds of Stegosaur Tracks from the Upper Jurassic Lourinhã Formation, Portugal. *Acta Palaeontol. Pol.* **2011**, *56*, 651–658. [CrossRef]

21.   Guillaume, A.R.D.; Costa, F.; Mateus, O. Stegosaur Tracks from the Upper Jurassic of Portugal: New Occurrences and Perspectives. *Ciências Terra/Earth Sci. J.* **2022**, *20*, 37–60. [CrossRef]

22.   Lapparent, A.F.; Zbyszewski, G. Les Dinosauriens Du Portugal. *Mémoires Des Serv. Géologiques Du Portugal.* **1957**, *2*, 1–63.

23.   Bonaparte, J.; Mateus, O. A New Diplodocid, *Dinheirosaurus Iourinhanensis* Gen. et Sp. Nov., from the Late Jurassic Beds of Portugal. *Rev. Del Mus. Argent. De Cienc. Nat. "Bernardino Rivadavia" E Inst. Nac. De Investig. De Las Cienc. Nat.* **1999**, *5*, 13.

24.   Tschopp, E.; Mateus, O.; Benson, R.B.J. A Specimen-Level Phylogenetic Analysis and Taxonomic Revision of Diplodocidae (Dinosauria, Sauropoda). *PeerJ* **2015**, *2015*, e857. [CrossRef] [PubMed]

25.   Mateus, O. *Lourinhanosaurus antunesi*, a new upper Jurassic allosauroid (Dinosauria: Theropoda) from Lourinhã, Portugal. *Memórias Acad. Ciências Lisb.* **1998**, *37*, 111–124.

26.   Mateus, O.; Maidment, S.C.R.; Christiansen, N.A. A New Long-Necked 'Sauropod-Mimic' Stegosaur and the Evolution of the Plated Dinosaurs. *Proc. R. Soc. B Biol. Sci.* **2009**, *276*, 1815. [CrossRef]

27.   Ramalho, M.M.R. Contribution à L' Étude Micropaleontologique et Stratigraphique Du Jurassique Supérieur et Du Crétacé Inférieur Des Environs de Lisbonne (Portugal). *Memórias Serviços Geológicos Port.* **1971**, *19*, 1–212.

28.   Mateus, O.; Telles Antunes, M. *Draconyx loureiroi*, a New Camptosauridae (Dinosauria, Ornithopoda) from the Late Jurassic of Lourinhã, Portugal. *Ann. Paléontologie* **2001**, *87*, 61–73. [CrossRef]

29.   Rotatori, F.M.; Moreno-Azanza, M.; Mateus, O. Reappraisal and New Material of the Holotype of *Draconyx loureiroi* (Ornithischia: Iguanodontia) Provide Insights on the Tempo and Modo of Evolution of Thumb-Spiked Dinosaurs. *Zoöl. J. Linn. Soc.* **2022**, *195*, 125–156. [CrossRef]

30.   Eddy, D.R.; Clarke, J.A. New Information on the Cranial Anatomy of *Acrocanthosaurus atokensis* and Its Implications for the Phylogeny of Allosauroidea (Dinosauria: Theropoda). *PLoS ONE* **2011**, *6*, e17932. [CrossRef] [PubMed]

31.   Goloboff, P.A.; Morales, M.E. TNT Version 1.6, with a Graphical Interface for MacOS and Linux, Including New Routines in Parallel. *Cladistics* **2023**, *39*, 144–153. [CrossRef]

32.   Hendrickx, C.; Araújo, R.; Mateus, O. The Non-Avian Theropod Quadrate I: Standardized Terminology with an Overview of the Anatomy and Function. *PeerJ* **2015**, *2015*, e1245. [CrossRef] [PubMed]

33.   Carpenter, K. Variation in a Population of Theropoda (Dinosauria): *Allosaurus* from the Cleveland-Lloyd Quarry (Upper Jurassic), Utah, USA. *Paléontol. Res.* **2010**, *14*, 250–259. [CrossRef]

34. Chure, D.J. *A New Species of Allosaurus from the Morrison Formation of Dinosaur National Monument (UT-CO) and a Revision of the Theropod Family Allosauridae*; Columbia University: New York, NY, USA, 2000.

35. Gilmore, C.W. Osteology of the Carnivorous Dinosauria in the United States National Museum, with Special Reference to the Genera *Antrodemus* (*Allosaurus*) and *Ceratosaurus*. *Bull. U.S. Natl. Mus.* **1920**, *I–XI*, 1–159. [CrossRef]

36. Currie, P.J.; Zhao, X.-J. A New Carnosaur (Dinosauria, Theropoda) from the Jurassic of Xinjiang, People's Republic of China. *Can. J. Earth Sci.* **2011**, *30*, 2037–2081. [CrossRef]

37. McClelland, B.K. Anatomy and Kinesis of the *Allosaurus* Skull. Ph.D. Thesis, Texas Tech University, Lubbock, TX, USA, 1990.

38. Paul, G.S.; Carpenter, K. Case 3506 *Allosaurus* Marsh, 1877 (Dinosauria, Theropoda): Proposed Conservation of Usage by Designation of a Neotype for Its Type Species *Allosaurus fragilis* Marsh, 1877. *Bull. Zoöl. Nomencl.* **2010**, *67*, 53–56. [CrossRef]

39. Paul, G.S. *Predatory Dinosaurs of the World*; A New York Academy of Sciences Book; Touchstone: New York, NY, USA, 1988; ISBN 0-671-61946-2.

40. Dalman, S.G. Osteology of a Large Allosauroid Theropod from the Upper Jurassic (Tithonian) Morrison Formation of Colorado, USA. *Vol. Jurassica* **2014**, *XII*, 69–106.

41. Carrano, M.T.; Loewen, M.A.; Evers, S.W. Comment (Case 3506)—Conservation of *Allosaurus* Marsh, 1877 (Dinosauria, Theropoda): Additional Data in Support of the Proposed Neotype for Its Type Species *Allosaurus fragilis* Marsh, 1877. *Bull. Zool. Nomencl.* **2018**, *75*, 59–64. [CrossRef]

42. Smith, D.K. Patterns of Size-Related Variation within *Allosaurus*. *J. Vertebr. Paléontol.* **2010**, *19*, 402–403. [CrossRef]

43. Rauhut, O.W.M. Post-Cranial Remains of 'Coelurosaurs' (Dinosauria, Theropoda) from the Late Jurassic of Tanzania. *Geol. Mag.* **2005**, *142*, 97–107. [CrossRef]

44. Rauhut, O.W.M. Theropod Dinosaurs from the Late Jurassic of Tendaguru (Tanzania). *Spec. Pap. Palaeontol.* **2011**, *86*, 195–239. [CrossRef]

45. Galton, P.M.; Carpenter, K.; Dalman, S.G. The Holotype Pes of the Morrison Dinosaur *Camptosaurus amplus* Marsh, 1879 (Upper Jurassic, Western USA)—Is It *Camptosaurus*, *Sauropoda* or *Allosaurus*? *Neues Jahrb. Für Geol. Und Paläontologie Abh.* **2015**, *275*, 317–335. [CrossRef] [PubMed]

46. Chure, D.J. A Reassessment of the Gigantic Theropod *Saurophaganax maximus* from the Morrison Formation (Upper Jurassic) of Oklahoma, USA. *Sixth Symp. Mesoz. Terr. Ecosyst. Biota* **1995**, *6*, 103–106.

47. Hone, D.W.E.; Farke, A.A.; Wedel, M.J. Ontogeny and the Fossil Record: What, If Anything, Is an Adult Dinosaur? *Biol. Lett.* **2016**, *12*, 20150947. [CrossRef]

48. Madsen, J.H., Jr.; Welles, S.P. *Ceratosaurus (Dinosauria, Theropoda) a Revised Osteology*; Stringfellow, J., Ed.; Utah Geological Survey: Salt Lake City, UT, USA, 2000; Volume 2, ISBN 1557913803.

49. Hendrickx, C.; Mateus, O. *Torvosaurus gurneyi* n. Sp., the Largest Terrestrial Predator from Europe, and a Proposed Terminology of the Maxilla Anatomy in Nonavian Theropods. *PLoS ONE* **2014**, *9*, e88905. [CrossRef]

50. McIntosh, J.S. Annotated Catalogue of the Dinosaurs (Reptilia, Archosauria) in the Collections of Carnegie Museum of Natural History. *Bull. Carnegie Mus. Nat. Hist.* **1981**, *18*, 1–67. [CrossRef]

51. Mojon, P.-O. Dinosauriens Éocretacés Des Faciès Purbeckiens (Berriasien Inférieur) Du Jura Méridional (S.-E. de La France). *Arch. Sci. Compte Rendu Seances Soc.* **2001**, *54*, 1–5. [CrossRef]

52. Blows, W.T. *Reptiles On The Rocks*; Isle of Wight Museum Publication: Newport, UK, 1978; pp. 1–60.

53. Gerke, O.; Wings, O. Multivariate and Cladistic Analyses of Isolated Teeth Reveal Sympatry of Theropod Dinosaurs in the Late Jurassic of Northern Germany. *PLoS ONE* **2016**, *11*, e0158334. [CrossRef] [PubMed]

54. Diedrich, C. Upper Jurassic Tidal Flat Megatracksites of Germany—Coastal Dinosaur Migration Highways between European Islands, and a Review of the Dinosaur Footprints. *Paleobiodivers Paleoenviron* **2011**, *91*, 129–155. [CrossRef]

55. Tamura, M.; Okazaki, Y.; Ikegami, N. Occurrence of Carnosaurian and Herbivorous Dinosaurs from Upper Formation of Mifune Group, Japan. *Mem. Fac. Educ. Kumamoto Univ.* **1991**, *40*, 31–45.

56. Zanno, L.E. A Taxonomic and Phylogenetic Re-Evaluation of Therizinosauria (Dinosauria: Maniraptora). *J. Syst. Palaeontol.* **2010**, *8*, 503–543. [CrossRef]

57. Ikegami, N. A Therizinosaurid Dinosaur from the Upper Cretaceous Mifune Group in Kyushu, Japan. *J. Vertebr. Paleontol.* **2005**, *25*, 73A.

58. Gradstein, F.; Gale, A.; Kopaevich, L.; Waskowska, A.; Grigelis, A.; Glinskikh, L.; Görög, Á. The Planktonic Foraminifera of the Jurassic. Part II: Stratigraphy, Palaeoecology and Palaeobiogeography. *Swiss J. Palaeontol.* **2017**, *136*, 259–271. [CrossRef]

59. Wilhem, C. Maps of the Callovian and Tithonian Paleogeography of the Caribbean, Atlantic, and Tethyan Realms: Facies and Environments. *Geol. Soc. Am. Digit. Map Chart Ser.* **2014**, *17*, 1–9. [CrossRef]

60. Francischini, H.; Sales, M.A.F.; Dentzien–Dias, P.; Schultz, C.L. The Presence of Ankylosaur Tracks in the Guará Formation (Brazil) and Remarks on the Spatial and Temporal Distribution of Late Jurassic Dinosaurs. *Ichnos* **2018**, *25*, 177–191. [CrossRef]

61. Mateus, O. Late Jurassic Dinosaurs from the Morrison Formation (USA), the Lourinhã and Alcobaca Formations (Portugal), and the Tendaguru Beds (Tanzania): A Comparison. *New Mex. Mus. Nat. Hist. Sci. Bull.* **2006**, *36*, 223–231.

62. Turner, C.E.; Peterson, F. Biostratigraphy of Dinosaurs in the Upper Jurassic Morrison Formation of the Western Interior, U.S.A. In *Vertebrate Paleontology in Utah*; Gillette, D.D., Ed.; Utah Geological Survey: Salt Lake City, UT, USA, 1999; Volume 99, pp. 77–102.

63. Evanoff, E.; Carpenter, K. History, Sedimentology, and Taphonomy of Felch Quarry 1 and Associated Sandbodies, Morrison Formation, Garden Park, Colorado. *Mod. Geol.* **1998**, *22*, 145–169.

64. Carpenter, K. Vertebrate Biostratigraphy of the Morrison Formation near Canon City, Colorado. In *Modern Geology*; Overseas Publishers Association: Geneva, Switzerland, 1998; Volume 23, p. 418.

65. Kirkland, J.; DeBlieux, D.D.; Hunt-Foster, R.K.; Foster, J.R.; Trujillo, K.; Finzel, E. The Morrison Formation and Its Bounding Strata on the Western Side of the Blanding Basin, San Juan County, Utah. *Geol. Intermt. West* **2020**, *7*, 137–195. [CrossRef]

66. Gates, T.A. The Late Jurassic Cleveland-Lloyd Dinosaur Quarry as a Drought-Induced Assemblage. *Palaios* **2005**, *20*, 363–375. [CrossRef]

67. Maidment, S.C.R. Diversity through Time and Space in the Upper Jurassic Morrison Formation, Western U.S.A. *J Vertebr Paleontol* **2023**, *43*, 5. [CrossRef]

68. Mocho, P.; Royo-Torres, R.; Escaso, F.; Malafaia, E.; de Miguel Chaves, C.; Narváez, I.; Pérez-García, A.; Pimentel, N.; Silva, B.C.; Ortega, F. Upper Jurassic Sauropod Record in the Lusitanian Basin (Portugal): Geographical and Lithostratigraphical Distribution. *Palaeontol. Electron.* **2017**, *20*, 1–50. [CrossRef] [PubMed]

69. Vavilov, N.I. *Origin and Geography of Cultivated Crops*; Cambridge University Press: London, UK, 1992; ISBN 0521111595.

70. Ward, L.F. The Mesozoic Flora of Portugal Compared with That of the United States. *New Ser.* **1895**, *1*, 337–346. [CrossRef] [PubMed]

71. Galton, P.M. The Ornithopod Dinosaur *Dryosaurus* and a Laurasia–Gondwanaland Connection in the Upper Jurassic. *Nature* **1977**, *268*, 230–232. [CrossRef]

72. Brikiatis, L. Late Mesozoic North Atlantic Land Bridges. *Earth-Sci. Rev.* **2016**, *159*, 47–57. [CrossRef]